ISTANBUL TECHNICAL UNIVERSITY ★ GRADUATE SCHOOL

DEVELOPMENT OF DIFFUSION BONDING PROCESSES FOR METAL ALLOYS TO USE PRODUCTION OF PCHE

M.Sc. THESIS

Ahmet Furkan EROL

Department of Materials Science and Engineering

Material Science and Engineering Programme

JULY 2022

ISTANBUL TECHNICAL UNIVERSTIY ★ GRADUATE SCHOOL

DEVELOPMENT OF DIFFUSION BONDING PROCESSES FOR METAL ALLOYS TO USE PRODUCTION OF PCHE

M.Sc. THESIS

Ahmet Furkan EROL
521171018

Department of Materials Science and Engineering

Material Science and Engineering Programme

Thesis Advisor: Prof. Dr. M. Kürşat KAZMANLI

JULY 2022

İSTANBUL TEKNİK ÜNİVERSİTESİ ★ LİSANSÜSTÜ EĞİTİM ENSTİTÜSÜ

BASKILI DEVRE ISI DEĞİŞTİRİCİ ÜRETİMİ İÇİN METAL ALAŞIMLARININ DİFÜZYON BAĞLAMA SÜREÇLERİNİN GELİŞTİRİLMESİ

YÜKSEK LİSANS TEZİ

Ahmet Furkan EROL

521171018

Malzeme Bilimi ve Mühendisliği Anabilim Dalı

Malzeme Bilimi ve Mühendisliği Programı

Tez Danışmanı: Prof. Dr. M. Kürşat KAZMANLI

TEMMUZ 2022

Ahmet Furkan Erol, a M.Sc. student of ITU Graduate School student ID 521171018 successfully defended the thesis/dissertation entitled "DEVELOPMENT OF DIFFUSION BONDING PROCESSES FOR METAL ALLOYS TO USE PRODUCTION OF PCHE", which he prepared after fulfilling the requirements specified in the legislations, before the jury whose signatures are below.

Thesis Advisor :	**Prof. Dr. M. Kürşat KAZMANLI** Istanbul Technical University	.....
Jury Members :	**Prof. Dr. Murat BAYDOĞAN** Istanbul Technical University	.....
	Dr. Fatma BAYATA SOLAK Istanbul Bilgi University	.....

Date of Submission : 3 June 2022
Date of Defense : 29 July 2022

To my family,

FOREWORD

This study, IDEALAB A.Ş. it covers the experimental development of the diffusion bonding method used in the development process of the heat exchanger designed in-house. Therefore, I would like to thank especially Mr. Edip SEVİNÇER, Mr. Talha Ensar BAŞ and IDEALAB family for all their support in the emergence of this thesis.

I would like to thank my esteemed advisor, Prof. Dr. M. Kürşat KAZMANLI who always stands behind me with his understanding and his experience and guidance in the graduate process.

I would like to thank my dear friend and also as research assistant, İbrahim Göksel HIZLI, for not leaving me alone in this process, rushing to my aid in every troubled process, and taking a close interest in my thesis.

Finally, I would like to express my endless thanks to my mother Emine EROL, to my father Süleyman EROL, to my sister Dr. Esra EROL ERGAN and to my brother for their support and love throughout the education and training process until the emergence of this thesis.

July 2022 Ahmet Furkan EROL

Mechanical Engineer & Energy Systems Engineer

TABLE OF CONTENT

Page

ABBREVIATIONS

PCHE **:** Printed Circuit Heat Exchanger

EDS **:** Energy Dispersive Spectroscopy

kN **:** Kilo-Newton

MPa **:** Mega pascal

HV **:** Vickers Hardness Value

mm **:** Millimeter

SEM **:** Scanning Eelctron Microscopy

GMAW/GTAW **:** Gas Metal Arc Welding/Gas Tungsten Arc Welding

SYMBOLS

A : Angstrom ($1x10^{-10}$ meter)

° : Degree

°C : Centigrade

µm : Micron

Co : Initial Density of One of The Diffusion Pairs

Cs : Concentration on Surface

Cx : Density of a point x distance from the surface or cross section

d : Trace Diameter [mm]

D : Diffusion Coefficient

Db : Ball Diameter [mm]

$\frac{dc}{dx}$: Concentration Gradient

erf : Error Function

F : Force

kgf : Kilogramme Force

$\Delta Q_{surface\text{-}diffusion}$: Activation Energy Required for Surface Diffusion

$\Delta Q_{grain\ boundary\ diffusion}$: The Activation Energy Required for Grain Boundary Diffusion

$\Delta Q_{volumetric\ diffusion}$: Activation Energy Required for Volumetric Diffusion

x : The Distance From the Surface of the Point Where Cx is Measured

t : Time

J : Flux

T_E : Base Material Melting Temperature

T_D : The Temperature at Which Diffusion Bonding Takes Place

LIST OF TABLES

Page

LIST OF FIGURES

Page

DEVELOPMENT OF DIFFUSION BONDING PROCESSES FOR METAL ALLOYS TO PRODUCE PCHE

SUMMARY

The phase state of carbon dioxide above the critical pressure and critical temperature is called supercritical CO_2 (sCO_2). Since the density of sCO_2 at the critical point is higher than the density of the liquids at the critical point, it allows the pumping power in the compressor to be greatly reduced, thus increasing the efficiency of thermal-electrical energy conversion.

The sCO_2 cycle has great potential in waste heat recovery systems, air-independent propulsion systems, due to its high power density, high efficiency, compact and modular structure.

In order to use a heat exchanger in the sCO_2 cycle, a compact heat exchanger resistant to high pressure and temperature should be developed. In order to develop a heat exchanger that will meet these requirements, the diffusion bonding process, which can be applied in complex geometries, provides strength as much as the base material, and has high corrosion resistance, comes to the fore. Since the heat exchangers that can meet the high pressure and high temperature requirements of sCO_2 are printed circuit heat exchangers (PCHE) type heat exchangers, the diffusion coupling method developed within the scope of the thesis has been used in the production of printed circuit heat exchangers.

Heat exchangers are equipment that allow the heat energies of two fluids to pass from a high temperature fluid to a low temperature fluid. In some areas of use, it is of great importance that the heat exchanger designs be compact and resistant to high pressure and high temperature. Printed circuit heat exchangers (Printed Circuit Heax Exchanger-PCHE) come to the fore because they are one of the types of heat exchangers that meet these conditions. The compactness, high pressure and temperature resistance of this type of heat exchanger is directly related to the production method of the heat exchanger. Diffusion bonding has been used in the production of micro-channel heat exchanger, which is the subject of this thesis, because of the precision welding process requirement. In addition, the strength of the weld in the region of diffusion bonding is in some cases as much as the base material.

In printed circuit heat exchangers, micro-channel plates are placed on top of each other to ensure heat transfer between the fluids with counterflow in the channel. When two plates are welded together in order to withstand high pressure and temperature, the strength of the weld area must be either the same or close to the base material. In addition to the fact that traditional welding methods (melt welding, solder, etc.) cannot provide as much strength as diffusion bonding welding, the material pairs that can be

used in traditional welding methods are limited. Not every material can be welded with each other. Material selection possibilities are wider in diffusion bonding method.

The diffusion bonding process, which plays a critical role in the production of heat exchangers mainly due to such advantages, has been developed within the scope of this thesis.

The basis of the diffusion bonding process is explained by the diffusion mechanism. Concentration and concentration changes, which are the basic parameters in the diffusion process, are revealed by Fick's laws. Diffusion takes place on an atomic scale between the materials to be used in diffusion bonding. The diffusion coupling mechanism has been studied in this context. The parameters affecting the diffusion bonding are: temperature, pressure, time, surface quality and atmosphere where diffusion bonding takes place. The parameters optimized in the thesis work are temperature, pressure and time. Surface quality and atmosphere were kept constant in each sample.

316L stainless steel material was chosen for use in heat exchanger design due to reasons such as resistance to high temperature, resistance to high pressure, that is, high strength, cheap and easy availability, and suitability for the diffusion bonding process. For this reason, 316L stainless steel is used in the diffusion bonding process. The properties of 316L stainless steel material are explained in the thesis. In addition to diffusion bonding of 316L-316L material pair, samples using nickel as intermediate material were also examined. The test matrices of the relevant samples were prepared and sample optimization was made. Temperature, pressure and time were used as optimization parameters. 316L-316L and 316L-Ni-316L samples were also tested with destructive and non-destructive examinations using these optimization parameters, and the test results were also compared. Tensile test and microhardness test were performed as tests of samples prepared within the scope of destructive testing. Optical microstructure examinations, SEM and EDS examinations were also carried out within the scope of non-destructive examination. The prepared samples were examined and evaluated.

As a result of the literature search, all samples were prepared under 8.5 MPa pressure and in Argon atmosphere. In the study, first of all, temperature optimization was made. The samples prepared at 950°C and 1050°C were fixed for 60 minutes and compared. As a result of the temperature optimization, it was observed that the samples prepared at 950°C and 60 minutes failed the tensile tests. In the second optimization phase, the temperature was kept constant at 1050°C and the optimization was made for 120 and 180 minutes and the results were evaluated. It has been seen in tensile tests, 316L-Ni-316L diffusion bonding sample produced at 1050°C for 180 minutes, under 8.5 MPa pressure and argon atmosphere gave the best results. In the tensile test, the maximum tensile stress was measured as 407 MPa.

As a result of the development of the diffusion bonding process, a printed circuit heat exchanger (PCHE) was produced by using the sample parameters that gave the best results as a result of the tensile tests. The heat exchanger was tested in a test bench installed at 80 bar, 453°C. The parameters have been measured. It has been seen that it meets the technical requirements in terms of performance. In addition, the hydrostatic test of the heat exchanger was carried out at 200 bar at room temperature using water as a fluid, and the leak test was carried out under 10 bar pressure at room temperature by blowing air into the heat exchanger and foaming the outside with a special solution. The heat exchanger has successfully passed these tests as well.

Thus, the diffusion bonding process developed for the designed printed circuit heat exchanger (PCHE) was successfully carried out.

Keywords: *Supercritical CO_2, sCO_2, Diffusion, Diffusion Bonding, PCHE, Heat Exchanger, Diffusion Bonding Mechanism, 316L, Tensile Tests, Microstructure, SEM-EDS*

BASKILI DEVRE ISI DEĞİŞTİRİCİ ÜRETİMİ İÇİN METAL ALAŞIMLARININ DİFÜZYON BAĞLAMA SÜREÇLERİNİN GELİŞTİRİLMESİ

ÖZET

Karbondioksitin kritik nokta yani kritik basınç ve kritik sıcaklık üzerindeki faz durumuna süper kritik CO2 (sCO_2) denir. sCO_2'nin kritik noktadaki yoğunluğu, sıvıların kritik noktadaki yoğunluğundan fazla olması sebebi ile kompresördeki pompalama gücünün büyük ölçüde azaltılmasına olanak sağlamakta, dolayısıyla termal-elektrik enerji dönüşümü verimliliğini arttırmaktadır.

sCO_2 çevrimi yüksek güç yoğunluğu sağlaması, yüksek verimliliğe sahip olması, kompakt ve modüler yapıda olması gibi sebeplerden ötürü atık ısı geri kazanım sistemlerinde, havadan bağımsız tahrik sistemlerinde çok büyük potansiyele sahiptir.

sCO_2 çevriminde bir ısı eşanjörünün kullanılabilmesi için yüksek basınca ve sıcaklığa dayanıklı kompakt bir eşanjör geliştirilmelidir. Bu gereksinimleri karşılayacak bir ısı değiştirici geliştirmek için karmaşık geometrilerde uygulanabilen, baz malzeme kadar mukavemet sağlayan, korozyon direnci yüksek kaynak metodu olan difüzyon bağlama işlemi öne çıkmaktadır. sCO_2'nin yüksek basınç ve yüksek sıcaklık gereksinimlerini karşılayabilen ısı değiştiriciler baskılı devre ısı değiştiriciler (PCHE) tipi ısı değiştiriciler olduğundan dolayı, baskılı devre ısı değiştiricilerin üretiminde, tez kapsamında geliştirilen difüzyon bağlama metodu kullanılmıştır.

Isı değiştiriciler iki akışkanın ısı enerjilerinin sıcaklığı yüksek akışkandan sıcaklığı düşük akışkana geçmesini sağlayan ekipmanlardır. Bazı kullanım alanlarında ısı değiştirici tasarımlarının kompakt olması, yüksek basınca ve yüksek sıcaklığa dayanıklı olması büyük önem arz etmektedir. Baskılı devre ısı değiştiriciler (Printed Circuit Heax Exchanger-PCHE) bu şartları sağlayan ısı değiştirici çeşitlerinden biri olması nedeniyle ön plana çıkmaktadır. Bu tip ısı değiştiricilerin kompakt olması, yüksek basınca ve sıcaklığa dayanıklı olması, ısı değiştiricinin üretim yöntemiyle doğrudan alakalıdır. Difüzyon bağlama bu tezin konusu olan mikro kanallı ısı değiştirici üretiminde hassas kaynaklama işlemi gerekliliğinden kullanılmıştır. Ayrıca, difüzyon bağlamanın olduğu bölgedeki kaynağın mukavameti, bazı durumlarda baz malzeme kadar olmaktadır Bu sebeplerden ötürü, difüzyon bağlama metodunun geliştirilmesi ve baskılı devre ısı değiştirici (PCHE) üretiminde difüzyon bağlama methodunun kullanılması, teknik isterlere uygun ısı değiştiricinin geliştirilmesinde kritik rol oynamaktadır.

Baskılı devre ısı değişticilerde mikro kanallı plakalar üst üste yerleştirilerek, kanaldaki ters akışla akışkanlar arasındaki ısı transferi sağlanmış olur. Yüksek basınç ve sıcaklığa dayanabilmesi için iki plaka birbirine kaynatıldığında, kaynak bölgesinin mukavemetinin baz malzemeyle ya aynı ya da yakın mukavemetli olması gerekliliği

ortaya çıkmaktadır. Geleneksel kaynak yöntemleri (eritme kaynağı, lehim vb.) difüzyon bağlama kaynağı kadar mukavemet sağlayamamasının yanı sıra, geleneksel kaynak yöntemlerinde kullanılabilecek malzeme çiftleri limitlidir. Her malzeme birbiriyle kaynak yapılamamaktadır. Difüzyon bağlama metodunda malzeme seçim olanağı daha geniştir.

Temelde bunun gibi avantajlarından ötürü, ısı değiştirici üretiminde kritik rol oynayan difüzyon bağlama prosesi bu tez kapsamında geliştirilmiştir.

Difüzyon bağlama prosesisinin temeli difüzyon mekanizmasıyla açıklanmaktadır. Difüzyon prosesinde temel parametreler olan, konsantrasyon ve konsantrasyon değişimleri Fick kanunları ile ortaya konmuştur. Difüzyon bağlamada kullanılacak malzemeler arasında atomik ölçekte difüzyon gerçekleşmektedir. Difüzyon bağlama mekanizması bu bağlamda incelenmiştir. Difüzyon bağlamaya etki eden parametreler şunlardır: sıcaklık, basınç, zaman, yüzey kalitesi ve difüzyon bağlamanın gerçekleştiği atmosferdir. Tez çalışmasında optimize edilen parametreler sıcaklık, basınç ve zamandır. Yüzey kalitesi ve atmosfer her numunede sabit tutulmuştur.

Yüksek sıcaklığa dayanıklılığı, yüksek basınca dayanıklılığı yani yüksek mukavetli olması, ucuz ve rahat bulunabilirliği, difüzyon bağlama prosesi için uygunluğu gibi nedenlerden ötürü 316L paslanmaz çelik malzemesi, ısı değiştirici tasarımında kullanılmak üzere seçilmiştir. Bu sebeple difüzyon bağlama prosesinde 316L paslanmaz çelik kullanılmıştır. 316L paslanmaz çelik malzemesinin özellikleri tez kapsamında açıklanmıştır. 316L-316L malzeme çiftinin difüzyon bağlamasının yanı sıra ara malzeme olarak nikel kullanılan numuneler de incelenmiştir. İlgili numunelerinin test matrisleri hazırlanıp, numune optimizasyonu yapılmıştır. Optimizasyon parametreleri olarak sıcaklık, basınç ve süre kullanılmıştır. 316L-316L ve 316L-Ni-316L numuneleri de bu optimizasyon parametreleri kullanılarak tahribatlı ve tahribatsız muayenelerle test edilmiştir ve test sonuçlarının karşılaştırılması da yapılmıştır. Çekme testi ve mikrosertlik testi tahribatlı muayene kapsamında hazırlanan numunelerin testleri olarak yapılmıştır. Optik mikroyapı incelemeleri, SEM ve EDS incelemeleri de tahribatsız muayene kapsamında yapılmıştır. Hazırlanan numuneler incelenmiş ve değerlendirilmiştir.

Literatür araştırması sonucunda bütün numuneler 8.5 MPa basınç altında ve Argon atmosferinde hazırlanmıştır. Çalışmada öncelikle sıcaklık optimizasyonu yapılmıştır. 950°C ve 1050°C'de hazırlanan numuneler 60 dakika süre ile sabitlenerek karşılaştırma yapılmıştır. Sıcaklık optimizasyonun sonucunda, 950°C ve 60 dakikada hazırlanan numunelerin çekme testlerinde başarısız olduğu görülmüştür. İkinci optimizasyon safhasında ise sıcaklık 1050°C'de sabit tutularak 120 ve 180 dakika sürelerde optimizasyon yapılmıştır ve sonuçlar değerlendirilmiştir. Çekme testlerinde görülmüştür, 1050°C'de, 180 dakika süre ile, 8.5 MPa basınç ve argon atmosferi altında üretilen 316L-Ni-316L difüzyon bağlama numunesi en iyi sonucu vermiştir. Çekme testinde maksimum çekme gerilmesi 407 MPa, olarak ölçülmüştür.

Difüzyon bağlama prosesi geliştirme çalışmaları sonucunda çekme testleri sonucunda en iyi sonucu veren numune parametreleri kullanılarak baskılı devre ısı değiştirici (PCHE) üretimi yapılmıştır. Isı değiştirici 80 bar, 453°C'de kurulan test bremzesinde test edilmiştir. Parametreler ölçülmüştür. Performans olarak teknik gereklilikleri sağladığı görülmüştür. Ayrıca, ısı değiştiricinin hidrostatik testi akışkan olarak su kullanularak oda sıcaklığında 200 barda, sızıntı testi ise ısı değiştirici içerisine hava basılarak, dış tarafına da özel bir solüsyonla köpürtülerek yine oda sıcaklığında 10 bar basınç altında gerçekleştirilmiştir. Isı değiştirici bu testlerden de başarılıyla geçmiştir.

Böylelikle tasarlanan baskılı devre ısı değiştirici (PCHE) için geliştirilen difüzyon bağlama prosesi başarıyla gerçekleştirilmiştir.

Anahtar kelimeler: *Süperkritik CO_2, sCO_2, Difüzyon, Difüzyon Bağlama, PCHE, Isı Değiştirici, Difüzyon Bağlama Mekanizması, 316L, Çekme Testleri, Mikroyapı, SEM-EDS*

1. INTRODUCTION

Heat exchangers are equipment that allows energy to be exchanged between two fluids. In some cases, heat exchangers are required to be compact and resistant to high pressures and temperatures. Micro-channel, printed circuit heat exchangers stand out as the heat exchanger type that meets these technical requirements among the heat exchangers in the market.

Due to the complex and sensitive geometry of micro-channel printed circuit heat exchangers, their production is difficult compared to other types of heat exchangers. Welding micro channels to each other is a very arduous task with traditional welding methods. Diffusion bonding method is seen as a reasonable production type to be used in the production of this type of heat exchanger.

Diffusion bonding methodology and the diffusion bonding process required for the production of a printed circuit heat exchanger (PCHE) were carried out. First of all, it is explained why the diffusion bonding process needs to be developed within the scope of this thesis. It has been mentioned what a printed circuit heat exchanger (PCHE) is and what it is used for. It is also mentioned in the analytical design criteria. In the other stage, diffusion is mentioned in general in order to examine the diffusion bonding process in a more micro dimension. Then, diffusion bonding mechanism, diffusion bonding parameters, comparison of diffusion bonding with other welding methods, inspection methods in which the quality of diffusion bonding is controlled, areas and materials where diffusion bonding is applied, equipment where diffusion bonding is performed, and national diffusion bonding studies and potentials are explained.

1.1 Printed Circuit Heat Exchanger

The aim of the development of the diffusion bonding process, which is the main subject of the thesis, is to ensure that the printed circuit heat exchangers meet the desired technical requirements. These requirements was explained in this chapter.

1.1.1 Introduction of PCHE

Heat exchangers are devices that provide heat exchange between fluids at different temperatures. An example sCO_2 Brayton cycle waste heat recovery system in which compact heat exchangers will be used is given in Figure 1.1. There are two compact heat exchangers in the cycle, the recuperator and the cooler. In the scope of the thesis, the development process of the diffusion bonding process to be used in the production of the recuperator through which the sCO_2 fluid passes in the supercritical phase is explained. The working principle of the system and the task of compact heat exchangers in the cycle are explained below.

Exhaust gas from the waste heat source passes through a heat exchanger as shown in Figure 1.1 and transfers its heat to sCO_2 at high pressure. The CO_2 gas, whose temperature rises with the exhaust gas heat, is expanded in a turbine and its energy is converted into shaft power. This shaft power is used to generate electricity with the help of an alternator. Thus, useful electrical energy is produced from waste heat.

The heat recovery cycle has been determined as the cycle model to be used in the waste heat recovery system. In this cycle, the heat of the high temperature fluid exiting the turbine is transferred to the fluid exiting the compressor in the heat exchanger, thereby increasing the overall cycle efficiency.

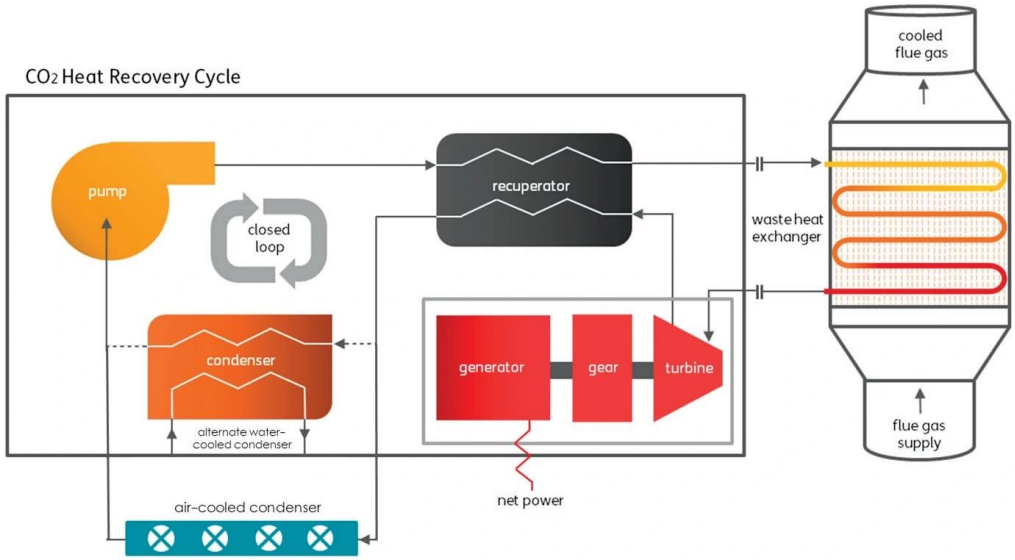

Figure 1.1 : Waste Heat Recovery System Cycle Model Schematic Illustration.

Printed circuit heat exchangers are produced by diffusion bonding of thin metal plates with channels opened by chemical etching techniques. Parts are welded using a binder material in the commonly used heat exchangers. Thanks to chemical etching, channels of very small diameters can be opened, and thanks to diffusion bonding, a seamless weld is obtained by connecting the metal layers to each other in a cellular structure at a temperature below the melting point. In this way, extremely compact heat exchangers that can easily operate at high temperatures and pressures are obtained. Because almost no thermal resistance is formed, it does not adversely affect the strength of the material, and no blockage is observed in the channels thanks to the use of binders (such as solder). Due to these advantages, micro-channel printed circuit heat exchangers produced by diffusion bonding method are used in many areas such as fuel cell systems, chemical reaction processes, marine and terrestrial facilities, cooling and air conditioning, and their usage areas are constantly expanding [1].

The operating pressures, temperatures, materials of manufacture, corrosion resistance, compactness, flow capability and working fluids of compact heat exchangers are given in Table 1.1. The number of heat exchangers that are both very compact and capable of operating under high temperature and pressure that is few. The heat exchangers that stand out in Table 1.1 as such heat exchangers are; brazed fin plate, fin-plate, diffusion bonded printed circuit board and Marbond. Brazed finned plate heat exchangers can operate at lower temperature and lower pressure than heat exchangers manufactured by diffusion bonding. Because there are many difficulties in brazed manufacturing that can withstand high temperature and high pressure. In diffusion bonding, the material is connected to each other in a cellular structure and becomes monolithic. All of the above-mentioned that indicated in Table 1.1 heat exchangers have high corrosion resistance and have a wide range of working fluid options.

The diffusion bonding process is actually a different soldering method. Since the method used in the diffusion bonding process is very different from traditional soldering, it has a special place in the literature as a welding method. From this perspective, printed circuit heat exchangers produced by diffusion bonding can also be compared with brazed-fin plate heat exchangers. From this point of view, diffusion bonded heat exchangers rise to much higher pressure values than brazed-fin plate heat exchangers.

Table 1.1 : Working Conditions of Compact and Comparision Heat Exchangers [2-5].

Type of Heat Exchanger	Properties						
	Compactness (m2/m3)	**Fluid**	**Material**	**Temperature Interval (°C)**	**Pressure (bar)**	**Corrosion Resistance**	**Multi Fluid**
Packinox Plate	≤300	Gases, Liquids, Two Phases fluid	Stainless Steel, Titanium	<300	32	Good	No
Spiral	≤200	Liquid-Liquid, Two Phases fluid	Stainless Steel, Titanium	<400	25	Good	No
Brazed Fin-Plate	800 – 1500	Gases, Liquids, Two Phases fluid	Aluminium, Stainless Steel, Nickel Alloys	From Cryogenic to 650	90	Good	Yes
Plate-Fin	700 – 800	Gases, Liquids, Two Phases fluid	Titanium, Stainless Steel	<500	>200	Excellent	Yes
Diffusion Bonded Printed Circuit	200 - 5000	Gases, Liquids, Two Phases fluid	Stainless Steel, Nickel Alloys, Titanium	-200 ile 900	>400	Excellent	Yes
Polymer	450	Gas-Liquid	Polyvinylidene difluoride Polypropylene	≤150	6	Excellent	No
Body Plate	-	Liquids	Stainless Steel, Titanium	≤350	70	Good	No
Marbond	≤10000	Gases, Liquids, Two Phases fluid	Stainless Steel, Nickel Alloys, Titanium	-200 ile 900	>900	Excellent	Yes

1.1.2 Analytical design of PCHE

The thermal capacity of the designed heat exchanger was determined as 25 kW. During the determination of this value, the costs of the heat exchanger and the test setup were taken into account.

After determining the 25 kW recuperator capacity, the sCO_2 power generation cycle thermodynamic model was created and the cycle suitable for 25kW recuperator capacity was designed. As a result of these studies, the recuperator inlet and outlet pressure and temperature values and fluid mass flow rates were determined. These boundary conditions provided input to the computer aided design and simulations. The technical requirements of the heat exchanger are shared in Table 1.2.

Table 1.2 : Technical Requirements and Boundary Conditions of PCHE.

Parameters	Requirements
PCHE Thermal Capacity	25 kW
Efficiency	≥ 0.90
Printed Circuit Heat Exchanger Compactness	> 850 m^2/m^3
Cold Side Fluid	Water
Cold Side Fluid Inlet Temperature	63°C
Cold Side Fluid Outlet Temperature	323°C
Cold Side Fluid Inlet Pressure	200 bar
Cold Side Fluid Outlet Pressure	199 bar
Hot Side Fluid	sCO_2
Hot Side Fluid Inlet Temperature	453°C
Hot Side Fluid Outlet Temperature	87°C
Hot Side Fluid Inlet Pressure	79.2 bar
Hot Side Fluid Outlet Pressure	78.2 bar
Mass Flow of CO_2	0.06 kg/s

PCHE is designed for sCO_2 fluid for both side. However, due to technical issues, water was used in hydrostatic, leakage and performance tests. Showing that one side works for sCO_2 will be proof that both sides will work with the same fluid.

In this context, some correlations and equations are used. In Figure 1.2 [3], a graphic explanation of the equation which is indicated in equation 1.1 used as a basis for the heat exchanger analytical design can be found. A heat exchanger was designed by making detailed fluid mechanics and heat convection calculations.

$$Q = U * A * \Delta T \tag{1.1}$$

In equation (1.1) where, Q represents heat flow rate that unit is Watt (W), U is overall heat transfer coefficient that unit is $W/m^2.K$, A indicates heat flow area that unit is metersquare (m^2) and ΔT shows temperature differences that unit is Kelvin (K). Here,

overall heat transfer coefficient is pretty important parameter in terms of computing capacity of heat exchanger.

Figure 1.2 also shows that formula of overall heat transfer coefficient and explain how heat transfer occur among three material.

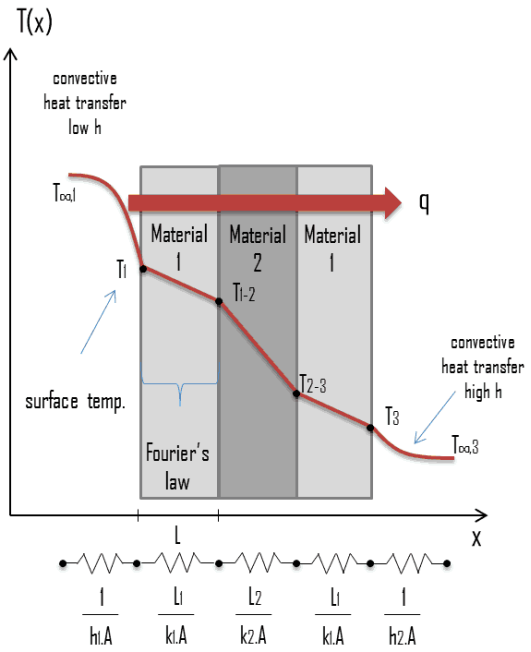

Figure 1.2 : Explanation of Heat Transfer and Overall Heat Transfer Equation [3].

$$Q = U * \Delta T = \frac{(T\infty,1)-(T\infty,3))}{\left(\frac{1}{h1}\right)+\left(\frac{L1}{k1}\right)+\left(\frac{L2}{k2}\right)+\left(\frac{L1}{k1}\right)+\left(\frac{1}{h2}\right)} \quad (1.2)$$

In equation (1.2) that has relation with Figure 1.2, the h parameter represents the heat convection. The parameter k is the heat conduction coefficient. L is the thickness of the material between the two materials that will conduct heat. For the heat exchanger, this thickness is very low (1.5 mm). The h values for the heat exchanger were found by making in-depth calculations on fluid mechanics and heat transfer. The values of these found heat convection coefficients are considerably larger than the heat conduction coefficient. Even though the changes in the microstructure due to diffusion bonding reduce the heat transfer coefficients of 316L and Nickel approximately 16 times from the values in the literature [4], the performance of the heat exchanger is only affected by 10% capacity loss from this change. Calculations were made by adding 20% safety factor and the heat exchanger was designed with this safety factor. In this case, even the decrease in the heat transfer coefficient of 16 times has guaranteed that the heat exchanger capacity will remain within the technical

requirements. For these reasons, the heat transfer coefficients of the materials were not taken into account while making the heat exchanger analytical calculation. Therefore, it was not necessary to measure the heat transfer conduction coefficients of the samples.

Hydrostatic testing requirements are contained in ASME Sec VIII Div1 2015, UG-99 [5]. According to this code, the pressure vessel hydrostatic test pressure should be at least as much as the value calculated below at each point.

$$Ph = 1{,}3 \times MAWP \times LSR \tag{1.3}$$

$$LSR = \frac{S_{test}}{S_{design}} \tag{1.4}$$

In the above equations, LSR is obtained by dividing the maximum allowable stress of the pressure vessel material at test temperature (S_{test}) by the maximum allowable stress at design temperature (S_{design}). MAWP represents the maximum allowable working pressure. As stated in MAWP ASME Code Case 2766, the hydrostatic pressure value for plate heat exchangers pressure vessel can be taken as the design pressure of the heat exchanger in calculations not to take in to account pressure vessel. The variation of the maximum allowable stress value with temperature for SS316/316L material is given in the at Figure 1.3 below. The maximum allowable stress value is 138 MPa at test conditions (20 °C) and 108 MPa at design temperature (500 °C).

2010 SECTION II, PART D (METRIC)

TABLE 1A (CONT'D)
SECTION I; SECTION III, CLASSES 2 AND 3;* SECTION VIII, DIVISION 1; AND SECTION XII
MAXIMUM ALLOWABLE STRESS VALUES *S* FOR FERROUS MATERIALS
(*See Maximum Temperature Limits for Restrictions on Class)

Line No.	Maximum Allowable Stress, MPa (Multiply by 1000 to Obtain kPa), for Metal Temperature, °C, Not Exceeding														
	–30 to 40	65	100	125	150	200	250	300	325	350	375	400	425	450	475
20	138	138	138	138	138	134	126	119	116	114	112	111	110	108	108

Figure 1.3 : ASME SS316/316L Material Maximum Allowable Stress Variation with Temperature [5].

Diffusion bonding should provide tensile strength at room temperature. Temperature extrapolation was calculated using the ASME standard. This makes it unnecessary to perform a tensile test at the operating temperature of the heat exchanger. With the ASME formulation, the maximum pressure the heat exchanger should have at that

temperature was calculated. The calculated value is below the technical requirement. Since it is not the subject of the thesis, it was thought that more details were not needed.

The printed circuit heat exchanger channel geometries determined according to the conditions mentioned above are given in the Table 1.3 below.

Table 1.3 : Channel Geometry.

Channel Width	1 mm
Channel Depth	0.5 mm
Wall Thickness	1.5 mm
Fin Thickness	0.7 mm
Plate Thickness	2 mm

1.1.3 CFD analysis of PCHE

CFD analyzes were carried out to determine the pressure drop values at the inlet and outlet ports of the heat exchanger. In these analyzes, the section from the connection points of the inlet and outlet ports of the heat exchanger to the heat exchanger core region was examined for sCO_2 and water. The flow control volume drawn for the analyzes is given in Figure 1.4 and the mesh structure is given in Figure 1.5. Half of the port geometry is modeled symmetrically as the control volume

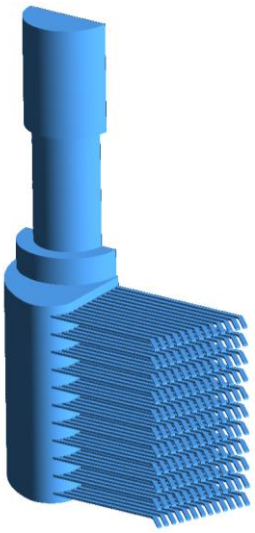

Figure 1.4 : Symmetrical Port Control Volume Prepared For Pressure Drop Analysis.

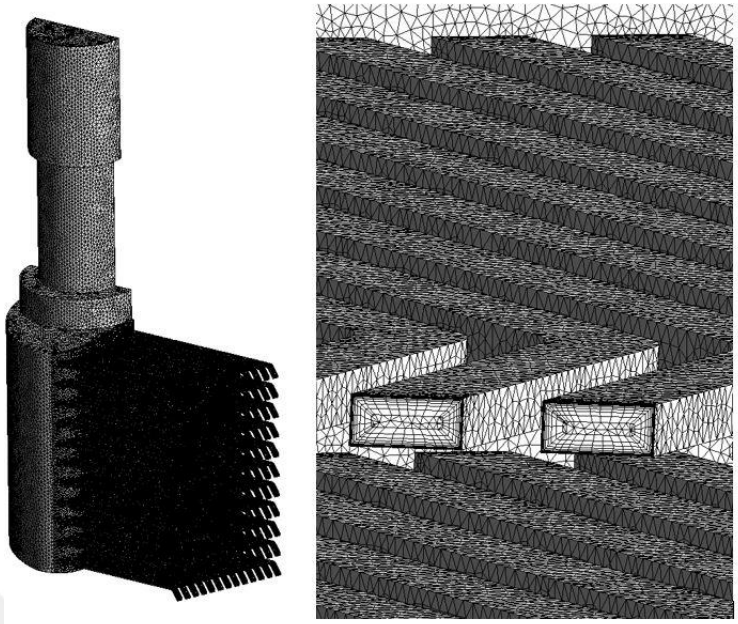

Figure 1.5 : Symmetrical Port Network Structure Prepared For Pressure Drop Analysis.

There are 6.6 million nodes and 14.5 million elements in the prepared fluid mesh structure. Boundary conditions used in heat exchanger channel analyzes were used in the analyses. In the analyzes for water, the inlet and outlet ports were analyzed together, and for gas, the inlet and outlet ports were analyzed separately because the temperatures were different at the inlet and outlet. The results obtained in the analyzes are given in Table 1.4 below.

Table 1.4 : Pressure Drop CFD Analysis Results.

Fluid	**Pressure Drop (Bar)**
Water	0.48
sCO_2 -Inlet-Hot	0.0569
sCO_2 -Outlet-Cold	0.0116
Total sCO_2	0.0685

In the analysis results, a very low pressure drop value was observed on the sCO_2 gas side. Due to the low viscosity and low velocity of the gas, the pressure drop is low. The average velocity of the hot fluid in the channel at the inlet of sCO_2 gas in the

channel is 7.81 m/s at the exit and the average speed of the cold fluid in the channel is 1.68 m/s. On the water side, a higher pressure drop occurred due to the high viscosity and density of water compared to sCO_2 gas. The average water flow rate in the channel is 3.88 m/s. Most of the pressure drop on the water side is due to the sudden contraction at the channel entrance and the sudden expansion at the channel exit. The pressure drop and pressure distribution from the water side inlet to the outlet are given in Figure 15 below and the pressure distribution on the middle section is given in Figure 1.6. The pressure drop of the gas side hot fluid sCO_2 inlet port is given in Figure 1.7, and the pressure distribution in the middle section is given in Figure 1.8. The pressure drop of the gas side cold fluid sCO_2 outlet port is given in Figure 1.9, the pressure distribution in the middle section is given in Figure 1.10.

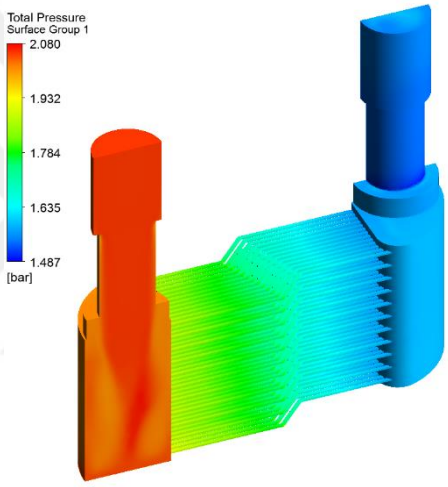

Figure 1.6 : Pressure Distribution From Water Inlet to Outlet.

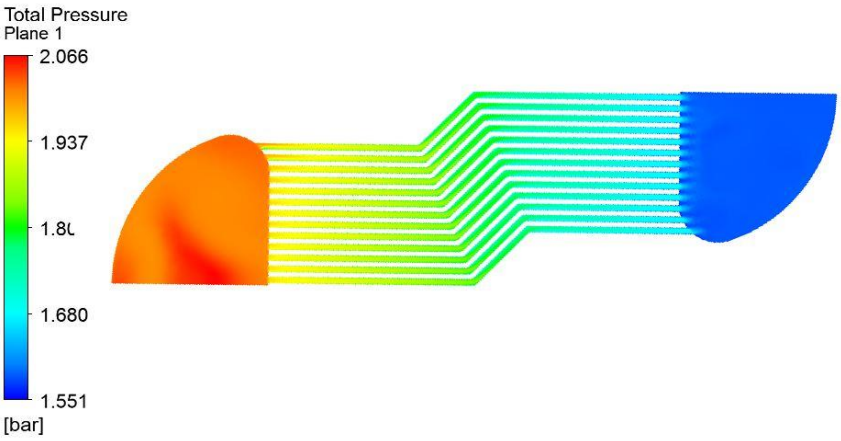

Figure 1.7 : Water Mid Section Pressure Distribution.

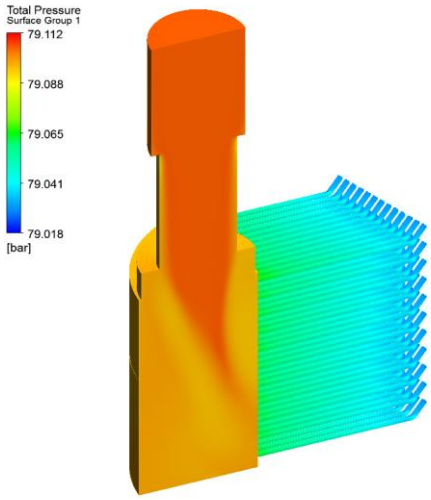

Figure 1.8 : sCO_2 Gas İnlet Port Pressure Distribution.

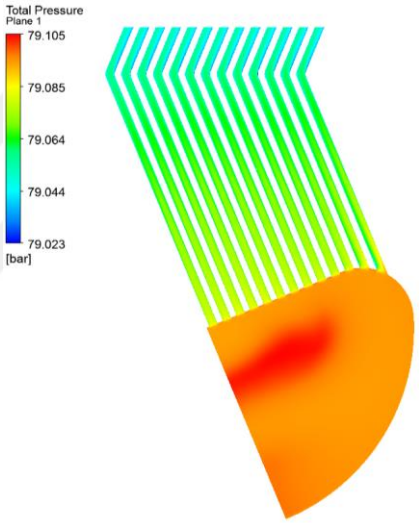

Figure 1.9 : sCO_2 Hot Mid Section Pressure Distribution.

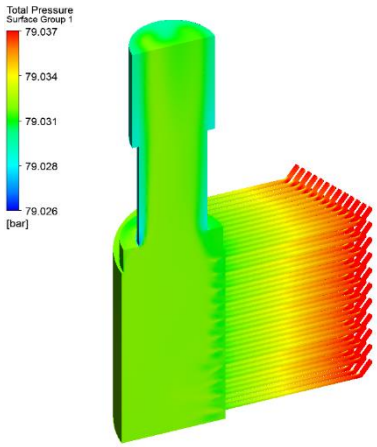

Figure 1.10 : sCO_2 Cold Outlet Port Pressure Distribution.

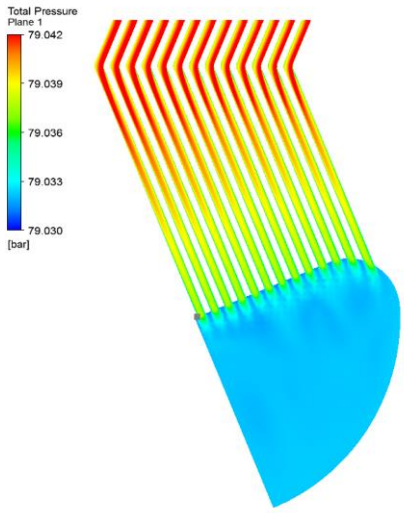

Figure 1.11 : sCO_2 Cold Middle Section Pressure Distribution.

As a result of the analysis, the total pressure drop on the water side, including the channels from the inlet to the outlet, was determined as 2.024 bar and 0.16 bar on the sCO_2 side.

Semi-circular channel geometry, which is one of the first designs, was used in the geometry used in the analyzes where temperature distributions were simulated. As a result of iterations, this rectangular shaped channel has evolved into geometry. Since this geometry change will have a minor effect on the temperature distribution profile, it was not necessary to repeat the analyzes.

As a result of the temperature distribution, it is clearly seen that the heat distribution is under the influence of the incoming fluid. In the region where the hot fluid enters, high temperature values are read, and in the region where the cold fluid heats up, low temperature values are read. The general operating characteristics of counter-flow heat exchangers are clearly visible. Similar to the temperature profile on the solid material, it is seen that the distribution of the hot and cold fluid changes according to the temperature difference.

When the CFD analyzes to see the pressure drops are examined, it is seen that the pressure drops are very low. When this situation is examined in the sCO2 cycle, the low pressure drop becomes even more important. The reason is that the presence of equipment with low pressure drop in the cycle will cause the pump used to consume lower power. In this case, the efficiency of the cycle will also increase

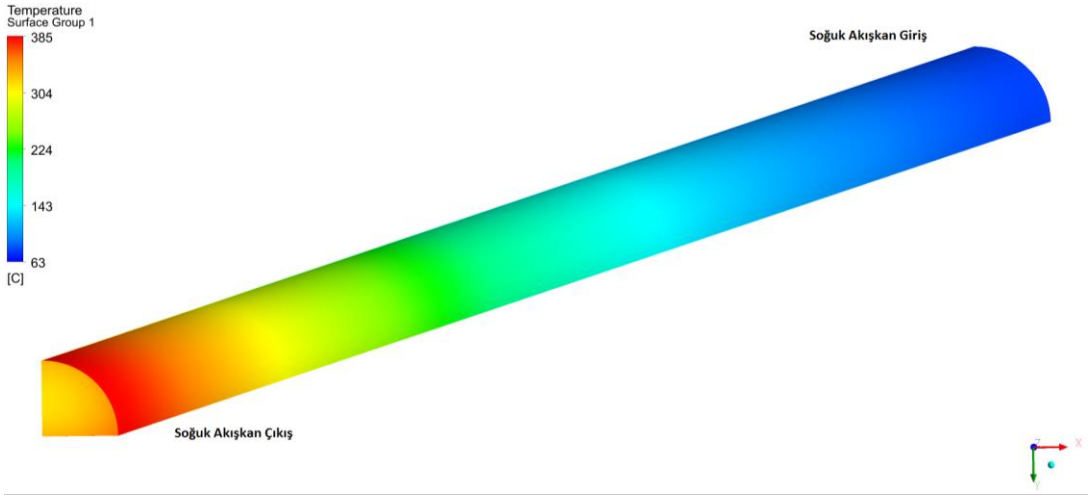

Figure 1.12 : Cold Channel Temperature Distribution.

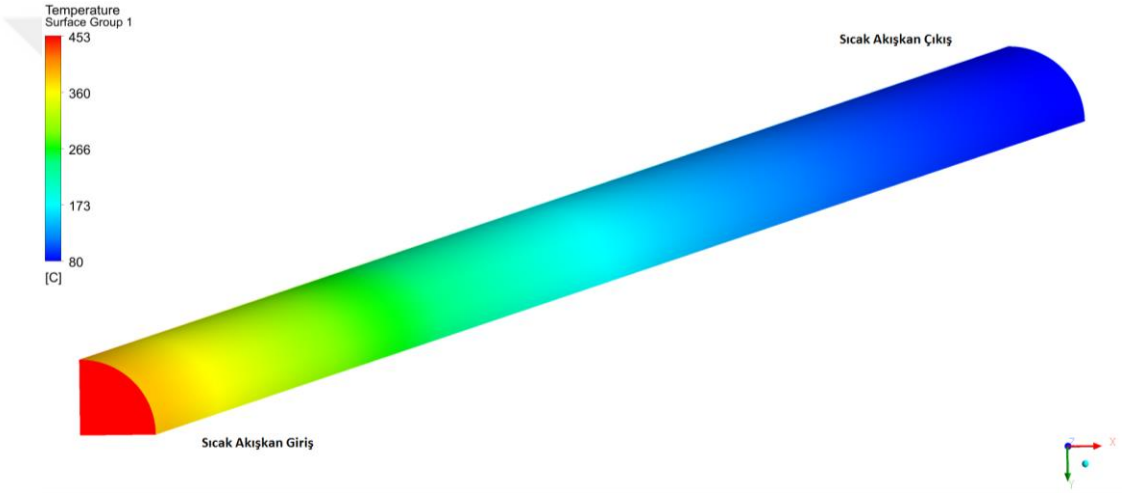

Figure 1.13 : Hot Channel Temperature Distribution.

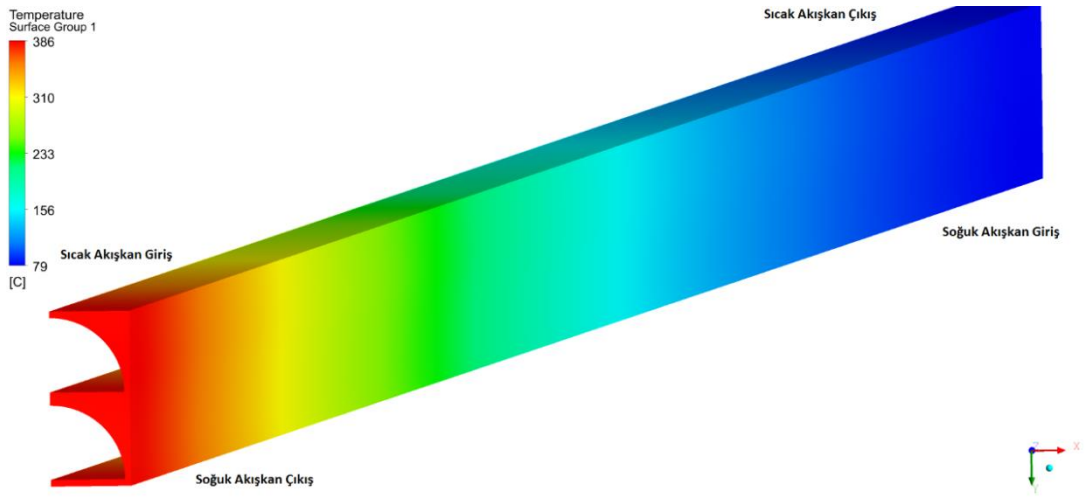

Figure 1.14 : Temperature Distribution On Solid Material.

As shared in Figure 1.12 ,it is seen that the temperature of the cold fluid increases regularly from the inlet to the outlet. It is seen that it normally occurs in the solid interface region where the heat is transferred in the exit region to its highest value. As the temperature profile increases towards the solid contact surface in the free flow region in the pipe, this increase rate increases especially in the contact region.

It is observed that the temperature of the hot fluid decreases regularly from the inlet to the outlet as shared in Figure 1.13. It is seen that it normally occurs in the solid interface region where the heat is transferred in the exit region to its lowest value. As the temperature profile decreases towards the solid contact surface in the free flow region in the pipe, this decrease rate increases especially in the contact region.

It is seen that the inlet fluids dominate on the solid material. It is seen that the temperature of the solid material increases in the region where the hot fluid is located, and the temperature decreases in the region where the cold fluid exits as shown at Figure 1.14.

1.1.4 FEM (Finite Elements Methods) analysis of PCHE

Structural analyzes of the inter-channel which are the most critical area of the micro-channel heat exchanger, were carried out using the finite element method. In these studies, firstly, thermal analysis was carried out to determine the temperature distributions on the parts. Stress distributions were determined by using temperature distributions obtained in thermal analysis as load in structural analysis.

Details of the geometric structure of the micro-channel heat exchanger channel, of which the critical design was carried out, were given in Table 1.3.

The geometric representation of the boundary conditions used in the evaluation of the thermomechanical stress levels of the heat exchanger channel is shared in Figure 1.15. In addition, according to Figure 1.15, thermal analysis boundary conditions information is shared in Table 1.5, and structural analysis boundary conditions information is shared in Table 1.6. Structural and thermal analyzes were carried out in 2D and the number of channels in the form of 2x2, 4x4 and 8x8 were evaluated. This evaluation was carried out in order to determine how much the number of channels considered affects the results.

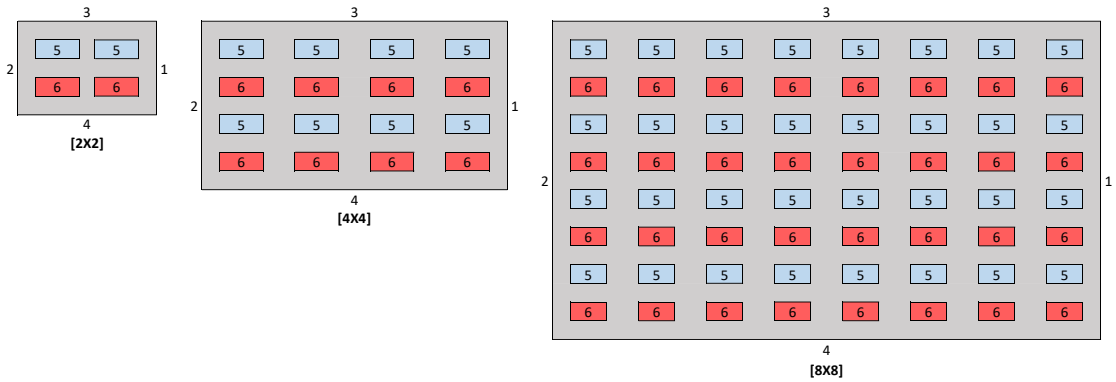

Figure 1.15 : Channel Geometry Analysis Boundary Conditions Geometric Representation.

Table 1.5 : Channel Geometry Thermal Analysis Boundary Conditions.

Boundary Condition	Hydrostatic Test	Design
1, 2	Simetry	Simetry
3, 4	Lineer Periyodic	Lineer Periyodic
5	22°C	324.336°C
6	22°C	453°C

Table 1.6 : Channel Geometry Structural Analysis Boundary Conditions.

Boundary Condition	Hydrostatic Test	Design
1	Simetry	Simetry
2	Free	Free
3, 4	Lineer Periyodic	Lineer Periyodic
5	200bar	80bar
6	1bar	1bar

0.08mm element is used in the thermal and structural analysis mesh structure. In order to be more sensitive in the results on the channel walls, the mesh structure has been made more sensitive at the rate of 1/10. The geometry and details of the created mesh structure are shared in Figure 1.16 and Table 1.7.

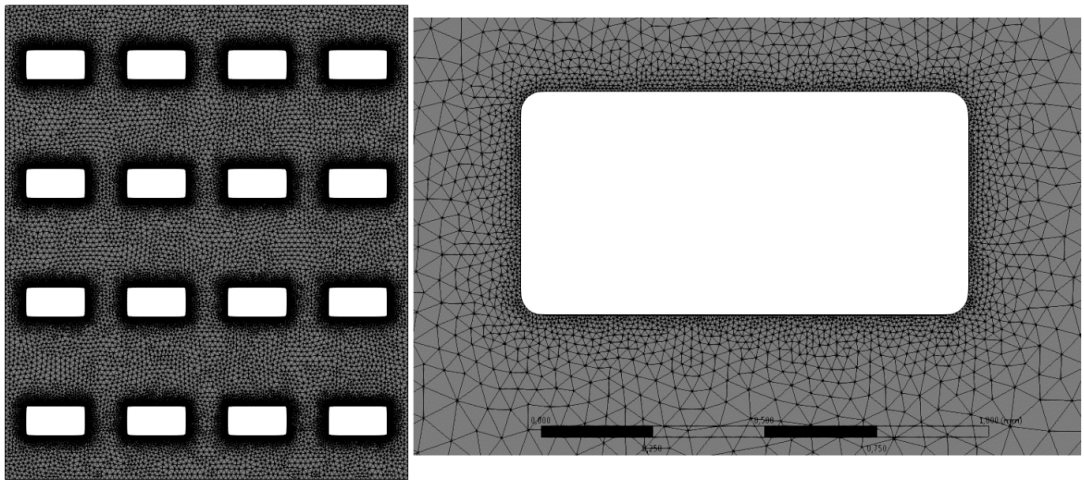

Figure 1.16 : Mesh Structure.

Table 1.7 : Channel Geometry Network Structure Details.

Cells	Element Type	Number of Nodes	Element Number
2x2	Triangular	43.715	21.034
4x4	Triangular	173.487	83.644
8x8	Triangular	705.097	340.526

After the thermal analysis, the temperature distributions on the channel are shared in Figure 1.17.

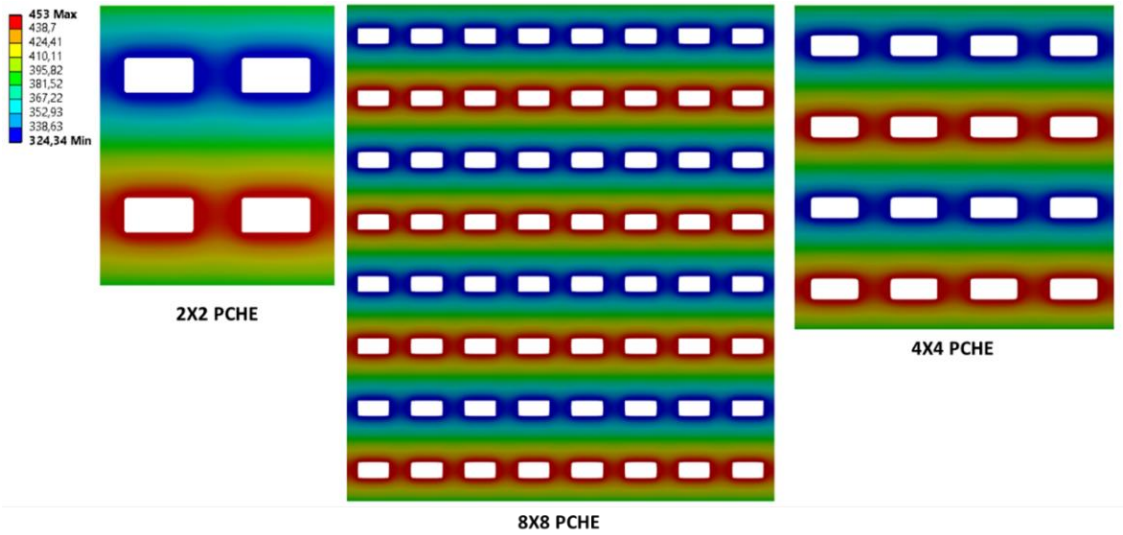

Figure 1.17 : Temperature Distribution as a result of Thermal Analysis [°C].

After the thermal analysis, the temperature distributions on the channel were taken as the thermal load, and the boundary conditions and pressure values shared in Figure 1.15, and Table 1.6 were applied for all conditions and cells. As a result of the analyses, the stress distributions were obtained depending on the distance with the path shared in Figure 1.18, schematically. In addition, it was seen as a result of the analysis that the number of channels did not affect the results.

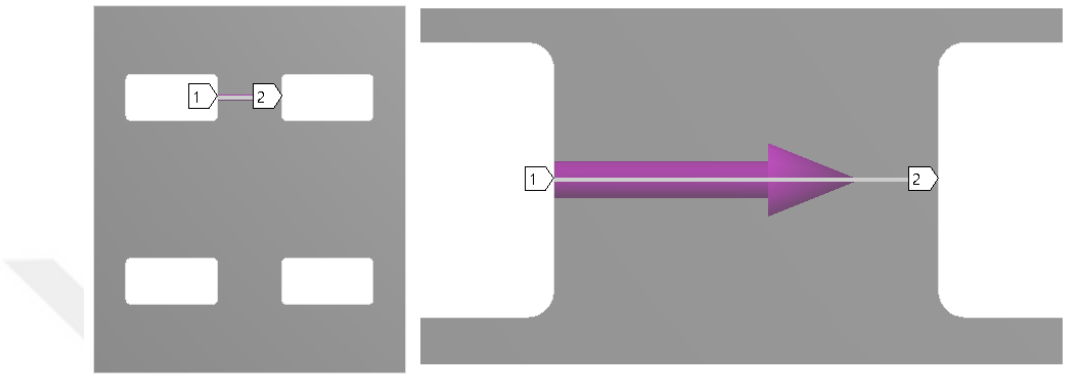

Figure 1.18 : Schematic Representation of Stress Distribution on a Channel Wall.

It has been seen by the structural analyzes that the duct stress is maximum 84 MPa for the hydrostatic test to be carried out under 200 bar pressure at room temperature. The allowable safety stress of 316L is 138 MPa at room temperature. This value is well below 84 MPa. This shows that the design is safe for hydrostatic testing.

Likewise, it was seen again with the structural analyzes that the channel stress is a maximum of 75 MPa at the design temperature (500°C) and at the design pressure (80 bar). The allowable safety stress of 316L is 107 MPa at 500°C. This value is also below 75 MPa. This shows that the design is safe for the working conditions of the heat exchanger. [6]

1.2 Diffusion

It is known that vibration levels increase when atoms in equilibrium are heated. Sometimes these vibrational levels become so intense that atoms begin to shift. The movement of atoms from one place to another is defined as diffusion in solids. Diffusion mechanisms are in four groups and their details are shared in Table 1.8.

Table 1.8 : Diffusion Mechanism [7].

Diffusion Mechanism	Explanation	Mechanism Layout
Interstitial Mechanism	It is the movement that occurs towards the spaces in the arrangement of atoms. Here, the atom first moved to space 2. Afterwards, it moved to spaces 3, 4, 5 and 6, respectively. However, this diffusion process requires large amounts of energy. Therefore, this mechanism can only occur in heterodiffusion of atoms smaller than the atoms of the base metal.	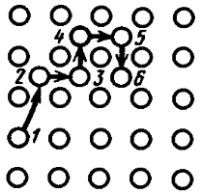
Vacancy (Substitutional) Mechanism	The jumping of an atom into a vacant position in an adjacent position is called the vacancy mechanism. Here, atoms are replaced by spaces. With spaces, atoms exhibit a reverse motion.	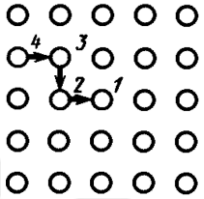
Mutual Displacement Mechanism	There can be exchanges between two adjacent atoms. This requires the expenditure of a large amount of energy, because each atom must be moved a distance of two atomic diameters. In addition, the lattice must be disrupted locally in order for the mechanism to occur.	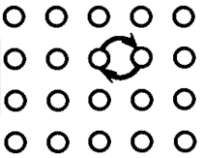
Ring Mechanism	In the 1940s, it was claimed that the ring mechanism was too difficult due to distortion and the Kirkendall effect. In 1950, Zeger suggested that diffusion would be possible without too much warping, as a result of three or four atoms being displaced in a circular order instead of two atoms being interchanged.	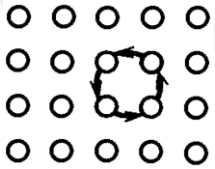

Diffusion in solids is divided into three groups as “volumetric diffusion”, “grain boundary diffusion” and “surface diffusion”. Volumetric diffusion is diffusion in a crystal lattice. It takes a lot of energy for this to happen. Grain boundary diffusion is the diffusion that occurs in faulty regions of materials at the atomic level. Grain boundary diffusion is much faster than volumetric diffusion because it is in the form of atom flow into the spaces. The energy required for grain boundary diffusion is half that required for volumetric diffusion [8]. Atoms on a metal surface have weaker bonds compared to their positions in the lattice. Therefore, the energy requirement in surface diffusion is even lower than in grain boundary diffusion. The activation energy required for diffusion activation can be summarized as follows:

$$\Delta Q_{\text{surface diffusion}} < \Delta Q_{\text{grain diffusion}} < \Delta Q_{\text{volumetric diffusion}}$$

Although volumetric diffusion is much slower than surface diffusion, the diffusion of matter is much greater. That is, it is inversely proportional to the energy requirement. This is because the diffusion cross section in surface and grain boundary diffusions is quite small compared to volumetric diffusion. So the total volume is much larger in volumetric diffusion.

Two laws, I.Fick's Law and II.Fick's Law, have been established to determine the amount of diffusing material in the diffusion mechanism. In I.Fick's law, it is possible to determine the amount of diffusing material passing through a fixed section a. Here, concentration differences cause the particles to move in a certain direction. The mathematical expression for what is known as I.Fick's law is shared below:

$$J_A = -D\left(\frac{dc}{dx}\right) \tag{1.4}$$

Where equation 1.4; $\frac{dc}{dx}$: concentration gradient, J : flux (m is the displacement of the metal mass t perpendicular to this plane from surface A in time t), D : diffusion coefficient. If the concentration gradient dc/dx is a nonzero value, a diffusion rate exists. If the dc/dx activation energy is equal to zero (0), there is no concentration change. The flux continues until the concentration is homogeneous in the material [9].

If there is no steady state in a diffusion event, for example, in cases where it is difficult to determine the mass flow at a constant concentration difference, I.Fick's law is insufficient. For this reason, II.Fick's law is used to determine the diffusion coefficient. While transforming I.Fick's law into II.Fick's law, a volume element limited to two parallel surfaces with a distance of dx is used [9]. Since the concentration will thus remain dependent on x and t, the following expression can be used for most cases:

$$dc/dt = D\left(\frac{d^2c}{dx^2}\right) \tag{1.5}$$

Applying some boundary conditions for this equation, the following expression is obtained:

$$\frac{(Cx-Co)}{(Cs-Co)} = 1 - erf\left(\frac{x}{2\sqrt{Dt}}\right) \tag{1.6}$$

Where equation 1.5 and 1.6; Cs : concentration at the surface Cx : density of a point at a distance x from the surface or cross section Co : the initial density of one of the diffusion pairs x : The distance from the surface of the point where Cx is measured D : co-diffusion coefficient t : diffusion time erf : error function

The concentration parameters specified in this equation are presented in Figure 1.19 as a concentration profile. Here, the relationship between concentration and diffusion distance is shown.

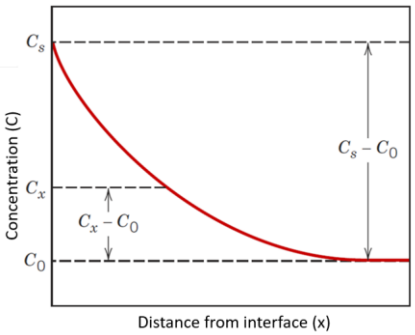

Figure 1.19 : Concentration Profile for Unsteady State Diffusion [10].

In addition, the variation of the diffusion distance with time and position depending on the concentration is also shared in Figure 1.20. “t” represents temperature. As can be seen here, the amount of diffusion within the unit area increases with the increase in temperature [10].

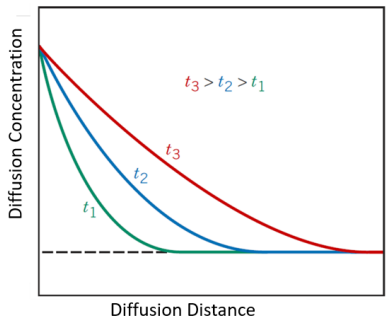

Figure 1.20 : Concentration Profile for Different Temperatures in Unsteady State Diffusion Bonding [10].

1.3 Diffusion Bonding

Welding applications are evaluated in two classes as fusion (melting) and pressurized solid state welding. Compared to fusion welding applications, solid state welding applications require the distance between workpieces to be at atomic scale in order to establish bonds between atoms. However, conditions such as surface geometry, chemical conditions, and physical state prevent atoms from joining together on an atomic scale. In reality, surfaces are not ideally smooth and clean. Even if it is a surface that has been machined with great precision, a surface shows microscopic disturbances

at the height of hundreds or even thousands of molecular layers. So when the two parts are put together, only these broken structures will come into contact. Also, any solid surface holds oxygen atoms that form strong chemical bonds with the surface atoms. The simplest way to remove all these obstacles is offered by fusion welding.

In fusion welding, the parts to be joined are melted at the edges and the absorbed substances are evaporated or melted. These substances are closed into the interatomic distance that is formed spontaneously by forming a welding pool. As the weld pool is cooled (with molten filler metal, if any) it fuses into a single body, forming a permanent joint.

In pressure solid state welding, the parts to be joined are brought together on an atomic scale by plastic deformation in the weld zone. Sometimes the mating surfaces are cleaned by vacuum, reducing atmosphere (oxygen-free environment), or autoclave cleaners. Full strength coupling is achieved through physical contact, chemical bonds between atoms on the workpiece surface (metallic, ionic, covalent or combination thereof) and volumetric transformations.

Pressure solid state welding can be subdivided into many subsections, such as resistance welding, pressurized gas welding, diffusion bonding, friction welding, ultrasonic bonding, explosion welding, and stored energy welding.

As the name suggests, diffusion bonding involves the diffusion of atoms across the interface at the solid surface of the weld and sometimes in the liquid state (when a molten interstitial material is used). The applied bonding pressure (or press load) causes the edges to move within the range of atomic forces. If there is a molten intermediate layer, the determining factor is the press load that removes the intermediate layer from the joint zone. Press load is applied until all the intermediate layer is combined.

Diffusion bonding is a solid state welding method. This welding method is based on solid state diffusion. Diffusion is the migration of atoms from high-energy regions to low-energy regions in order to reduce the free energy (chemical potential difference) of the material. Diffusion in the material begins to accelerate at the recrystallization temperature. Temperature, time, diffusing medium and potential difference are the main parameters affecting diffusion. These parameters, therefore, also affect diffusion

bonding. It can be briefly listed the mechanisms of diffusion bonding as follows; plastic deformation, creep, diffusion and recrystallization [11].

Sometimes, the diffusion bonding may be referred to as a pressure combiner, auto vacuum welding, thermo compression welding, solid state welding, or solid phase welding. This can cause confusion in understanding the essence and mechanism of the diffusion bonding. In order to eliminate these confusions, many definitions have been made since the first applications of this process. However following definiton is accepted as definition of “Diffusion Bonding”;

"Diffusion bonding of materials in solid state is a process for making a monolithic joint through the formation of bonds at atomic level, as a result of closure of the mating surfaces due to local plastic deformation at elevated temperature which aids interdiffusion at the surface layers of the materials being joined." [12].

Diffusion bonding is a very economical process. It does not contain any expensive solder, special wires or special electrodes, fluids and shielding gases. Moreover, no further processing is required afterwards. Therefore, there is no additional material loss and no processing requirement. A diffusion bonded product does not normally gain weight as it would with welded or brazed components. The properties of the base metals in the weld zone remain almost as they are. Therefore, there is no need for any heat treatment after joining. The amount of energy required for diffusion bonding is, for example, between one-fourth and one-sixth of that required for resistance welding.

The environmental advantages of diffusion bonding are that the working environment is high hygienic standards and free from ultraviolet radiation, harmful gas emissions, metal spatter and finely divided dust.

A major limitation of the diffusion bonding process is the time spent vacuuming the vacuum chamber and preparing the parts for assembly. Currently, studies are continuing to eliminate this situation and it is thought that a solution will be found in a short time.

Recently, diffusion bonding has gone beyond its application to materials that can be joined by conventional welding and vacuum brazing, and has been applied to many small and large workpieces, competing with existing diffusion welding and brazing processes. Diffusion bonding is an application that is expected to gain more and more importance with the increasing use of alloy steels, special alloys, non-metallic and

composite materials. It is envisaged that there will be a two-way development for diffusion bonding. First, further perfecting the diffusion bonding technique and procedure, improving heating methods, press load transfer and mechanical components. The second is to reveal the potential of this application in much more critical materials and application areas.

1.3.1 Diffusion bonding mechanism

The success of the diffusion bonding process is ensured by three variables that need constant monitoring and careful adjustment. These variables are bonding temperature, bonding pressure (or compressive load) and dwelling time (applied pressure time)

The bonding temperature should be between 50 and 80% of the melting point of the metal that has lowest melting temperature in the bonding [12]. High temperature helps the diffusion of atoms to each other across the weld interface and this aids in surface deformation (crushing surface imperfections).

The bonding pressure or pressure load must ensure a tight contact between the surfaces of the parts. The pressure value should assist the deformation of the surface imperfections and be sufficient to fill the gaps in the bonding area. If the pressure is not sufficient, all the cavities on the surface will be left unfilled and the strength of the joint area will be adversely affected. The pressing load disperses the oxide films, creating a clean surface and facilitating the diffusion process.

The dwelling time at a given bonding temperature and bonding pressure should often be kept to a minimum due to physical and economic considerations. Dwelling time should be sufficient for a close contact to be established and for diffusion processes to take place. Excessive time can leave voids in the bonding zone, change the chemical composition of the metal, or cause the formation of brittle intermetallic phases (in the case of bonding dissimilar metals or alloys).

The vacuum in the bonding zone is usually maintained at 10^{-1} – 10^{-3} Pa. Sometimes, inert gas (dry argon or dry helium with a dew point below 216 K), hydrogen, or various gas mixtures may be present in the environment inside the furnace [13]

For the bonding area to be tough, there must be good surface contact, the edges must be smooth and fit snugly against each other. Soft metals such as aluminum, magnesium, tin and gold require surface treatments before diffusion bonding so that

their surface roughness is not over 40 – 80 μm. Hard alloys, heat-resistant metals, high-temperature alloys, tool steels and non-metals require a more thorough surface coating. In such cases, the roughness on the surface should be 2.5 μm and below [13].

In order for an adequate diffusion bonding/welding to be made, mechanical proximity must be ensured in metal-to-metal contact and obstructive surface forms must be levelled. In a diffusion bonding, it is a three-step process as shared in Figure 1.21.

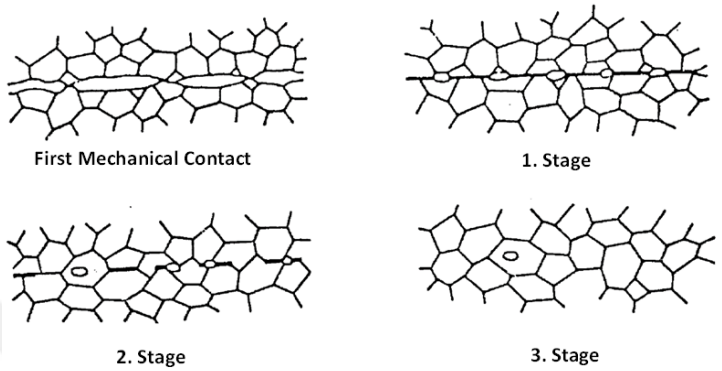

Figure 1.21 : Diffusion Bonding Mechanism [13].

In order to form a bond by diffusion, the junction surfaces must be as close as a few A (1 angstrom=1x10 $^{-10}$ meters). However, the height of the best surface roughnesses that can be obtained even with precision manufacturing methods applied in the industry is more than 100 A. In this case, when the surfaces touch, some of the protrusions come into contact only in a very limited area.

In addition, oxide film layers with a thickness ranging from 10 to 1000 A are formed on the surface of the parts. This oxide layer is dissolved by the base material by applying heat to the environment. In addition, these oxide film layers are broken by the pressure applied to the surfaces and are pushed out of the bonding surface in the further steps of the diffusion bonding. The application of pressure to the surfaces also provides several A level convergence.

1.3.2 Parameters effecting on diffusion bonding

The parameters affecting the diffusion bonding are temperature, pressure load, time, surface conditions and working atmosphere.

1.3.2.1 Temperature

In the diffusion bonding process, temperature is an important parameter as it affects deformation, oxide solubility, allotropic transformations, recrystallization, diffusion and the process in a short time. When the temperature of a material is increased, the diffusion coefficient (D) and the flux of atoms (J) increase. At high temperatures, it becomes easier to exceed the activation energy required for the diffusion of atoms. This is because the strength of the main materials decreases with the increase in temperature. Thus, both the plastic deformation in the first stage and the creep of surface roughnesses are facilitated. In this way, it is faster to obtain the contact area required for bonding. In industry, the temperature value used for diffusion bonding is $0.5TE < TD < 0.8TE$. Here, TE is the melting temperature of the base materials, and TD is the temperature at which the diffusion bonding process is performed [12]. It is necessary to determine the temperature at which the diffusion bonding process takes place, taking into account the applied pressure load, in a way that does not impair the microstructure of the base material. Choosing this temperature as high as possible will both increase the quality of the bonding and enable the process to take place faster [14].

In practice, the temperature value used in diffusion bonding should be applied as high, constant and homogeneous as possible. In addition, the speed of heating and cooling is one of the parameters that highly affect the quality of the bonding. In the literature, it has been stated that the diffusion rate doubles with every 20°C increase in temperature. The application of higher temperatures than necessary during bonding causes grain coarsening and a decrease in material strength [15].

1.3.2.2 Pressure load

The pressure load is necessary to ensure a tight contact between the parts. The pressure load depends on the diffusion bonding temperature to be applied, the mechanical properties of the materials to be bonded and the degree of forming required. In practice, the upper limit of the pressure load is determined as the yield strength of the main materials at the bonding temperature. During assembly-bonding, this pressure load can be applied hydraulically, pneumatically or mechanically [15].

The pressure load applied during joining-bonding affects in the following ways:

- It breaks the insoluble surface oxides and increases the metal-to-metal contact area.
- By bringing the surfaces to be joined closer to each other at the distance between atoms, it activates the force of attraction between atoms.
- It creates a chemical potential difference for diffusion.
- It helps plastic deformation of surface roughness [16].

In addition, the following points should be considered so that the pressure load to be applied in practice does not cause negative effects:

- The compressive load to be applied is large enough to increase the creep rate and plastic deformation of the surface roughnesses; It should be chosen small enough not to cause microscopic deformation of the parts to be joined.
- The pressure load should be kept below the yield strength of the parts to minimize the plastic volume deformation of the parts to be joined.
- The rate at which the compressive load is applied has no effect on bonding deformation or strength [17].

In the studies carried out, successful trials have been made at pressures ranging from 0.007 to 4000 MPa, but it has been stated that pressures between 7-21 MPa are sufficient [18]. It has been stated that in the case of joining dissimilar metals, the choice of pressure load should be determined according to the weakest of the two materials [12].

1.3.2.3 Processing time

The duration of the bonding is an indirect parameter; It is related to temperature, pressure load and type of joint. Time is inversely proportional to pressure and temperature. The time required for each material or pair of materials can vary from a few seconds to several hours. If the surface to be joined is dirty and processing is carried out at low temperatures, the diffusion bonding time should be increased [19]. On the other hand, long duration increases the cost of the process, triggers the formation of cavities in the joint area, the change of composition and the formation of intermetallic compounds, thus causing negativities that deteriorate the mechanical properties of the joint. As a result; Sufficient time for diffusion bonding is the time period in which fusion can be achieved by ensuring mutual contact on the surfaces, sufficient for the movement of atoms and holding at this stage [15]. It has been

determined that prolonging the bonding time at constant pressure load and temperature can increase the bond strength up to a point. This situation is shared in Figure 1.22 [17].

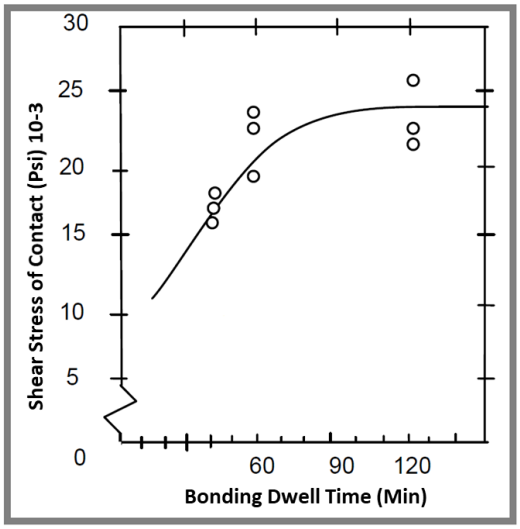

Figure 1.22 : Relationship Between Contact Shear Strength and Bonding Dwelling Time [17].

It has been determined that metallurgical effects do not have much effect on the bonding time. Keeping the bonding time short in industrial applications is important in terms of economy [18].

The time spent in diffusion bonding consists of two phases. The first stage is the maturation (incubation) process. At this stage, the contact area between the surfaces increases and extreme deformation zones occur. In the second phase, recrystallization events with intense creep are dominant, in which shear and grain boundary migration are observed [16].

1.3.2.4 Surface conditions

In diffusion bonding, the surface conditions of the materials to be joined are very important in terms of ensuring contact between the two metals and therefore quality bonding [20]. Surface conditions affecting the quality of diffusion bonding are surface roughness, surface films and surface spacing. Roughnesses affect the time it takes to reach full contact between surfaces. In diffusion bonding, especially long wavelength surface roughnesses are important. Because in this case, both a multi-directional pressure load is required and a long time will be needed to eliminate the gaps. Surface roughness is the main cause of post-bonding residual pores. In addition, the oxide

layers prevent the contact of the surfaces to be bonded, delay the bond formation and prevent the grain boundary diffusion in the intermediate section, causing the formation of gaps. It has the same effect as oxide films at intervals such as oil, grease, dust. Chemical etching and acid cleaning methods are used to remove oxide film layers [15].

Although a metal surface has been prepared with care, there are various foreign materials. The states of these substances in the surface layers are represented in Figure 1.23. Plastic deformation does not occur in the region indicated by A and represents the main material. B represents the base metal layer found together with the oxide layers. C indicates the oxide layer. D is the layer where oxygen ions are absorbed. E represents the layer of water molecules, F represents the oil molecules and finally G represents the ionized dust particles [12].

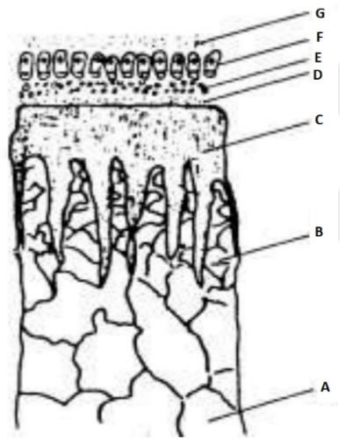

Figure 1.23 : Cross section of layers of a metal surface [12].

The residues on the metal surface are two parts: oxide film layers, which are quite fragile, and organic or inorganic layers such as oil, grease, dust. Residues such as oil, dust, and even fingerprints have more or less the same effect as oxide films. Therefore, it must be removed from the surface before bonding. Chemical etching and acid cleaning methods are used to remove oxide films. Other residues are removed by washing and drying at temperatures up to 300°C.

In reality, the negative effect of the foreign material layers on the surface at the source is not just the creation of a physical barrier. The attraction forces between atoms interact as follows: Atoms on the surface want to share their electrons with other atoms. However, when surfaces are dirty, these surface soils become saturated by sharing electrons with atoms of the metal. Thus, the surface attraction forces (surface energies) on the surface are reduced. It has been shown that even a half-atom layer of

oxygen greatly reduces the adhesion force [21]. All metals except gold are covered with an oxide film at room temperature. Oxide layers seen in steels are 0.04 – 0.05 μm thick [12]. It has the ability to dissolve iron and zirconium surface dirt. The time taken for the formation of a certain film thickness in various metals is shared in Table 1.9 [21], [12].

Table 1.9 : Oxide Film Formation Times and Film Thickness in Some Metals [21], [12].

Metal	Film Thickness, [μm]	Time, [second]
Copper	$3x10^{-3}$	30
Aluminium	$12x10^{-4}$	15
Iron	$2x10^{-3}$	40
Molibdenium	$2x10^{-3}$ - $3x10^{-3}$	40
Germanyum	$2x10^{-3}$ - $3x10^{-3}$	80

Degreasing is a general part of the surface cleaning process. Alcohol, trichloroethylene, acetone, clarifiers and many other cleaning agents can be used. Generally recommended degreasing techniques are complex and involve gradual pickling and rinsing in various solvents. As some of these cleaners are toxic, precautions should be taken for safety when used. Vacuum heating can also be used to achieve clean surfaces. The usefulness of this method is highly dependent on the nature of the films on the surface and the type of metal. Organic, aqueous or gaseous adsorbed layers can be easily removed by high temperature vacuum heat transfer. It is possible to dissolve oxides attached to some metals at high temperature. Some materials such as zirconium, titanium, tantalum, colombium are examples [22]. The result is well-bonded surfaces with surfaces that are better prepared and protected at lower temperature and pressure.

1.3.2.5 Environment/atmosphere

During diffusion bonding, a protective atmosphere should be used to avoid oxide film layers at the part surfaces and at the interface. For this reason, the process is carried out under vacuum or in an inert gas atmosphere. Although there are situations where satisfactory results can be obtained in normal atmosphere with metals with unstable or high oxygen solubility oxides, these are very few.

Argon, helium and nitrogen gas can be used as inert gas. Although hydrogen gas is used to reduce the amount of oxygen, it causes hydrate formation in titanium, zirconium, hafnium, niobium and tantalum alloys. For this reason, it is necessary to be careful when using hydrogen. Since inert gases reduce the effect of oxygen in the atmosphere only to a certain degree, vacuum is used for metals with stable oxides. Vacuum can dissolve oxide films at approximately $1.3x10^{-3}$ Pa levels. However, in practice vacuum levels of $1.3x10^{-5}$ Pa are preferred. During the vacuum, the bonding interfaces of the part are protected from oxidation, and the foreign materials on the surface are also dissolved. Studies have shown that the joints made in vacuum provide better strength than the joints made under the protection of inert gases that are not sufficiently pure, even if the vacuum is not very high [17]. Gas percentages corresponding to various vacuum degrees are given in Table 1.10 [23].

Table 1.10 : Gas Content Per Unit Volume at Certain Pressures [23].

Pressure [Pa]	**Total [%]**	**O_2 [%]**	**N_2 [%]**
101080	100	20.1	79.9
133	0.13	0.03	0.1
13.3	0.013	0.003	0.01
1.3	0.0013	0.0003	0.001
0.13	0.00013	0.00003	0.0001

Despite its advantages, vacuum can be expensive, especially the initial investment cost of the vacuum medium is high. A satisfactory diffusion bonding can be achieved by good use of shielding gas environments and by the right methods. It has been proven that in some cases, it is possible to bond small parts with considerable fast without protection [8], [17], [18].

1.3.3 Application of diffusion bonding

Diffusion bonding offers many advantages over other welding methods. Due to these advantages, the fields where diffusion bonding is used are general engineering, aerospace, nuclear, electronics, defense and energy sectors.

It is used in general engineering because it does not have disadvantages such as the formation of brittle intermediate metal structures in existing welding technologies. At the same time, the production of geometric shapes (hollow, closed wall, etc.) with very complex shapes, for which production is insufficient with applications such as casting and forging, becomes possible with diffusion bonding technology. In addition, with this capability, it becomes more possible to apply high-strength coating technologies.

Diffusion bonding enables the production of cheaper, more efficient, lighter and easier to design parts in the aerospace field. In the aviation industry, diffusion bonding is used instead of butt-face or overlap-shaped joints by forging and traditional welding methods [24].

Large-scale companies such as Northrop, Rockvel, Douglas Aircraft are used in the production of F 15 missile nests from titanium alloys, explosion nozzles for bombers, the main landing tailgate of T38 aircraft, wind blades by diffusion bonding and super plastic forming using 1000 – 5000 tons presses have made gains in term of cost [25], [26].

The purpose of diffusion bonding in defense industry applications; is to produce structures and elements that cannot be produced more economically and integratedly than other techniques. For example, in welded joints of martensitic structure where the presence of hydrogen is a problem, diffusion bonding is applied instead of conventional welding methods. As presented in Figure 1.24, the points in the window frame that provide cooling for the sensors in the rocket head were produced with the diffusion bonding [27]. It provides great convenience as it can be combined with steel and aluminum diffusion bonding, which is also used in the production of glider type aircraft [28].

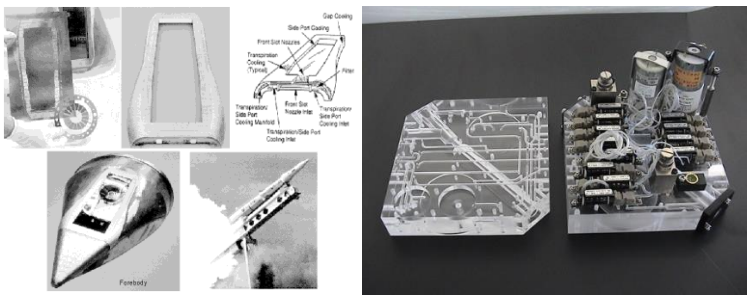

(a) (b)

Figure 1.24 : a) Rocket Head Window Frame Channel Application b) Bio-chip Sample [28].

Electronic circuit manufacturers use many joining techniques in jobs such as connecting the chip to a substrate after producing an integrated circuit from silicon parts, connecting chips and circuits with electrically conductive materials. In the microelectronics industry, diffusion bonding is carried out by using a gold foil as an interlayer for bonding silicon chips to their copper or Ni-Fe-based framework. In addition, diffusion bonding technology provides great convenience and production opportunity, since the main materials in biochip production do not contain free electrons. In addition, the need for interlayer transition possibility for biochips is made possible by diffusion bonding of multiple layers. As a result, diffusion bonding makes it possible to manufacture complex and nearly smooth inner channels that cannot be produced by conventional fabrication methods. The biochip produced by FUJI denolo company is shared in Figure 1.24 as an example [29].

In order to meet the high pressure and temperature requirements, as a result to increase efficiency in energy and nuclear applications, heat exchangers must meet these requirements. For this, the connection areas of the heat exchangers must have high strength at high temperatures. The regions joined by diffusion bonding can meet this need because they are very close to the strength of the main materials, and in some cases the same strength. In this way, with high efficiency energy conversion systems, the same powers can be obtained with compact structures more than 10 times. The size and weight comparison of a heat exchanger produced by diffusion bonding method and a heat exchanger produced with current technologies is presented in Figure 1.25 [30].

Figure 1.25 : Comparison of Diffusion Bonding and Traditional Methods in Heat Exchanger Production [30].

1.3.4 Diffusion bonding equipments

Engineering today relies on the use of high-strength and high-temperature steels and alloys and the joining of these materials in a strong, ductile, and corrosion-resistant manner. Diffusion bonding is seen as the most suitable method for such a bonding quality. Specially designed equipment is needed for diffusion bonding.

A wide variety of diffusion bonding equipment has been developed in terms of design and application. In each case, the diffusion bonding equipment must contain all the necessary components to perform the welding and auxiliary operations.

A typical diffusion bonding unit consists of two subunits, an electromechanical and a power source. The function of the electromechanical subunit is to close and empty the process chamber, form, transport and weld the workpieces, perform all the auxiliary operations and control all the steps. Accordingly, the diffusion bonding unit consists of a vacuum chamber, a vacuum pumping system, a system that transmits the movements to the workpiece, an auxiliary component to monitor and control the temperature of the contact area, vacuum and electrical devices. The power supply unit is actually a combination of heating sources. These can be resistant, induction, radiation, lasers, an electron beam, a radiant heater, a flow of electric current, and a combination of these.

The most important distinction of the diffusion bonding unit is the use of vacuum. Even at low vacuum values, the impure content of the atmosphere in the process chamber is lower than the waste content of commercially pure argon. Vacuum, apart from its protective effect, provides a faster and more complete degassing of the materials to be joined and the removal of oxides, dirt and deposits from both the surface and volume of the materials [12].

Since diffusion bonding is a joining method that requires heat and pressure, the joining process; Special equipment designed in accordance with the shape and dimensions of the materials, the atmosphere and temperature required by the process is needed. In most cases, the diffusion bonding device is designed by the user or to meet the user's requirements.

Electrical energy is generally used for the heating process to obtain the junction temperature. Most of the time, electrical energy is passed through resistors to heat the welding chamber. Heating is provided by resistors wrapped around this chamber.

In rare cases, the joining process is carried out by heating the samples in the furnace environment with the prepared special apparatus.

Another heating method is induction. The biggest advantage of using induction is that different winding numbers can be used according to different materials [31].

Another issue as important as obtaining the temperature in diffusion bonding is to control the temperature at constant degrees. In the diffusion bonding method, which requires longer times than other bonding methods, the temperature must remain constant throughout the process.

Various systems are used in the application of the force required to create the bonding pressure. These systems can be counted as mechanical, hydraulic and isostatic systems. Mechanical or hydraulic systems are mostly used for bonding small parts. In the bonding of more complex shaped and large parts, it is difficult to provide equal pressure along the bonding surface. For this reason, isostatic gas pressure systems are generally applied in the bonding of these parts [32].

The working groups of the equipment in which diffusion bonding is carried out are generally presented in Figure 1.26 [12].

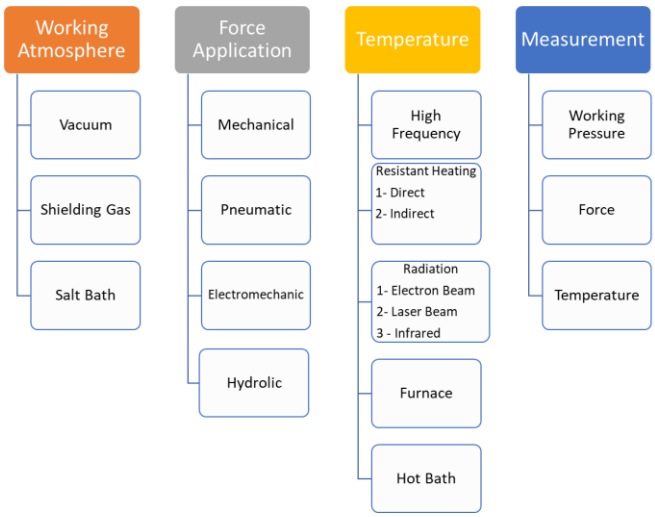

Figure 1.26 : Diffusion Bonding Equipment Working Groups [12].

In isostatic systems, bonding is carried out in a pre-ventilated environment. This method is used in welding processes of easily broken metals or welding processes between metals and ceramic materials. This system also provides superiority by eliminating the compressive stresses in the material [32].

In mechanical and hydraulic systems, suitable presses should be used to provide the relevant pressure for the press load that helps diffusion to take place. Presses should be used in a structure that will meet the requirements not only in terms of load but also in terms of size. The most important thing is that the pressure can be kept constant for a certain period of time. The most important advantage of the press system is the ease of use it provides and the perfect control of production with this system. In the systems where the press is applied, the materials of the molds that apply the press should also be selected according to the application temperature and pressure [12].

In diffusion bonding, the most affecting the quality of the coalescence is the atmospheric environment. For this, as previously stated, applications are made in the under vacuum, shielding gas and salt bath.

In these applications, the aim is to remove the oxide film layers and to eliminate the elements such as dirt, oil and residue on the material surfaces. For this, the isolation of the diffusion bonding atmosphere must be provided very well. Insulation must be provided not only for protective atmosphere and vacuum, but also for temperature. For this reason, bonding parameters such as vacuum and temperature must be constantly monitored. Various adjustment and measurement systems that regulate pressure and temperature cause the diffusion bonding device to have a complex structure [31].

The diffusion bonding process is carried out in units whose general concept is shared in Figure 1.27. The parts (2) to be joined are loaded into a vacuum chamber (1). A vacuum system (3) is used to protect the workpieces against oxidation during assembly. The heat is provided by the induction of the high frequency oscillator (5). The pressing load applied to the workpieces is provided by a hydraulic system (6). When the joining process is completed, the bonding surface is lowered to the determined temperature in the vacuum chamber [33].

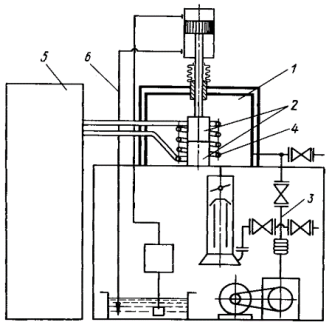

Figure 1.27 : Diffusion Bonding Vacuum Furnace Concept [33].

Since the vacuum process makes diffusion bonding devices very expensive, furnaces in which oxide layers are removed with the help of inert gases are used instead of vacuum. When the quality of diffusion bonding in vacuum and inert gas environments is compared, vacuum environment provides a much higher quality bonding. However, economic factors make it difficult to prefer vacuum outside of mass production. In this case, the preparatory processes required for the bonding surfaces gain more importance. Considering this, diffusion bonding should be performed. The concept of the diffusion bonding device, in which inert gases are used instead of vacuum, is shared in Figure 1.28 [33].

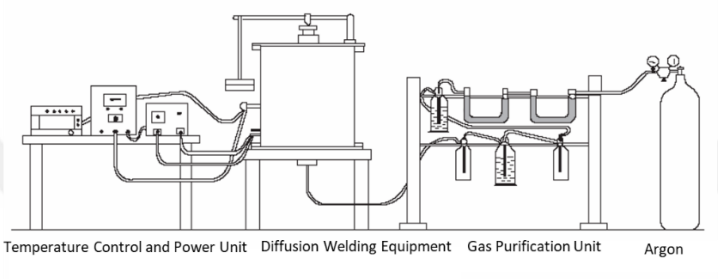

Figure 1.28 : Diffusion Bonding Furnace Concept (Inert Gas) [33].

The use of diffusion bonding is increasing due to the benefits it provides in many areas. For this reason, diffusion bonding furnaces have been produced by many companies in order to make this process suitable for mass production. These companies that make limited production. One of these company is mostly interested in the production of laboratory scale furnaces. Since diffusion bonding furnaces are generally special production furnaces, it is not possible to clearly determine their properties in the form of shelf products. However, we can determine the limits of oven capabilities based on the products produced by the companies. In diffusion bonding furnaces, it is possible to press at levels above 10-3 Pa, at temperatures above 2000°C and up to 4,000 kN. All these parameters should be determined depending on the geometry and material to be applied [33].

1.3.5 Comparison of diffusion bonding with other welding methods

It has many advantages over diffusion bonding, fusion welding and soldering methods. This can be clearly seen from the table presented in Table 1.11 [33].

Table 1.11 : Comparison of Diffusion Bonding with Other Welding Methods [33].

Properties	Fusion Welding	Diffusion Bonding	Soldering
Method of Joint	Source of oxygen and pressure	Pressure (Without Fused)	Fused joint, Pressure and Fused joint
Heating	Local	Local, Bulk	Local, Bulk
Temperature	Melting Temperature of Main Parts	The range of 0.5 – 0.7 times the melting temperature of the main parts.	A temperature above the melting point of the solder
Surface Preparation	Roughly	Detailed	Detailed
Quality of Bonding	Ductile	Precision-bored	Capillary
Materials	Metals ve Alloys	Metals, Alloys, Nonmetallics	Metals, Alloys, Nonmetallics
Different Materials Weldings	Limited	Most of materials	Most of materials
Solidification Fragility	Strong	None	Weak
Porosity	Constriction, air holes	None	Constriction, air holes, diffusion
Overlap by Heat Treatment	No	Limitless	Limited
Basic Connection Types	End to end, Overlay	End to end, Overlay, conical insert, cylindrical, spherical, curvilinear	End to end, Overlay
Product Sensitivity	Low	Very High	High
Vibration Resistance	Low	Very High	High
Corrosion Resistance	Sufficient	Very High	Low
Strength	Strength close to main materials	As strengthful as main materials	Solder filler strength
Air Pollution and Radiation Emission	Yes	No	Yes

The most important feature of diffusion bonding is the high quality of the bonding site. It is the only joining process in which the properties of the main materials are preserved in the metal-metal and non-metal junction zone in monolithic structures. With correctly selected bonding parameters (temperature, press load and time), the material above and adjacent to the joint line will exhibit the same strength and flexibility as the base material. When the process is done in vacuum, the mating surfaces are not only protected from contamination such as oxidation, but the material is cleaned by separating or dissolving the oxides present. Therefore, in a diffusion bonding process, incomplete bonding, oxide residues, cold and hot cracks, gaps-cavities, distortion, loss of alloying elements etc. there are no situations. Since the edges are in full contact with each other, materials such as solder or electrodes are not needed. In terms of strength, ductility, sealing and corrosion resistance, diffusion bonded parts exhibit the same quality as main parts and meet the requirements of the most critical applications. Diffusion bonding has increased service life, quality and reliability by a factor of 10 to 12 for a wide variety of products. It also made it possible to develop new structures by simplifying techniques and procedures, eliminating the scarce and expensive materials. Another important feature of diffusion bonding is the high stability of its mechanical properties. Thus, it does not require quality control of each sample during production, making it possible to provide quality control more quickly with control methods such as sampling.

Diffusion bonding enables very complex shapes to have the same properties as base materials. It is very capable and suitable for situations that cannot be produced by conventional methods or require conventional processes with very high costs. In terms of dimensional tolerances, diffusion bonded products are the same as machined parts, and in some cases even better. Because the diffusion bonding process makes many fasteners redundant, it is less prone to stress-induced corrosion, a very important issue for long-life products. In diffusion bonding, the materials to be joined can range from a few microns (foils thickness) to several meters.

Recently, diffusion bonding theory has been developed and important results have been obtained on forming a monolithic bond between all kinds of inorganic materials without affecting the mechanical properties of the materials. Diffusion bonding is gaining more widespread use with the development of diffusion metallurgy.

One of the very automated bonding method is a diffusion bonding. It can adapt very quickly to the production of complex structures manufactured by rolling, casting or extrusion methods. The basic parameters of diffusion bonding (temperature, pressure head, atmosphere, vacuum and time) are easily programmable. In this way, it can be carried out with almost no human intervention. In addition, the high degree of realization of the diffusion bonding mechanism increases the quality and life of the products, which makes diffusion bonding even more attractive.

Diffusion bonding can be directly coupled to a complex structure. It supports many joining shapes such as end-to-end, overlapping, conical, spherical. For this, only the control of the heat source and the press load to be applied is sufficient.

As a result, this method has several advantages when comparing diffusion bonding with fusion and other solid state welding methods:

• Deformations and pre- and post-annealing requirements in fusion welding are not seen in this method.

• Two metallurgically incompatible metals that are completely different from each other, or a metal and a non-metal can be joined by this method.

• The press load time is independent of the bonding area. Therefore, large-area or complex-shaped connections can be joined at once.

• Undesirable metallurgical structures do not occur in the base materials in the bonding.

• Today, diffusion bonding is the most efficient and effective method for joining ceramics and composites with metals and other materials.

• There is no need for highly qualified operators for the process.

• Diffusion bonding is essentially a diffusion-controlled technique.

• The most important factor in joining ceramics is material brittleness. This means that the use of deformation during joining is not possible. For this reason, diffusion bonding is the only possible method of welding ceramics.

Along with these advantages, the disadvantages of the diffusion bonding method can be listed as follows:

• High hardware cost

• Special environment and apparatus requirement

• Requirement for shielding gas atmosphere or vacuum environment

• Need for very clean and precise surface preparation

• The possibility of formation of interphases, albeit small, with intermetallic compounds at the junction interface

• Sometimes very long times are needed for the bonding process [15].

1.4 Literature Survey

The literature review in this thesis is divided into three. One of them is “Diffusion Bonding”, another one is “Diffusion Bonding Applied Materials” , last subject is “Diffusion Bonded Heat Exchangers”.

1.4.1 Diffusion bonding

The diffusion bonding process is not a new technology. There are some recent studies. In early, diffusion bonding was modeled as solid-state modeling. Grain boundary also affects diffusion bonding performance. One of these studies that has includes these issues, in the late 1980s, colleagues A. F Hill and E. R. Wallach performed solid-state modeling of diffusion bonding. This article describes a theoretical model for diffusion bonding, which proposes a new and simplified cavity geometry. The mechanisms operating during diffusion bonding are based on those derived from pressure sintering studies, but the driving forces and velocity terms for these mechanisms have been modified to allow for quite different geometries of the two processes. Also included in this work is an analysis of the effect of grain size, which may result in an increase contributing to bonding from additional grain boundary diffusion, and therefore may be relevant to the aggregation of particularly fine grain size materials [34]. Materials properties are also significant important for diffusion bonding. One of the most important material of diffusion bonding process is low carbon steel. Therefore, low carbon steels may be relevant with solid state modeling. On top of the previous studies on solid state bonding, a study has been carried out by expanding on low carbon steel. Middle of the 2016, the team of K. Pongmorakot, S. Nambu, Y. Shibuta and T. Koseki carried out this study by solid state bonding of ultra-low carbon steels, hot pressing followed by isothermal retention at low temperatures ranging from 873 to 923 K. They found that the development of interfacial strength consisted of two stages; They

divided them into sections as the first stage, where the increase in interface strength is rapid and significant, and the second stage, where the increase is gradual. The strength development in the first phase took place primarily in the contact zones produced by hot pressing. In the second stage, on the contrary, they interpreted the evolution as due to the increase in contact areas due to the shrinkage of the gaps. In the first step, they did a molecular dynamics simulation to clarify the atomic behavior at the interface. The results revealed that the compression-induced disordered atomic arrangement was rearranged with increasing isothermal retention time, leading to better consistency and increased interfacial strength between contact sites [35]. Surface roughness is important in diffusion bonding. The effect of surface roughness on the formation of grain boundaries has been shown. C. Zhang and his friends conducted research that is named “Role of surface finish on interface grain boundary migration in vacuum diffusion bonding “. The aim of this study was to understand the role of surface finish on interfacial grain boundary migration during vacuum diffusion bonding of stainless steel. The results showed that two types of interfacial grain boundary migration were observed. One was interfacial grain boundary migration at the triple junction; and another was stress-induced interfacial grain boundary migration. Surface finishing had an obvious effect on the behavior of interfacial grain boundary migration. For smoother surface interface, grain boundary migration occurred mainly at triple junctions, while more strain-induced interface grain boundaries were produced for rougher surfaces. Mechanism analysis revealed that higher surface roughness on rougher surfaces is subjected to load and severely deformed, easily leading to inhomogeneous local state. They showed that the deformation on opposite sides of the interface grain boundary, as well as the difference in accumulated stored energies, thus produced more stress-induced interfacial grain boundary migration. In addition, the shear strength of the joint is consistent with the interfacial grain boundary migration rate, and higher interfacial grain boundary migration rate results in a higher shear strength of the joint [36]. Besides the surface roughness, the most important factor affecting the diffusion bonding is how much the diffusion between the materials will take place. For this reason, material selection is very important in diffusion bonding. 316L and Ni are popular materials due to their cheapness, high temperature and pressure resistance, and machinability. The study of 316L used as the interface material of the base material Ni should be considered in this context. In the past, some studies have been done on the 316L stainless steel as base material and Ni as interfacial

material used in this study in the context of diffusion bonding. One of these studies is Zi-Liang An et al., in their study named "High Temperature Performance of 316L-SS Joint Produced by Diffusion Bonding", basically investigated the diffusion bonding performance of 316L-SS steel under high temperature. Two types of bonding samples, with and without Ni foil interlayer between 316L–SS bar, were prepared by diffusion bonding for 1 hour under 10MPa uniaxial pressure in the temperature range of 850-1050°C. The relationship between bonding parameters and high temperature tensile strength of joints was investigated. Based on the test results, optimized processing parameters are suggested. It was stated in the study that the addition of the intermediate layer could decrease the room temperature strength but increase the high temperature strength. This was attributed to the conversion of Fe0.64Ni0.36 formed in the bonding process to FeNi3 at high temperature by Zi-Liang An et al [37]. Diffusion bonding has also been used in various micro-machines. Diffusion bonding method has been investigated with very different materials according to the usage area. Z.D. Wang, N.S. Pradeep and T. Takeda, colleagues, conducted research on micro heat exchangers, micro reactors and micro fuel cell systems, composite structures with laminar functional plates Usual fusion welding can hardly meet the joining requirement of micro-machines due to its limited efficiency and low precision. Diffusion bonding, on the other hand, may be a desirable technique for joining laminar plates. Its effectiveness, fast adhesion and small distortion have been successfully proven in various bonds of similar and dissimilar metals [38]–[40]. To date, there is limited open literature on the high temperature mechanical properties of diffusion bonding. In diffusion bonding, the bonding rate and the change in strength depending on temperature should also be examined. Much of the work by H. Nishi, and P. Weimar colleagues has focused on bonding parameters and their relationship to room temperature strength and bonding ratio [40], [41].

1.4.1.1 Current researches of diffusion bonding in Turkey

Diffusion bonding has remained an application that has been evaluated in the national academic framework. In Turkey, the diffusion bonding process is not commercially available as a product or service, and it has been evaluated within the framework of the studies of the academic community. In one of the studies on diffusion bonding in Turkey, the compatibility between aluminum and copper material pairs was examined. Sare Çelik conducted research on determination of diffusion welding conditions of

pure aluminum and copper under shielding gas. Studies have been carried out to determine the best diffusion bonding parameters of aluminum and copper materials. In the experimental study, it was determined that the most suitable parameters in the atmospheric environment created with argon gas are 560°C temperature, 4.5 MPa press load and 60 minutes dwelling time [7]. The effects on diffusion bonding by changing various parameters between nickel alloys and stainless steel material pairs were also investigated in studies conducted in Turkey. In this case, Sermin Koçer has focused on investigation of diffusion welding of high chromium nickel alloy stainless steel with unalloyed low carbon steel. Studies have been carried out to determine the best diffusion bonding parameters of unalloyed, low carbon steel and duplex stainless steel materials. In the experimental study, it was determined that the most suitable parameters in the atmospheric environment created with argon gas are 900°C temperature, 3 MPa press load and 15 minutes dwelling time [42]. The phases also have an effect on the diffusion bonding method. Studies have been done to investigate this. One of these works, "Formation and effect of interphases in diffusion welding of pure aluminum and pure copper" as subject was investigated by Levent Fidan. The bonding process was carried out by applying the parameters obtained within the scope of previous studies of pure aluminum and pure copper materials and the metallographic structure of the bonding area was examined [11]. The relationship between titanium and stainless steel in diffusion bonding has been investigated in Turkey. Barış Bilgin carried out this study which named "Joining Ti-6Al-4V/304L Material Pair by Diffusion Welding Using Copper Interlayer". Studies were carried out to determine the best diffusion bonding parameters of Ti-6Al-4V alloy and 304L stainless steel materials by using copper interlayer. In the experimental study, it was determined that the most suitable parameters in the atmospheric environment created with argon gas are 870°C temperature, 1 MPa press load and 90 minutes dwelling time [43]. Intermediate material was also placed between titanium and stainless steel to see its effect in diffusion bonding "Investigation of combatability of titanium and low carbon steel couple by diffusion welding using interlayer" was conducted as study by Evren Atasoy. Studies were carried out to determine the best diffusion bonding parameters by using silver alloy interlayer of titanium and low carbon steel materials. In the experimental study, it was determined that the most suitable parameters in the atmospheric environment created with argon gas are 850°C temperature, 3 MPa press load and 90 minutes dwelling time [44]. Titanium alloys have a special place in the

diffusion bonding method. For this reason, detailed studies have been carried out. Parameters were changed and examined. Serkan Öngören has focused on investigation of mechanical and microstructural properties of diffusion-welded joints of Ti-Al-V alloys. Studies have been carried out to determine the best diffusion bonding parameters of Titanium Grade 5 (Ti-6Al-4V) materials. In the experimental study, it was determined that the most suitable parameters in the atmospheric environment created with argon gas are 815°C temperature, 2.72 MPa press load and 90 minutes dwelling time [14]. Compatibility of titanium alloys with copper in diffusion bonding was also investigated. Kemal Aydın conducted research on investigation of combatability of titanium and copper materials by diffusion welding method. Studies were carried out to determine the best diffusion bonding parameters of titanium Grade5 (Ti-6Al-4V) and copper materials. In the experimental study, it was determined that the most suitable parameters in the atmospheric environment created with argon gas are 890°C temperature, 3 MPa press load and 60 minutes dwelling time [45]. Diffusion bonding method with ceramic structures was also investigated. In this context, its compatibility with copper was examined. Fatmagül Tolun performed investigation and analysis of compatibility of copper and porcelain materials by diffusion welding. Studies have been carried out to determine the best diffusion bonding parameters of porcelain and copper materials. In the experimental study, it was determined that the most suitable parameters in the atmospheric environment created with argon gas are 900°C temperature, 4.5 MPa press load and 60 minutes dwelling time [46]. The compatibility of titanium with ferritic stainless steels in diffusion bonding method by using intermediate materials was examined in Turkey. “Investigation of Compatibility of Titanium and Ferritic Stainless Steel Materials by Diffusion Welding Using Nickel Interlayer” was investigated by Aydan Yıldız. Studies have been carried out to determine the best diffusion bonding parameters of titanium and ferritic stainless steel materials using a nickel interlayer. In the experimental study, it was determined that the most suitable parameters in the atmospheric environment created with argon gas are 850°C temperature, 3 MPa press load and 30 minutes dwelling time [47].

Production-oriented services for many sectors in our country are carried out both on a national and international scale. Considering the areas where diffusion bonding is applied, it is an application that has the potential to reduce foreign dependency in critical products in many sectors such as defense, energy, aviation, space, electronics,

medical and nuclear. On the other hand, performing this process domestically in the international arena will increase exports.

The main reason why the diffusion bonding process is not used commercially in the national sense is the high initial investment cost. For this, it is not a commercially preferred application nationally. Considering the situation in the international arena, the preparation levels of the sectors where this process is applied are high. For this reason, it is possible to talk indirectly about a century of international experience in diffusion bonding technology. The demands of sectors with relatively advanced technological readiness, such as defense and energy, that can bear this initial investment cost in the national sense, will help overcome this obstacle. As it can be seen in the studies, there is no situation other than the "investment cost" that can prevent the methodological development of diffusion bonding.

1.4.2 Diffusion bonding applied materials

Today, the diffusion bonding method is applied to many pairs of the same or different materials. These materials are not only metallic but also used in ceramic and plastic materials. It is successfully used in metal - nonmetal or metal - metal joining processes as a combination.

The most commonly used material for diffusion bonding is titanium. Titanium alloys can be joined by diffusion bonding without the need for an intermediate layer. In addition, another reason for the widespread use of titanium in diffusion bonding is that the interface does not need cleaning. However, titanium is not amenable to fusion welding, which makes joining by diffusion bonding necessary. Titanium can dissolve surface residues, including its own oxide, when pressure is applied at high temperatures. However, in titanium, the oxygen in the solid solution increases the hardness and forms a stable phase, making bonding difficult and causing cracks on the surface. Therefore, a protective atmosphere or vacuum is required in titanium diffusion bonding. When argon is used as a shielding gas, argon insoluble in titanium is trapped in the interface. This causes a gap in the cross section. For this reason, it is necessary to ensure the mobility of argon in the bonding zone [48].

Diffusion bonding of aluminum alloys is hampered by persistent surface oxides. However, it has been found that high temperature and large-scale deformation in the bonding region break this oxide layer. Also, facilitation of bonding can be achieved

under lower pressure by using a surface coating or an intermediate layer [48]. Due to its lightness and high strength, it is becoming more and more important to combine Al alloys with other high strength alloys in many areas.

Steel materials can be easily joined by fusion welding methods. However, the need for diffusion bonding arises when the requirements in this joint are complex geometries and high weld strength. Steel materials are generally suitable for diffusion bonding. Therefore, they are economical in designing parts with complex shapes or assemblies that require large weld areas and vital performance [49].

The bonding matrix for the material pairs where diffusion bonding can be made is shared in Figure 1.29 [17].

	1	2	3	4	5	6	7	8	9	10	11	12	13	14	15	16	17	18	19	20	21	22	23	24	25	
1	X	X		X		X		X				X					X	X	X	X						1
2		X			X	X							X							X						2
3																X								X		3
4				X					X		X															4
5	X	X			X	X		X	X	X			X		X			X	X	X				X		5
6						X			X																	6
7							X		X																	7
8								X	X	X	X	X		X	X	X			X	X						8
9					X				X	X	X	X			X	X	X		X	X	X	X		X	X	9
10									X	X				X	X	X		X	X			X		X		10
11											X					X			X	X						11
12												X				X										12
13	X												X		X					X						13
14										X				X	X			X						X	X	14
15					X										X		X		X	X			X	X		15
16					X											X			X		X			X		16
17	X																X									17
18																	X									18
19	X				X			X	X	X					X				X		X			X		19
20	X			X				X		X					X					X			X	X		20
21									X										X	X	X					21
22																						X		X		22
23																										23
24									X		X				X				X					X		24
25																										25
	1	2	3	4	5	6	7	8	9	10	11	12	13	14	15	16	17	18	19	20	21	22	23	24	25	

1	Aluminium and Alloys	14	Tantalum and Alloys
2	Beryllium and Alloys	15	Titanium, Zirconium and Alloys
3	Chrome and Alloys	16	Tungsten and Alloys
4	Cobalt and Alloys	17	Uranium and Alloys
5	Copper and Alloys	18	Vanadium and Alloys
6	Gold and Alloys	19	Low Carbon Steels
7	Magnesium and Alloys	20	Stainless Steels
8	Molybdenum and Alloys	21	Cast Iron
9	Nickel and Alloys	22	Carbide
10	Niobium and Alloys	23	Ceramics
11	Palladium and Alloys	24	Glass
12	Platin, Iridium and Alloys	25	
13	Silver and Alloys		

Figure 1.29 : Matrix of Diffusion Bonding Applied Materials [17].

The metal pairs and interlayer materials suitable for the diffusion bonding method are shared in Table 1.12 [44] [50].

Table 1.12 : Metal Pairs and Interlayer Materials Suitable for Diffusion Bonding Method [44] [50].

Metal-1	Interlayer	Metal-2
Molybdenum	Titanium	Molybdenum
Mo-%0,5 Ti	Titanium	Mo-%0,5 Ti
Tungsten	Niobium	Tungsten
Niobium	Zirconium	Niobium
Tantalum	Zirconium	Tantalum
High Alloy Steel	Beryllium	High Alloy Steel
High Alloy Steel	Niobium-Beryllium	High Alloy Steel
Titanium	Molybdenum	Copper
Titanium	Niobium	Copper
Molybdenum	Nickel	High Alloy Steel
Zircaloy	Copper	Zircaloy
Berllium	Gold	Copper
Berillium	Ag-Cu	Copper
Berillium	Ag-Cu-In	Copper
Aluminium	Copper	Kovar
316L Stainless Steel	Nickel	316L Stainless Steel

The diffusion bonding process parameters for some metal pairs are presented in Table 1.13 [44], [50], [51].

Table 1.13 : Diffusion Bonding Parameters for Metal Pairs [44], [50], [51].

Metal-1	Metal-2	Interlayer	Temperature [°C]	Pressure [MPa]	Time [min]
Copper	Molybdenum	-	900	7.35	10
Copper	Steel	-	900	4.9	10
Copper	Nickel	-	900	14.7	20
Copper	Copper	-	800-850	4.9-6.9	15-20
Titanium	Nickel	-	800	9.8	10
Titanium	Copper	Molybdenum	950	4.9	30
Titanium	Copper	Niobium	950	4.9	30
Titanim	Copper	-	800	4.9	30
Molybdenum	Molybdenum	Titanium	915	6860	20
Molybdenum	Steel	-	1200	4.9	10
Tungsten Tantalum	Tungsten	Niobium	925	6860	20
Niobium	Tantalum	Zirconium	870	-	-
Zircaloy-2	Niobium	Zirconium	870	-	-
Steel	Zircaloy-2	Copper	1040	20.6	30-120
Berillium	Aluminium	Copper	550	4.9	10
Copper	Berillium	63-Ag-27	800	-	30
Steel	Kovar	-	1000-1110	24.5-10.6	20-25
Steel	Cast Iron	-	850-950	7.35	5-7
316L	316L	-	1100	10	120
316L	316L	Nickel	950	10	60

The tensile strength and corrosion resistance of stainless steel is better than aluminum alloy. The flow channel production and welding performances of various materials such as stainless steel, Nickel-based alloy and titanium were evaluated. When stainless steel is used, the size of the flow channel can be very small thanks to the good strength values of the stainless steel. As a result, high heat transfer performance is achieved when stainless steel is used despite poor thermal conductivity values. In order to evaluate the robustness of the heat exchanger, it must successfully pass the non-destructive examination, hydrostatic test and sealing tests [52].

As a result of the Figure 1.29, Table 1.12 and Table 1.13, the diffusion bonding mechanism of 316L/316L and 316L/Ni/316L material pairs and the parameters affecting this mechanism were determined.

1.4.3 Diffusion bonded heat exchangers

Studies have been carried out on the production of heat exchangers by diffusion bonding method. Studies have been carried out on the production of heat exchangers by diffusion bonding method. The company named "Heatric" is the leading company in the world in the production of heat exchangers with diffusion bonding. It manufactures heat exchangers on specific areas. There are studies done in this context. Li et al., in their study, give information about the properties of materials used in the manufacture of compact heat exchangers produced by diffusion bonding method. This study focused on SS316/316L and Nickel-based alloy Inconel 617, which can be used in nuclear technologies. 316 L and Inconel 617 are frequently used in compact heat exchangers manufactured by Heatric. The study focuses on the effect of Nitrogen addition for 316 L, while for Inconel 617 it focuses on the effect of diffusion coupling and cooling rate on Inconel 617 properties. As a result, it has been observed that SS316L material is compatible with fluids such as Helium, Nitrogen CO2 and liquid sodium, and the design temperature is up to 550 ℃ depending on the creep life and environmental conditions. Inconel 617 material, on the other hand, has been found to be compatible for most applications with an operating temperature of 900 ℃ and above [53]. Another diffusion coupling method was used to produce heat exchangers by Clark et al. They investigated the diffusion welding properties of alloy 800H, alloy 617, alloy N and alloy 242 in their study. In their study, they used the “Gleeble” thermomechanical testing machine, which is used to determine the diffusion bonding

parameters. The plates were welded under vacuum hot press. The image of the process using the heat exchanger produced in Figure 1.30, and the alloy 800 H plates, which are diffusion welded under vacuum hot press, are shared in Figure 1.31. The results were then analyzed by SEM X-ray spectroscopy method and the results obtained with the Thermocalc/DICTRA software developed to evaluate the parameters were compared. As a result, it has been observed that the use of Nickel interlayer improves diffusion welding, and it has been observed that alloy 617, alloy 800H and alloy 242 materials are welded very well with this technique, under 3 hours holding time, 1150 ℃ and 3-7 Mpa pressure, and make perfect bonding [54].

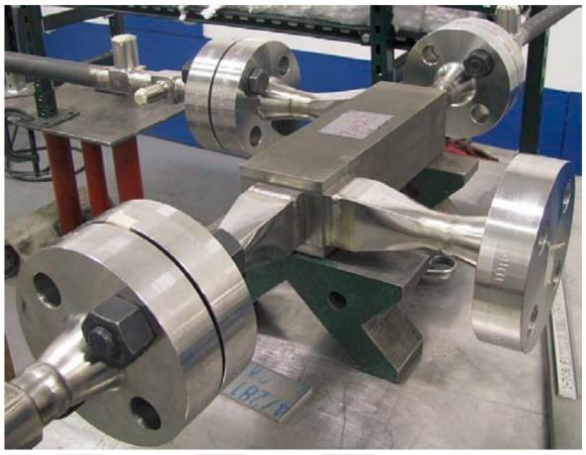

Figure 1.30 : Compact heat exchanger produced by diffusion bonding method using alloy 617 material produced to measure performance up to 900 C in a helium gas test setup [54].

Figure 1.31 : Alloy 800 H plates diffusion bonded under vacuum hot press [54].

2. METHODOLOGY

In experimental studies, firstly, the sample preparation process is run. Afterwards, examinations, equipment to be used, sample matrices are prepared. In the light of the information obtained from the literature review from the created matrix, the most appropriate parameters to be examined are determined and experiments are carried out. All these processes reveal the methodology of the study.

2.1 Diffusion Bonding Furnace and Test Equipments

In the diffusion bonding process, laboratory type resistance furnace of Nevola company was used as the heating source. The exterior of the furnace has been updated to supplement the vacuum and pressurization processes. In this way, it was possible to purge the furnace before diffusion bonding. Piston was used to apply the pressure load on the samples inside the furnace. Static load discs are used for the application of the force. The images of the furnace before and after the update are presented in Figure 2.1

Figure 2.1 : Diffusion Bonding Furnace.

Before the microhardness and metallographic inspection processes, the Ecopress 50 model molding device of Metkon company, which is a moulding (Bakalite) device, was used and the image of the device and the device in which sanding and polishing is done before microhardness and metallographic inspection processes. The electrolytic etching unit used for etching before the metallographic examination processes and after etching, Future Tech brand microhardness device was used for microhardness test. Shimadzu AG-IC brand and model tensile test device is used. The The ThermoFisher Quattro ESEM FE-SEM brand SEM-EDS device, in which SEM and EDS analyzes of metallographic examination processes are performed. Nikon Eclipse mr 100 optical microscope, in which optical microstructure examinations were made.

2.2 Material Selection and Material Properties of 316L

In this section, materials compatible with each other in the diffusion bonding process are presented. A cost-effective, durable material that can meet the technical requirements of the heat exchanger has been selected.

Recuperators are generally made of stainless steel. Gas inlet temperature in applications ranges from 593 ℃ to 816 ℃. For higher temperature applications, materials such as Inconel 625, Inconel 617 and Haynes 230 can be used, but their cost is high in most applications.

316L stainless steel was chosen as the material to provide the necessary structural properties in the micro-channel heat exchanger. 316L material is both easily available in the market and provides the necessary strength properties.

In addition to above reasons and tecnical criterias, it has been decided to manufacture the heat exchanger with 316L steel and materials suitable for this steel, due to reasons such as high pressure and temperature resistance as mechanical properties, and cost-effectiveness.

EN 1.4404/AISI 316L/DIN X2CrNiMo17-12-2 material chemical composition is given Table 2.1, mechanical properties at room temperature Table 2.2, mechanical properties at temperatures above room temperature is given Table 2.3, Its physical properties at a temperature of 20°C are given in

Table 2.4 and its weldability properties are given in Table 2.5 [55].

Table 2.1 : Chemical Composition of AISI 316L Stainless Steel (%).

Carbon (C)	Silicon (Si)	Manganese (Mn)	Potassium (P)	Sulfur (S)
≤ 0.030	≤ 1.00	≤ 2.00	≤ 0.045	≤ 0.015
Chromium (Cr)	**Molibdenum (Mo)**	**Nickel (Ni)**	**Nitrogen (N)**	**Iron (Fe)**
16.5-18.5	2.00-2.50	10.0-13.0	≤ 0.11	Rest

Table 2.2 : AISI 316L Stainless Steel Mechanical Properties At Room Temperature.

Mechanical Properties at Room Temperature (Longitudinal) Condition: Heat-treated solution			
Thickness	**Hardness HB 30**	**%0,2 Yield Strength**	**0,1% Yield Strength**
≤160/250 mm	≤215 HRC	≥200 N/mm^2	≥235 N/mm^2
Tensile Strength	Elongation after fracture (Lo=5*do)	Reduction in Area	**Impact Energy**
500-700 N/mm^2	≥%40/30	≥%60	≥ 100/60 J

Table 2.3 : AISI 316L Stainless Steel Mechanical Properties at Temperatures Above Room Temperature.

Mechanical Properties at Temperatures Above Room Temperature

Condition: Solution Heat Treated (Annealed)

0.2% Yield Stress Between 100°C and 550°C (N/mm2≥)

100°C	150°C	200°C	250°C	300°C	350°C	400°C	450°C	500°C	550°C
165	150	137	127	119	113	108	103	100	98

Average Coefficient of Expansion Between 100°C and 800°C (10^{-6} K^{-1})

100°C	200°C	300°C	400°C	500°C	600°C	700°C	800°C
16.0	16.5	17.0	17.5	18.0	19.0	19.5	19.5

Table 2.4 : Physical Properties of AISI 316L Stainless Steel [20°C].

Density (kg/dm3)	Specific Heat Capacity (J/g*K)	Heat Conduction (W/K*m)	Electrical Resistance (Ω*mm^2/m)	Modulus of Elasticity (kN/mm^2)	Magnetizability	Polishability
8.0	0.50	15	0.75	200	No*	No

(*) Austenitic steels can become slightly magnetized when quenched. Its magnetism can also be increased by cold forming.

Table 2.5 : AISI 316L Stainless Steel Weldability Properties.

Methods of Weld			
Shielded (Argon) Arc Welding MIG, WIG	Arc Welding	Resistance Welding	Autogenous Welding
Yes	Yes	Yes	Not Preferred

2.3 Diffusion Bonding Test and Analysis Methods

In diffusion bonding, tests are used to determine the bonding strength and quality. These tests are tensile test and microhardness test. In addition, the microstructure properties of the diffusion zone occurring at the interface of the bonded joints were analyzed using optical microscopy, scanning electron microscopy (SEM) and energy dispersive X-ray spectroscopy (EDS).

2.3.1 Tensile test

The tensile test is the test performed to determine the tensile strength of welded/bonded materials that will be subjected to tensile loads. The tensile test specimen must have the geometric structure given in Figure 2.2. The sample geometry is given by TSE standart that name is TS 138 EN 10002-1 for the tensile test are shared in Table 2.6 [56]. While the main dimensions that make up the tensile test specimen remain constant, the diameter D and Lt size that it is attached to the tensile test device may vary according to the jaws of the tensile test device.

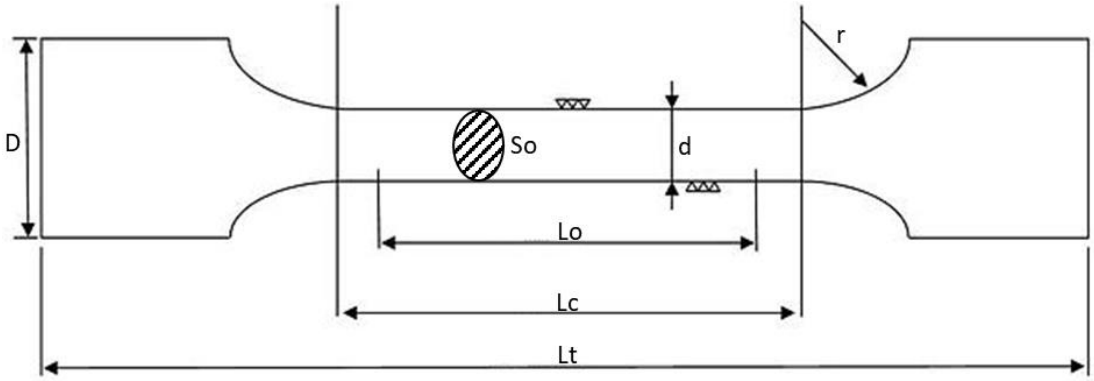

Figure 2.2 : Tensile Test Sample Dimensions.

Table 2.6 : Tensile Test Sample Dimensions According to TSE Standard (TS 138 EN 10002-1) [56].

r	**Nominal Dia.** d [mm]	**First Cross-Sectional Area** So [mm^2]	**First Measure Length** $Lo = k\sqrt{So}$ [mm]	**Minimum Parallel Length** Lc [mm]	**Total Length** Lt [mm]
5.65	20 ±0.15	314	100 ±1.0	110	Depends on the fixing method of the test pieces
	10 ±0.075	78.5	50 ±0.5	55	Device clamps in principle:
	5 ±0.04	19.6	25 ±0.25	28	It should be
					Lt > Lc +2d or 4 d

2.3.2 • Microhardness test

Hardness is a relative measure and can be defined as the resistance of materials to plastic deformation. The hardness of the materials actually provides information about the tensile strength of the material. For example, the hardness of steel materials is directly proportional to the tensile strength. In the micro-hardness measurement, the aim is to make a comparison by measuring the hardness differences between the main materials and the bonded area. Hardness measurement generally consists of measuring the resistance of the material to the indentation of a pyramid, conical or spherical standard tip into the material. An axial force is applied to the hard end to create a trace on the material. The hardness of the material is inversely proportional to the size of this indent.

Microhardness tests are divided into two groups according to the way they are performed under static and dynamic loads. Tests performed under static load are Rockwell, Brinell and Vickers hardness tests. The devices on which these tests are performed are not suitable for portable use.

In Vickers hardness test, a diamond square pyramid with 136° angle is used as a indenter. The average diagonal length d [mm] calculated by measuring the diagonals of the rectangular trace left by the pyramid tip pressed into the material with the load F [kgf], is substituted in the Vickers hardness formula and the hardness value is obtained as in Figure 2.3. Vickers hardness is not load dependent. It is useful to increase the load and thus the trace in order to reduce the measuring errors and to obtain an average value in heterogeneous structures. However, the diagonal length should not exceed two-thirds of the thickness of the part or layer whose hardness is measured. The load can vary between 1-120 kgf. 30 kgf can be selected as normal load. In the Vickers method, wide diagonals are obtained despite small depths due to the large pyramid angle. The residence time of the charge on the sample is approximately 20 seconds. As a result of this pressure, the pressure tip is removed from the sample and the test is completed [56].

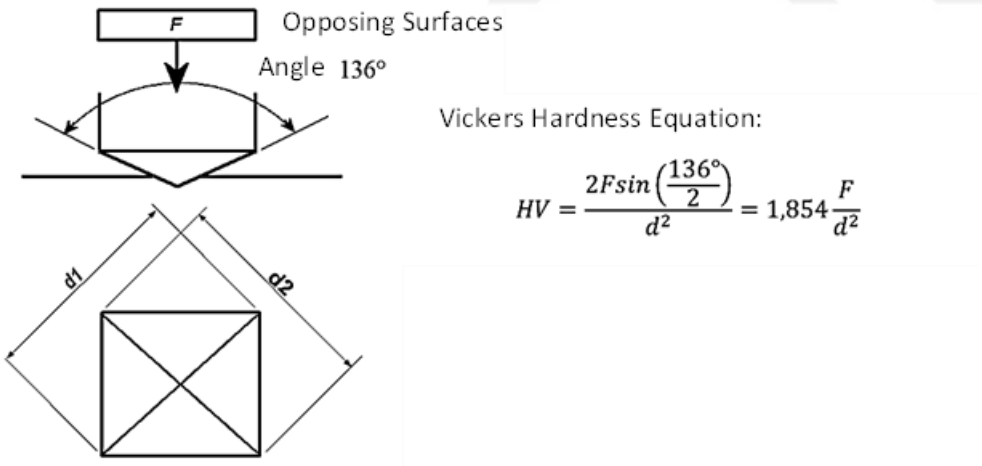

Figure 2.3 : Schematic Illustration of Vickers Hardness Measurement and Equation [56].

2.3.3 Scanning electron microscope (SEM)

The first of the non-destructive examinations is the metallographic analysis performed with the Scanning Electron Microscope. SEM is a type of electron microscope that obtains images by scanning the sample surface with a high-energy electron beam

focused on a very small area. Electrons interact with atoms in the sample to produce different signals that contain information about the topography and composition on the sample surface. With SEM, a resolution higher than 1 nanometer ($1x10^{-6}$ mm) can be achieved. With SEM analysis, the thickness, grain boundaries and interface of the connection intermediate layers can be examined in the region where the diffusion bonding is made. In this way, the differences between the joint area and the base material can be determined. In this study, SEM images of the samples were taken at 5000x magnification. Acc. Voltage was used as 15 kV. These parameters were sufficient to show the gaps and grain boundaries etc. on the samples.

2.3.4 Energy dispersive x-ray spectroscopy (EDS)

Energy dispersive x-ray spectrometry (EDS) shows the concentrations of elements by point and local, atomic and weight. For this reason, EDS has an important place in this study, which examines the diffusion bonding process in 316L and Ni. In the diffusion bonding process, the EDS analysis gave an idea to show how much the nickel and iron atoms diffuse between the materials with the effect of pressure and temperature. The obtained values were evaluated by tabulating in this context. 10.211 keV was used as the cursor value.

2.4 Diffusion Bonding Optimization and Test Matrix

During the preparation of the samples, a two-stage approach was preferred, first as temperature optimization and then as time optimization. In this approach, temperature optimization was performed for 950°C and 1050°C, and during this optimization process, the temperature was fixed at 60 minutes, the pressure load was 8.5 MPa, and the ambient atmosphere was argon. In the second stage, samples were produced for 120 and 180 minutes by fixing the temperature value, pressure load of 8.5 MPa and argon as the ambient atmosphere, which showed the best results. This two-step optimization process was also carried out for samples with a nickel interlayer. The two-stage optimization structure is summarized in the diagram shared in Figure 2.4. The diffusion bonding test matrix prepared for this two-step optimization is presented in Table 2.7. During sample preparation, 3 samples were prepared for each parameter set. Thus, the repeatability of the parameters was observed.

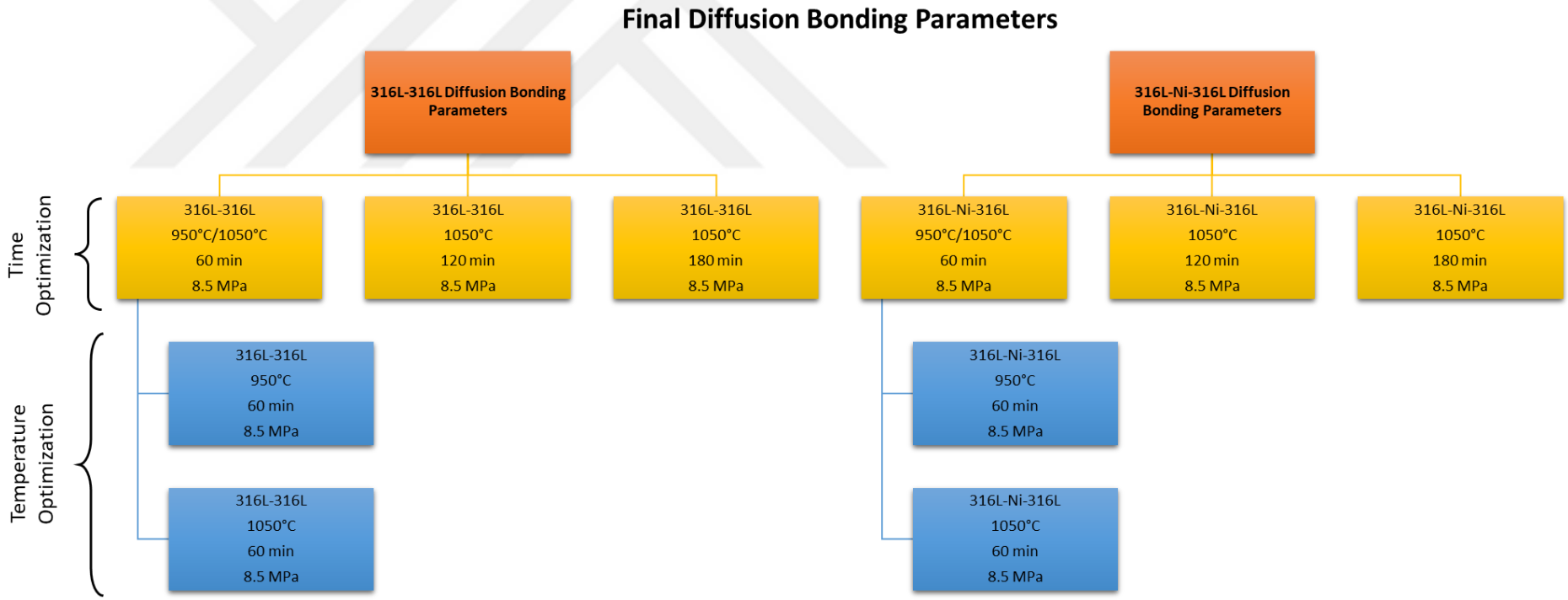

Figure 2.4 : Diffusion Bonding Optimization Diagram.

All samples were produced under Argon atmosphere and 8.5 MPa pressure. Three samples were produced, tested and analyzed to increase accuracy for each test parameter. Optical examinations, hardness tests and SEM, EDS analyzes were performed with metallographic samples. Sample matrix that preparation parameters for tests and analysis which is shared in Table 2.7.

Table 2.7 : Sample Test Matrix.

Sample No	Material Pair	Temperature [°C]	Time [min]	Pressure [MPa]	Atmosphere
1	316L-316L	950	60	8.5	Argon
2	316L-316L	1050	60	8.5	Argon
3	316L-Ni-316L	950	60	8.5	Argon
4	316L-Ni-316L	1050	60	8.5	Argon
5	316L-316L	1050	120	8.5	Argon
6	316L-316L	1050	180	8.5	Argon
7	316L-Ni-316L	1050	120	8.5	Argon
8	316L-Ni-316L	1050	180	8.5	Argon

2.5 Diffusion Bonding Sample Preparation Processes

In the sample preparation processes, first of all, material was procured and, a certificate was requested from the companies from which the material was supplied, whether the composition and mechanical properties specified for the 316L material were met. The certificates of the materials are shared in APPENDIX-1 and APPENDIX-2. Nevertheless, it has been verified by spectral analysis and tensile tests that the materials provide the requested composition and mechanical properties. The chemical composition of the materials was determined by spectral analysis and is shared in Table 2.8. After the material properties specified in the certificates and the requested properties matched, intermediate product production processes were started. The dimensions of tensile, microhardness and microstructure samples are presented in Figure 2.5.

Table 2.8 : 316L Stainless Steel Spectral Analysis Result.

Composition (%)								
C	Mn	P	S	Si	Cr	Ni	Mo	Fe
0.030	0.83	0.045	0.03	0.3	16.56	9.85	2.06	Rest

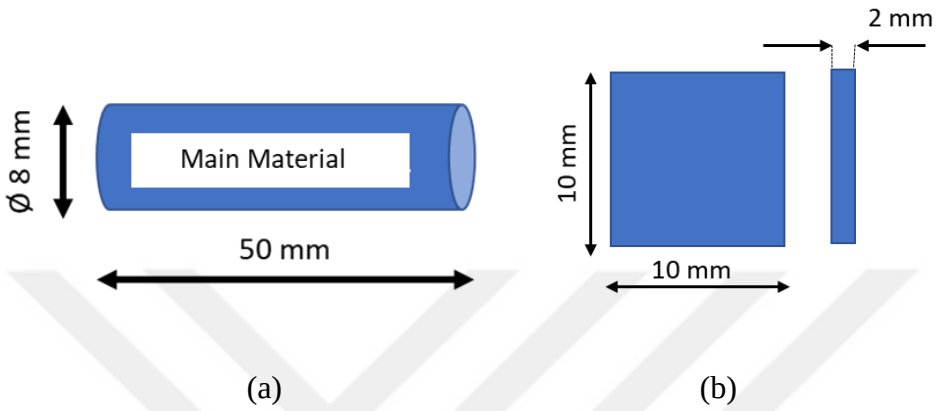

Figure 2.5 : a) Tensile Test Sample Raw Material Dimensions. b) Microhardness Test and Metallographic Inspection Material Dimensions.

After the preparation of the intermediate products, that is, the raw materials in the sample preparation stage, the production of diffusion bonding samples was started. The sample preparation processes for the diffusion bonding process are the same, but there are differences only in the sample raw material dimensions. The sample production process is the same except for sample sizes.

The first step in the production process of diffusion bonding samples is the sanding of the surfaces to be diffusion bonded. Surface roughness of 0.02 µm was obtained by gradually sanding the surfaces of the samples to be produced with 400, 800 and 1200 grit silicon carbide sandpaper on which diffusion bonding was to be applied. After the sanding process, the joint surfaces were cleaned with alcohol and dried. After the cleaning process, the materials were placed in the furnace. 20 micron was selected as nickel foil of thickness. The order of placement in the furnace is different for each sample type and is presented in Figure 2.6 and Figure 2.7. The necessary refractory material was used in order to prevent the samples from boiling with the piston in the furnace. In addition, carbon graphite materials were placed near the diffusion bonding sites of the samples in order to prevent oxidation in the junction area.

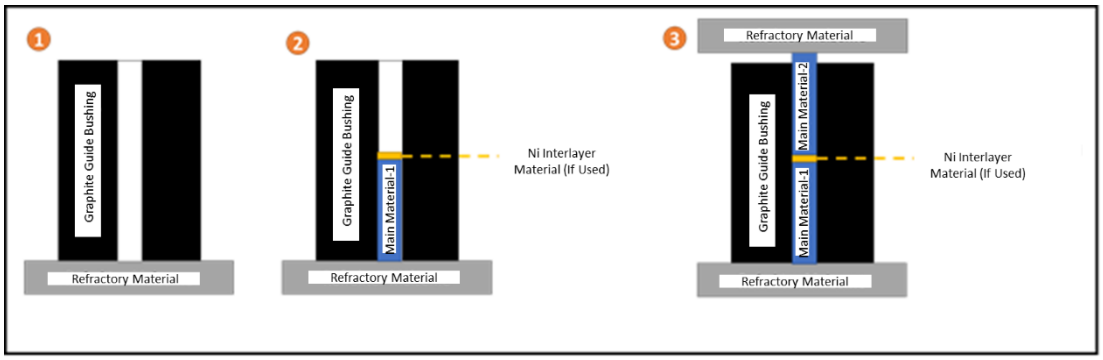

Figure 2.6 : Tensile Test Sample Furnace Layout Sequence.

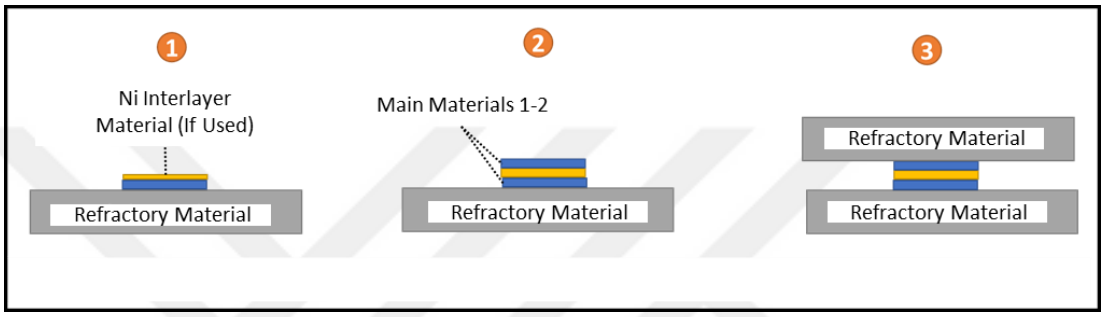

Figure 2.7 : Microhardness Test and Metallographic Inspection Raw Material Furnace Layout Sequence.

After the samples were placed in the furnace, the furnace atmosphere was cleaned 3 times with argon gas with a purity above 99.99%. Lastly, the furnace atmosphere was continuously supplied with argon gas with a positive pressure of approximately 1 bar. Argon gas flow rate was kept at approximately 3 lt/min. After the argon atmosphere was created, a pressure load of 8.5 MPa was applied as indicated in the sample matrix. Afterwards, the furnace was adjusted according to the temperature value specified for the relevant part in the sample matrix and the furnace atmosphere was heated at an average speed of 26 °C/min. When the temperature and pressure load reached the final level, the chronometer was kept and the furnace temperature, pressure load and argon atmosphere were fixed until the time specified in the matrix. When the time was up, the furnace was allowed to cool and the pressure load was removed. The samples were evacuated when the furnace atmosphere dropped to 250°C with an average speed of 15 °C/min.

After the tensile test specimens were bonded by diffusion, they were turned for the tensile test in the dimensions and the views of the tensile test specimens before, after and after diffusion bonding are presented in Figure 2.8. The samples, whose turning

process was completed, were subjected to tensile test by the authorized operator in accordance with the procedures.

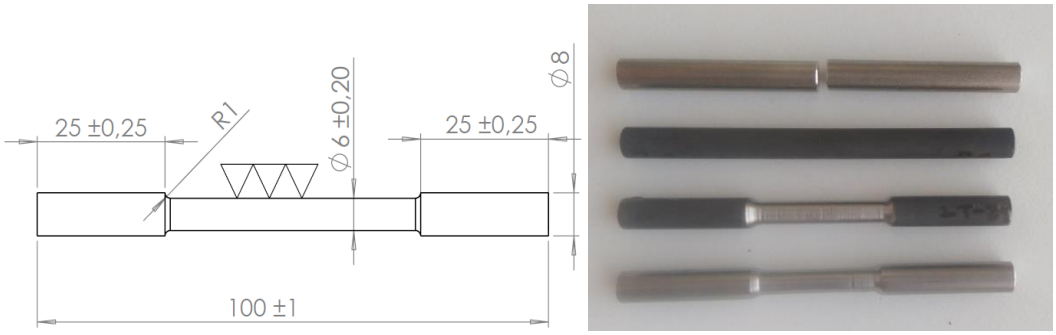

Figure 2.8 : Tensile Test Sample Turning Dimensions And Diffusion Bonding Tensile Test Samples According To TSE Standart (TS 138 EN 10002-1).

Microhardness and metallographic examination samples were first moulded in bakalite in the direction of the cross-sectional area after the diffusion bonding process. Afterwards, it was divided into two by a water-cooled laboratory type cutting device from the sections perpendicular to the diffusion bonding. 400, 800, 1200 grit silicon carbide sanding process was applied gradually on the surfaces to be tested and inspected. After the sanding process, the samples were subjected to polishing, which is the final surface treatment. This process was carried out gradually with 3 and 1µm felts. In addition, 3 and 1µm diamond paste was impregnated gradually during this process. The polished section surface was cleaned with alcohol and dried. 5 hardness measurements were made with the authorized personnel of the polished samples from the junction area towards both main material directions at 30µm intervals. Afterwards, it was electrolytically etched in volumetric 50%HNO_3 + 50%H_2O solution for 20 seconds for metallographic examination. The samples, whose surface preparation processes were completed, were subjected to optical microscope, SEM, and EDS analyzes by the authorized operator in accordance with the procedures. In Figure 2.9 samples prepared for microhardness and metallographic examination processes are shared.

After all these processes, the samples are ready for microhardness tests and metallographic analysis.

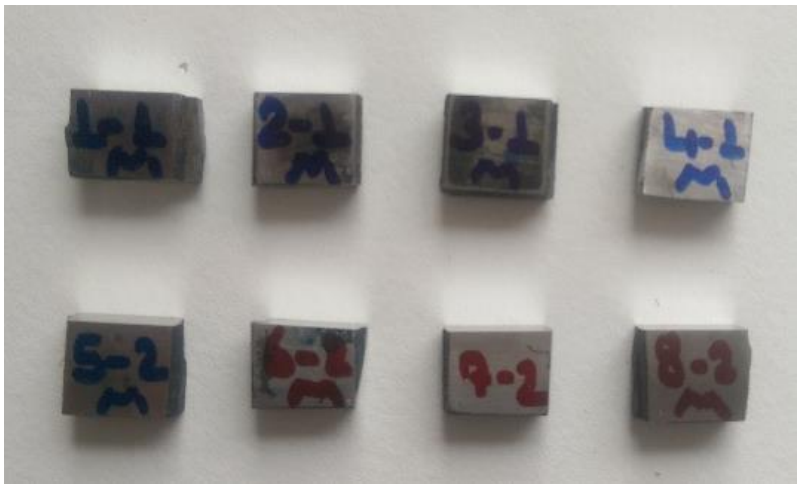

Figure 2.9 : Microhardness and Metallographic Inspection Samples.

2.6 Diffusion Bonding Temperature, Pressure and Time Cycle

The temperature, pressure load and time cycles of the diffusion bonding processes without an interlayer and with a Ni interlayer of the samples produced by the diffusion bonding method are presented in Figure 2.10 and Figure 2.11, respectively.

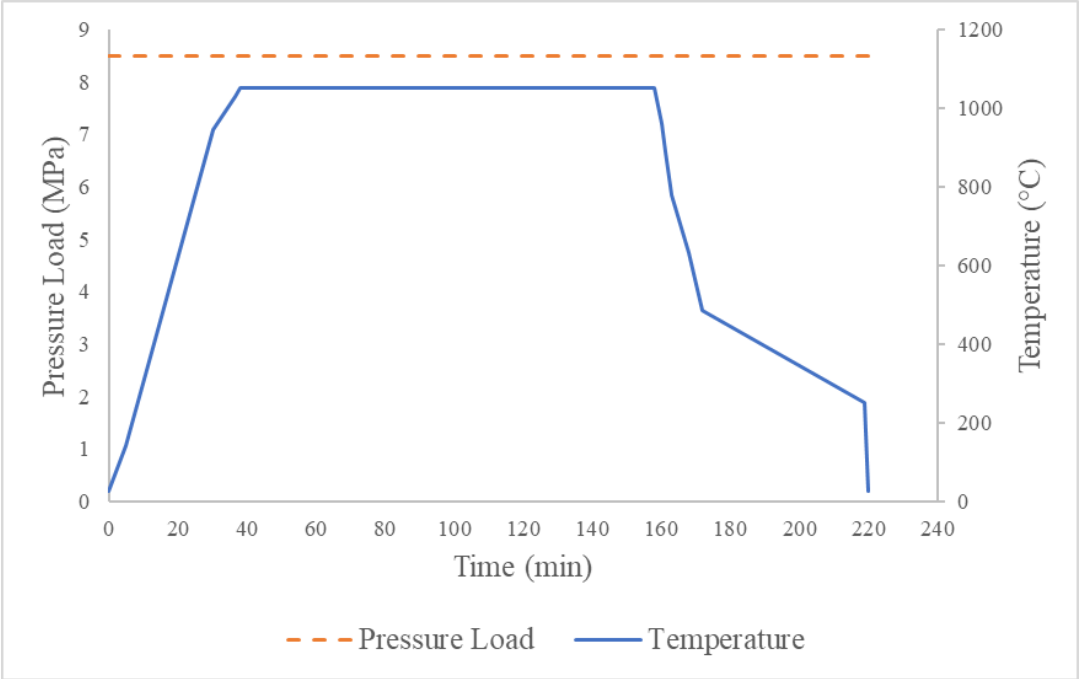

Figure 2.10 : 316L-316L Diffusion Bonding Cycle (1050°C, 120 min).

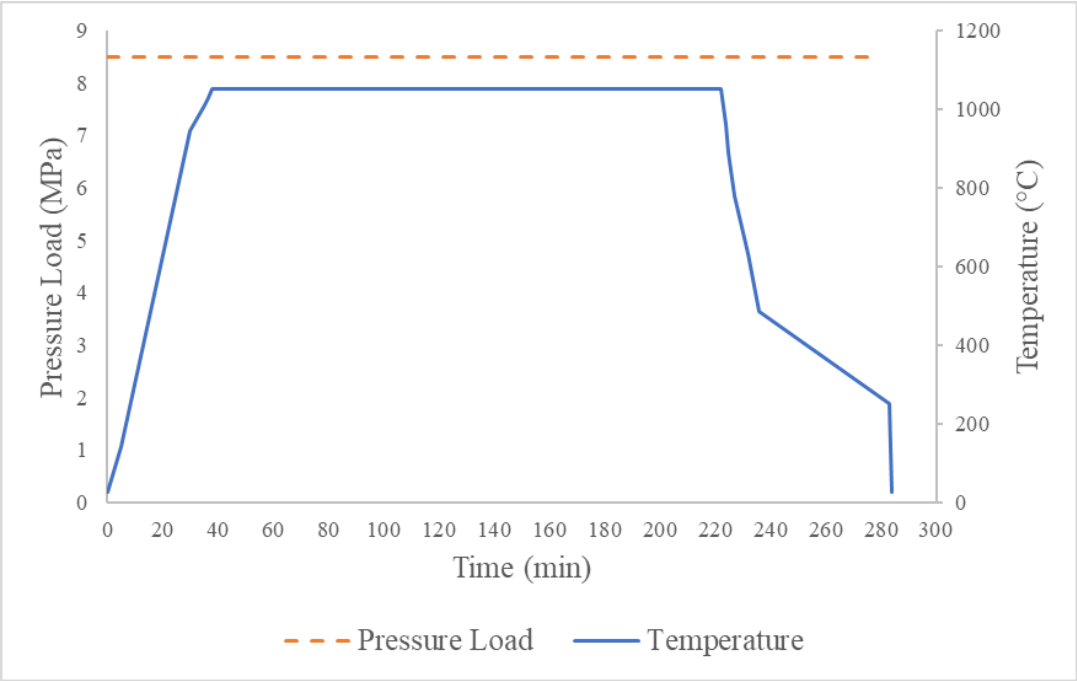

Figure 2.11 : 316L-Ni-316L Diffusion Bonding Cycle (1050°C, 180 min).

These cycles represent that how whole diffusion bonding processes combined into certain parameters in graph.

3. EXPERIMENTAL RESULTS AND DISCUSSIONS

Tensile tests, microhardness tests, optical microscope examinations, SEM-EDS examinations and graphics of the prepared samples were analyzed and interpreted in this part of the thesis.

3.1 Tensile Test Results

Tensile test specimens were produced using the parameters specified in the specimen matrix and shared details for the tensile test specimen preparation process. The produced parameters were subjected to tensile test. The images as a result of the tensile test of the samples produced with 316L stainless steel material and diffusion bonding are shared as sample in Figure 3.1. The maximum tensile strength and elongation in the tensile test results are shared in Table 3.1. Base material 316L tensile test results are shared in Figure 3.2. In addition, the load-strain and stress-strain curves are presented in as comparision Figure 3.3 and Figure 3.4

Figure 3.1 : Samples after tensile tests.

Table 3.1 : Tensile Test Results.

Sample No	Max. Tensile Strength [MPa]	Elongation [%]
Base 316L	650	37.0
1	N/A	N/A
2	220	6.8
3	N/A	N/A
4	217	5.4
5	284	5.7
6	268	7.0
7	394	14.8
8	**407**	15

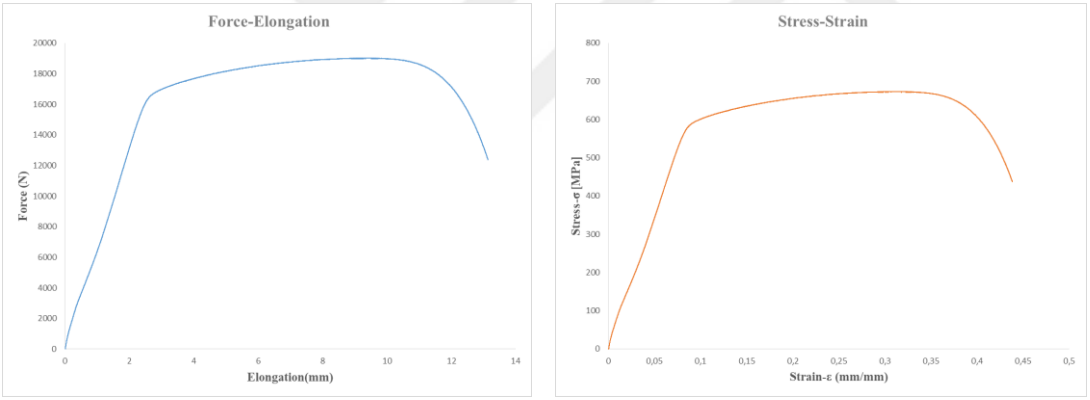

(a) (b)

Figure 3.2 : Base 316L Stainless Steel Material Tensile Test Results. a) Force-Elongation. b) Stress-Strain Curves.

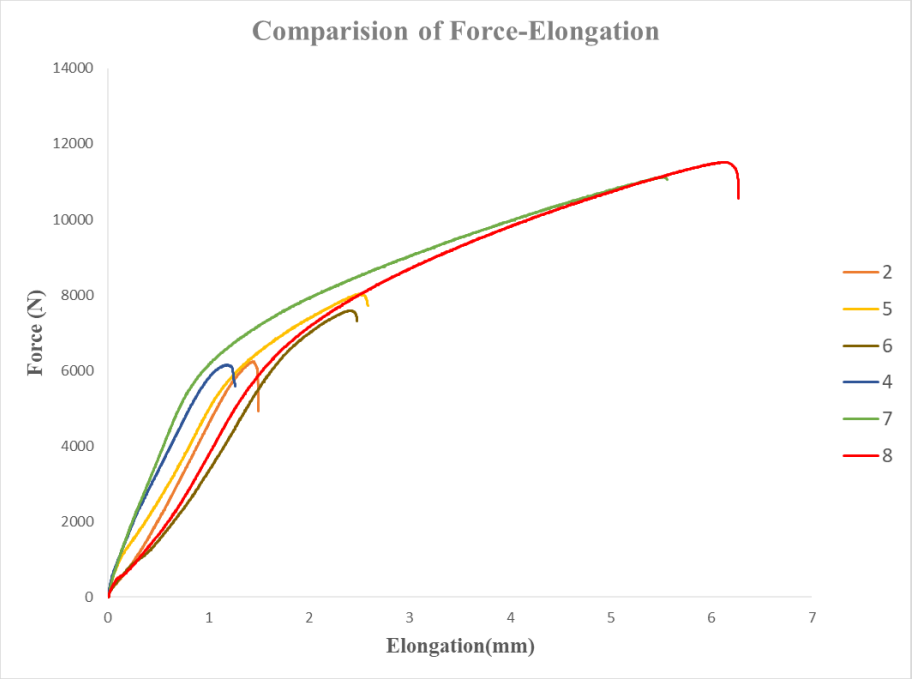

Figure 3.3 : Comparision of Force-Elongation of Samples.

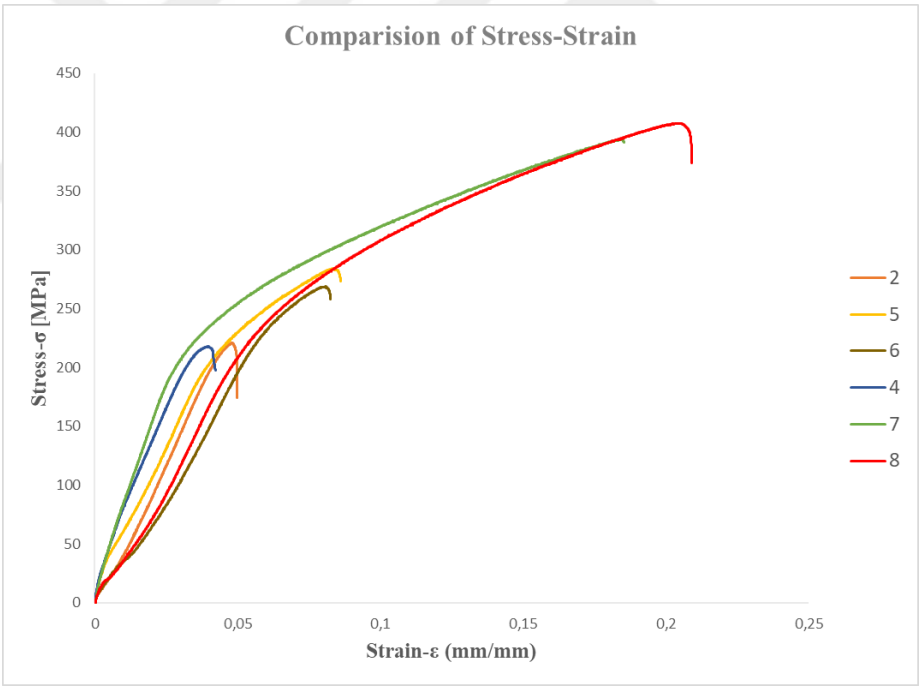

Figure 3.4 : Comparision of Stress-Strain of Samples.

Diffusion bonding samples which coded as 1 and 3 made at 950°C for the purpose of the tensile test could not be successful. As a result of the tensile test of base 316L type stainless steel, 650 MPa tensile strength was obtained. Maximum tensile strengths of 220, 284 and 268 MPa were obtained at 60, 120 and 180 minutes, respectively, in diffusion bonding without Ni interlayer at 1050°C and which also respectively samples

coded as 2, 5 and 6. Maximum tensile strengths of 217, 394 and 407 MPa were obtained at 60, 120 and 180 minutes, respectively, in diffusion bonding made using Ni interlayer at 1050°C and which also respectively samples coded as 4, 7 and 8. As a result of the diffusion bonding tests performed without the use of Ni interlayer, the maximum strength was obtained as 284 MPa for the samples combined at 1050°C for 120 minutes which sample coded as 5 . As a result of diffusion bonding tests using Ni interlayer, the maximum strength was obtained as 407 MPa on average for the samples joined for 180 minutes at 1050°C which sample coded as 8. It was observed that the tensile strength of the Ni interlayer samples prepared by diffusion bonding method at 1050°C, 120 minutes and 180 minutes was far ahead of the tensile strength of the other samples. It was also seen that the Ni interlayer significantly increased the tensile strength in diffusion bonding. The sample that gave the best results in the tensile tests was the sample with Ni interlayer, prepared by diffusion bonding method at 1050°C in 180 minutes that is sample 8.

3.2 Optical Microstructure Results

Optical microstructure samples were produced using the parameters specified in the sample matrix and shared details for the metallographic examination sample preparation process. The microstructures of the produced samples were examined by optical microscopy, and the results depending on the temperature, which is the first optimization step, are shared in Figure 3.5 and Figure 3.5.

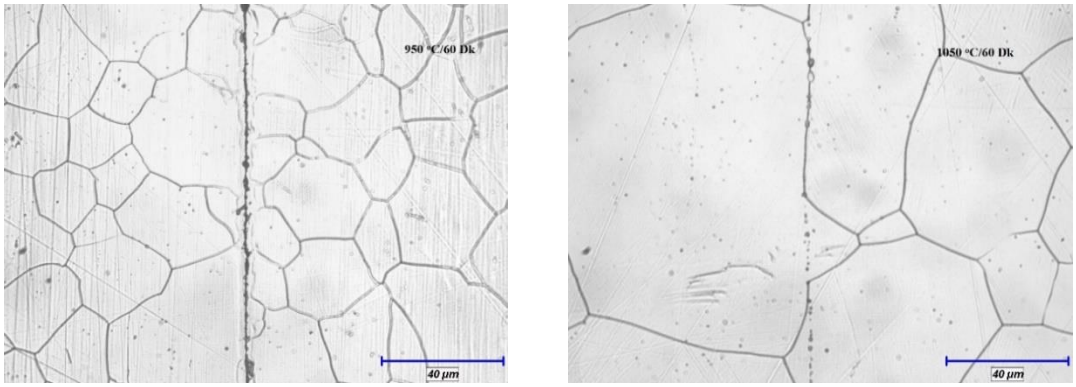

(a) (b)

Figure 3.5 : Microstructure images a) Sample No 1. b) Sample No 2.

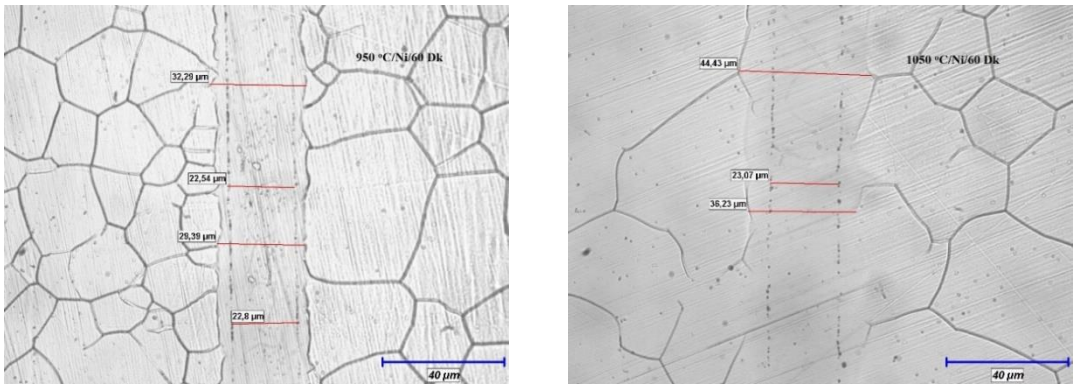

(a) (b)

Figure 3.6 : Microstructure images a) Sample No 3. b**)** Sample No 4.

In the temperature optimization process, which is the first stage of the sample matrix, it was observed that there were dense gaps in the junction areas of the samples that are sample 1 and sample 3, formed at 950°C. In Sample 1, an oxide layer is visible at the interface of two 316L materials. It is understood that the oxide layer is not removed at 950°C. In sample 2, it can be seen that this oxide layer relatively disappears at 1050°C. however, it was also observed that the grain boundaries were not completely removed. Here, the disappearance of the grain boundaries and the incomplete diffusion can be interpreted that the temperature of 1050°C remains the low temperature for the 316L material. Since diffusion increases with exponential increase in temperature, it is anticipated that higher temperature may be required. For the Sample 2, it is seen that the majority of the gaps are closed in the samples prepared at 1050°C during the one-hour sample preparation processes. It is seen that relatively better coalescence occurs in samples with Ni interlayer, and diffusion increases with the increase in temperature. After this stage, time optimization was started by using the temperature value of 1050°C, which gave the best results. 120 and 180 minutes were taken into consideration. In addition, when looking at Sample 1, it is seen that the grain sizes are small. The reason for this is thought that 950°C is not the temperature sufficient for the grain boundaries to grow. In sample 2, on the other hand, it was observed that 1050°C was sufficient temperature to enlarge the grain boundaries. In Sample 3, it is seen that the grain sizes are small on the left side and large on the right side. It is thought that the reason for this is either the temperature not being homogeneously distributed in the oven or the microstructure of the 316L used when it arrives.

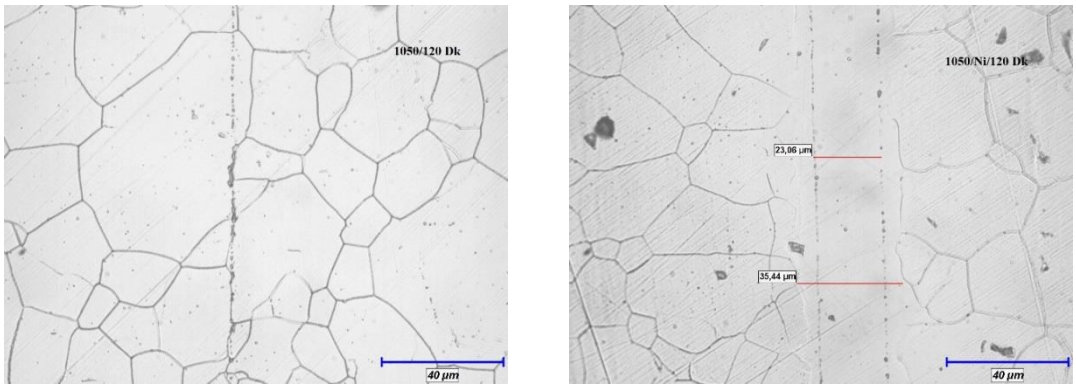

(a) (b)

Figure 3.7 : Microstructure images a) Sample No 5. b) Sample No 7.

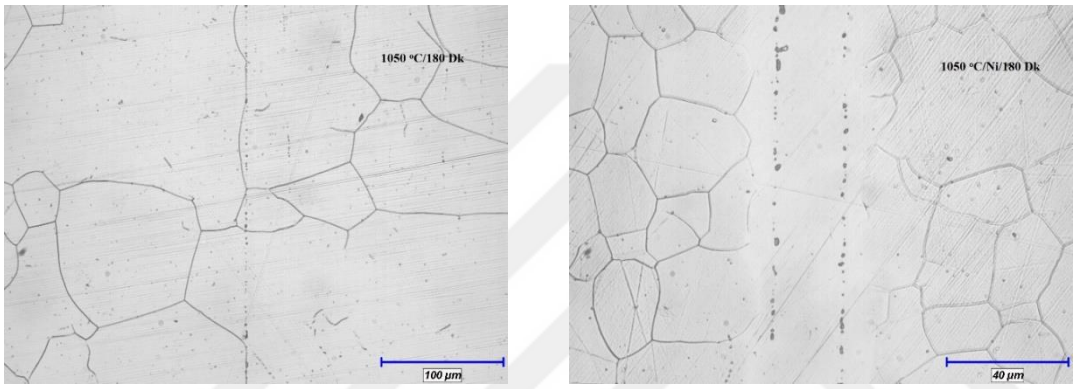

(a) (b)

Figure 3.8 : Microstructure images a) Sample No 6 b) Sample No 8

Samples formed at 1050°C temperature and 120 minutes are shown in Figure 3.7. Samples with and without Ni interlayer show better bonding than samples formed in 60 minutes. Microstructures of the samples created in 180 minutes are shown in Figure 3.8. Although there are traces of coalescence in the intermediate region in both samples, it is observed that the diffusion region of the samples with Ni interlayer has increased significantly. In the sample without an intermediate layer, it is extremely important that both material pairs form a common grain structure in the diffusion bonding region.

The effect of temperature on grain growth is clearly seen in Sample 6. In addition, this sample was exposed to 1050°C for 180 minutes. This is not the case in Sample 5, Sample 6 and Sample 7.

3.3 SEM-EDS Analysis Results

Samples were produced using the parameters specified in the sample matrix and shared details for the metallographic inspection sample preparation process. Produced samples were created in the form of temperature optimization in the first stage, as in the optical microstructure examination, in the second stage in the form of time optimization. The results of 60 min samples without Ni interlayer are shared in Figure 3.9.

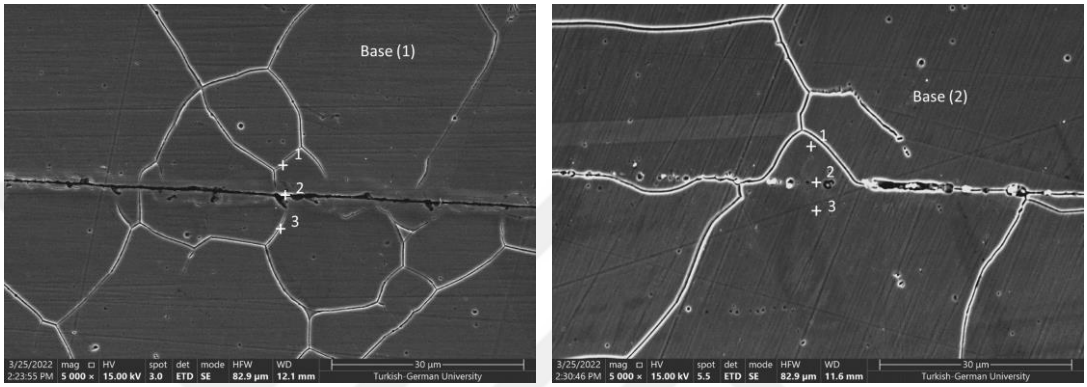

(a) **(b)**

Figure 3.9 : SEM Images a) Sample No 1. b) Sample No 2.

Table 3.2 : EDS Results (Figure 3-9-a).

Element	1		2		3	
	Weight %	**Atom %**	**Weight %**	**Atom %**	**Weight %**	**Atom %**
C (Kα)	0.47	2.129	0.634	2.619	0.37	1.684
O (Kα)	0.171	0.58	3.697	11.469	0.183	0.625
Si (Kα)	0.342	0.662	0.359	0.635	0.306	0.595
V (Kα)	-	-	0.132	0.128	-	
Cr (Kα)	17.7	18.527	22.638	21.611	17.457	18.348
Mn (Kα)	1.307	1.295	2.182	1.971	1.194	1.187
Fe (Kα)	69.009	67.253	60.285	53.58	69.237	67.751
Ni (Kα)	9.205	8.533	8.456	7.149	9.415	8.764
Mo (Lα)	1.798	1.02	1.618	0.837	1.838	1.047

Table 3.3 : EDS Results (Figure 3-9-b).

Element	1		2		3	
	Weight %	**Atom %**	**Weight %**	**Atom %**	**Weight %**	**Atom %**
C (Kα)	0.409	1.857	0.413	1.874	0.463	2.091
O (Kα)	0.186	0.634	0.27	0.919	0.317	1.075
Si (Kα)	0.328	0.638	0.321	0.623	0.32	0.618
Cr (Kα)	17.362	18.215	17.072	17.883	17.731	18.494
Mn (Kα)	1.091	1.084	0.683	0.678	1.15	1.135
Fe (Kα)	69.259	67.651	69.857	68.128	69.033	67.038
Ni (Kα)	9.594	8.914	9.539	8.85	9.319	8.609
Mo (Lα)	1.771	1.007	1.844	1.047	1.666	0.942

From the SEM photograph of the samples without Ni interlayer formed in 60 minutes, it is clearly seen that at 950°C there are dense gaps in the intermediate region, and at 1050°C, the interface mostly coalesces, but there are still micro-gaps. Elemental values of approximately 316L type stainless steel were revealed at 950°C and 1050°C from the EDS analyzes taken from the marked regions on the SEM images. In sample 1, gaps are seen at the diffusion bonding interface of 316Ls. In addition, as can be seen from the EDS results, the oxygen density is higher in the intermediate layer compared to sample 2 in terms of weight percent and atomic percent. Good bonding could not be achieved due to oxidation and gaps at the interface in Sample 1. The clearest indication of this is that it fails the tensile tests. In sample 2, gaps are seen again, however, it is also seen that the gaps are closed locally in some places due to the high temperature. It is seen that the oxygen density at the interface in sample 2 is less in weight percent and atomic percent than in sample 1. The possibility that the oxidation kinetics may have worked differently at high temperature may explain this situation.

It is also seen that the grain sizes in sample 1 remain relatively smaller than in sample 2 due to the low temperature. In other words, the grain size of sample 2 exposed to higher temperature increased more. Since the overgrowth of grain sizes will directly affect the strength of the material, the increase in grain size means that it should be

closely examined when exposed to high temperature. This interpretation should be interpreted in the light of the information that sample 1 was exposed to 950°C and sample 2 was exposed to 1050°C.

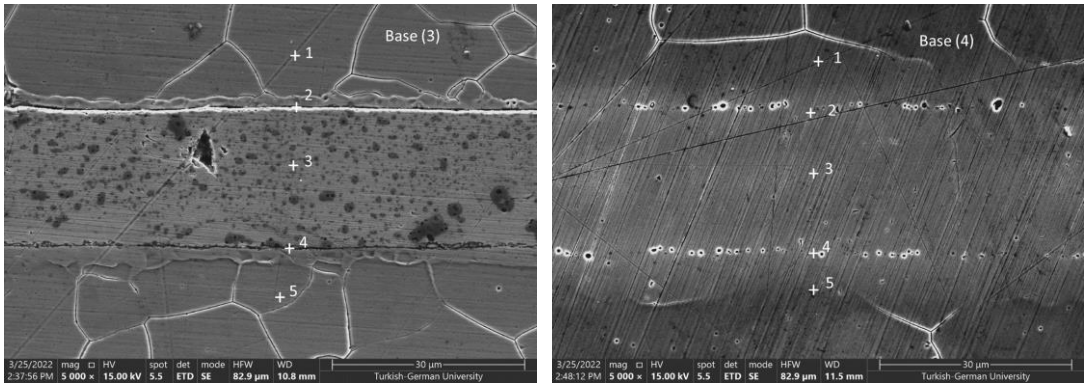

(a) (b)

Figure 3.10 : SEM Images a) Sample No 3. b) Sample No 4.

Table 3.4 : EDS Results (Figure 3-10-a).

Element	1		2		3	
	Weight %	**Atom %**	**Weight %**	**Atom %**	**Weight %**	**Atom %**
C (Kα)	0.419	1.906	2.351	9.452	0.429	2.023
O (Kα)	0.104	0.356	3.05	9.203	0.755	2.672
Si (Kα)	0.34	0.662	0.351	0.604	-	-
Cr (Kα)	17.695	18.586	21.759	20.205	-	-
Mn (Kα)	1.37	1.362	2.765	2.43	-	-
Fe (Kα)	69.001	67.48	24.254	20.968	0.804	0.815
Ni (Kα)	9.267	8.621	44.668	36.734	98.012	94.491
Mo (Lα)	1.802	1.026	0.802	0.404		

When Sample 3 and Sample 4 are examined, it is seen that Ni diffuses more into Fe in Sample 4 due to the high temperature. EDS results also support the image. In Sample 3, on the other hand, due to the low temperature, it is seen that the grain sizes are small, diffusion, that is, the diffusion of Ni into Fe, and the diffusion of Fe into Ni are more limited.

Table 3.4 : EDS Results (Figure 3-10-a) (Cont.).

Element	4		5	
	Weight %	Atom %	Weight %	Atom %
C (Kα)	0.812	3.576	0.414	1.878
O (Kα)	2.629	8.693	0.257	0.874
Si (Kα)	-	-	0.343	0.666
Cr (Kα)	3.888	3.957	16.788	17.582
Mn (Kα)	0.305	0.294	1.494	1.481
Fe (Kα)	5.176	4.903	68.922	67.204
Ni (Kα)	87.19	78.577	10.08	9.349
Mo (Lα)	-	-	1.702	0.966

Table 3.5 : EDS Results (Figure 3-10-b).

Element	1		2		3	
	Weight %	Atom %	Weight %	Atom %	Weight %	Atom %
C (Kα)	0.393	1.792	0.453	2.124	0.438	2.066
O (Kα)	0.15	0.513	0.133	0.468	0.604	2.139
Si (Kα)	0.213	0.416	-		-	-
Cr (Kα)	16.009	16.866	7.363	7.982	0.234	0.241
Mn (Kα)	0.653	0.651	0.492	0.504	-	-
Fe (Kα)	67.767	66.673	27.373	27.628	4.451	4.512
Ni (Kα)	13.337	12.444	63.293	60.768	93.245	89.923
Mo (Lα)	1.478	0.844	0.895	0.526		

In Sample 4, on the other hand, due to the high temperature, it is seen that the grain sizes are big, diffusion, that is, the diffusion of Ni into Fe, and the diffusion of Fe into Ni are more limited. EDS results also support this interpretation.

Table 3.5 : EDS Results (Figure 3-10-b) (Cont.).

Element	4		5	
	Weight %	**Atom %**	**Weight %**	**Atom %**
C (Kα)	0.434	2.041	0.416	1.915
O (Kα)	0.003	0.012	0.125	0.43
Si (Kα)	-	-	0.15	0.295
Cr (Kα)	7.77	8.442	13.312	14.143
Mn (Kα)	0.318	0.328	0.599	0.602
Fe (Kα)	29.875	30.223	57.077	56.459
Ni (Kα)	60.734	58.445	26.972	25.379
Mo (Lα)	0.866	0.51	1.348	0.776

The SEM photograph and EDS analyzes taken from the samples, which were diffusion bonded at 950°C and 1050°C and 60 min as dwell time using a Ni interlayer, are shown in Figure 3.10. SEM images of sample 3 do not show complete fusion between Ni and 316L as intermediate material. As seen in the SEM image of Sample 3, it is seen that the Ni material in the interlayer is not fully diffused with 316L. The failure of Sample 3 in the tensile test also supports this situation. The reason for this can be interpreted as the inability to achieve full coalescence at low temperature. As seen in the SEM image of Sample 3, it is seen that the Ni material in the interlayer is not fully diffused with 316L. The failure of Sample 3 in the tensile test also supports this situation. Sample 1 and Sample 3 are samples prepared at 950°C for 60 minutes. Both samples failed the tensile test. The reasons for its failure have been discussed above. When the region number 1 in sample 3 is examined, it is seen that there are 9.267% and 8.621% Ni by weight and atomic, respectively. Likewise, when the region number 5 in Sample 3 is looked at, it is seen that there are 10.08% and 9.349% Ni by weight and atom, respectively. Considering these Ni ratios, considering that the Ni ratio in base 316L is 9.85%, it was observed that the Ni diffusion was not fully realized in this sample. When looking at the 3rd region in sample 3, it is seen that the ratio of iron by weight is 0.815%. This rate shows that the diffusion is not sufficiently realized. Likewise, the Ni ratio in 1 and 5 in sample 3 is approximately the same as in base 316L. As can be

seen from the small increase in the Ni ratio in the 1 and 5 regions, Ni diffusion has taken place, but it is not sufficient. It is clearly seen that a better bonding was obtained with the increase in temperature, but the presence of micro-gaps between the Ni interlayer and the 316L base material. When looking at point 1 in both samples, it is seen that there is a nickel concentration. It was observed that the Ni ratio was 20 percent higher in the sample produced at 1050°C compared to the sample produced at 950°C. This result showed that the temperature difference increased the nickel diffusion. Also, it indicates that Ni diffusion from the intermediate Ni layer to the base material has occurred both of samples. When looking at the 5th point in both samples, it is seen that there is a nickel concentration. It was observed that the Ni ratio was 300 percent higher in the sample produced at 1050°C compared to the sample produced at 950°C, that is, the nickel diffused almost 3 times more at 1050°C than at 950°C. The effect of the temperature difference on diffusion was seen more clearly at the 5th point.. When looking at the 3rd point in both samples, it was seen that the iron diffusion was at these temperatures. The iron content is 1.5 times higher at 1050°C than at 950°C. The temperature difference at 100°C stood out as the factor that increased this iron diffusion.

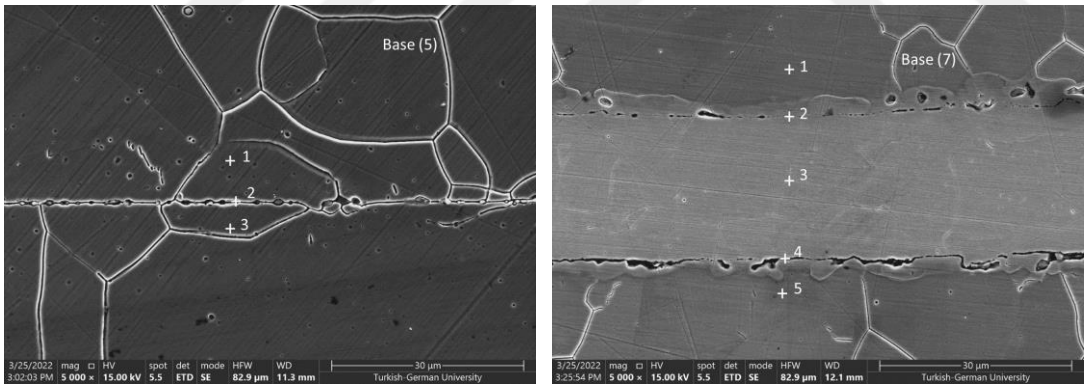

(a) (b)

Figure 3.11 : SEM Images a) Sample No 5. b) Sample No 7.

The difference between Sample 5 and Sample 7 is in the Ni layer. The temperature and time were kept constant. It is seen that the grain sizes are relatively close to each other. It can be said that it is a coincidence that the grain boundary appears to be smaller in sample 5. It is thought that this situation should not occur when more SEM images are taken from different places.

Table 3-6 : EDS Results (Figure 3-11-a).

Element	1		2		3	
	Weight %	**Atom %**	**Weight %**	**Atom %**	**Weight %**	**Atom %**
C (Kα)	0.315	1.433	0.082	0.377	0.307	1.401
O (Kα)	0.254	0.867	-	-	0.195	0.668
Si (Kα)	0.303	0.589	0.062	0.122	0.246	0.479
Cr (Kα)	17.473	18.354	18.254	19.41	17.042	17.951
Mn (Kα)	1.128	1.121	1.612	1.623	1.158	1.154
Fe (Kα)	69.533	68.001	71.315	70.604	70.073	68.723
Ni (Kα)	9.352	8.7	7.841	7.384	9.267	8.646
Mo (Lα)	1.642	0.935	0.834	0.48	1.711	0.977

Table 3-7 : EDS Results (Figure 3-11-b).

Element	1		2		3	
	Weight %	**Atom %**	**Weight %**	**Atom %**	**Weight %**	**Atom %**
C (Kα)	0.389	1.765	0.437	1.989	0.453	2.172
O (Kα)	0.203	0.692	0.086	0.294	-	-
Si (Kα)	0.307	0.596	0.297	0.578	-	-
Cr (Kα)	17.262	18.117	16.799	17.652	0.505	0.56
Mn (Kα)	1.098	1.09	1.328	1.321	-	-
Fe (Kα)	69.518	67.931	69.454	67.949	1.658	1.71
Ni (Kα)	9.492	8.823	9.999	9.305	97.385	95.559
Mo (Lα)	1.732	0.985	1.599	0.911	-	

In Sample 7, on the other hand, due to the high temperature, it is seen that the grain sizes are large, diffusion, that is, the diffusion of Ni into Fe, and the diffusion of Fe into Ni are more limited. EDS results also support this interpretation.

Table 3-7 : EDS Results (Figure 3-11-b) (Cont.).

Element	4		5	
	Weight %	**Atom %**	**Weight %**	**Atom %**
C (Kα)	0.46	2.097	0.328	1.494
O (Kα)	1.072	3.67	0.235	0.803
Si (Kα)	0.175	0.341	0.286	0.557
Cr (Kα)	9.102	9.588	17.194	18.066
Mn (Kα)	1.134	1.131	1.563	1.555
Fe (Kα)	29.22	28.658	69.087	67.588
Ni (Kα)	57.797	53.922	9.688	9.016
Mo (Lα)	1.04	0.594	1.618	0.921

The SEM photograph of the sample, which was diffusion bonded at 1050°C for 120 minutes without an intermediate layer, is shared in Figure 3.11, and it is seen that the in sample 5, there is no complete integration in the diffusion bonding region between the 316L materials. Despite all this, the concentration of grain boundaries in the diffusion bonding region emerges as a logical explanation for the high tensile force. This indicates that diffusion coupling took place well in Sample 5. The tensile test results also support this interpretation. When the SEM image of sample 7 is examined, it is seen that the integration has occurred relatively in the diffusion bonding region. It is seen that the weight ratio of iron in region 3 is 1.658%. This ratio indicates that iron diffusion takes place into pure Ni. Contrary to this, it is seen that the Ni diffusion does not occur as seen in the 1 and 5 regions. It is thought that the Ni atom in 316L does not have enough energy or enough time to both defect and displace. However, at the 4th point, the presence of almost the same ratio of iron and nickel indicates the point where complete diffusion takes place. Grain sizes are affected by temperature. It is seen from the SEM images of sample 5 and sample 7 obtained at the same temperature and time, that is, at 1050°C and for 120 minutes, that the grain sizes are approximately the same. This helps us to see the effect of the Ni interlayer on the strength more clearly. In the tensile test, 394 MPa for sample 7 and 284 MPa for sample 5 are obtained, and it will be useful to examine in the light of this information.

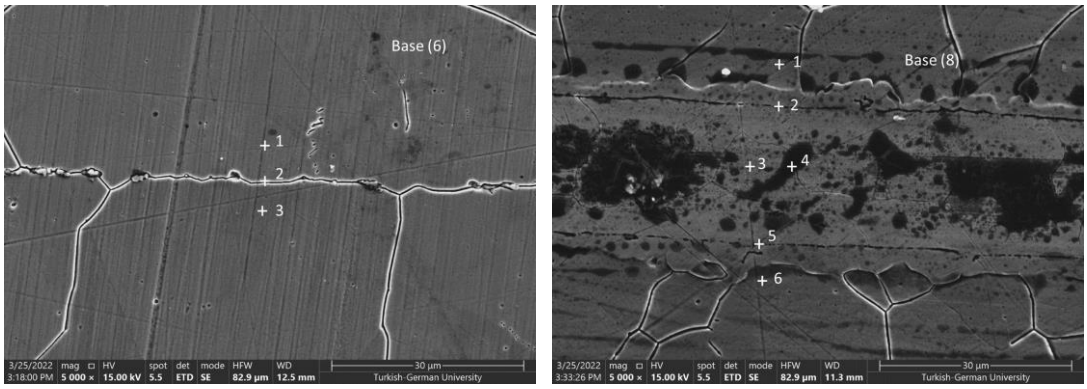

(a) (b)

Figure 3.12: SEM Images a) Sample No 6. b) Sample No 8.

Table 3-8 : EDS Results (Figure 3-12-a).

Element	1		2		3	
	Weight %	**Atom %**	**Weight %**	**Atom %**	**Weight %**	**Atom %**
C (Kα)	0.404	1.844	0.457	2.064	0.398	1.806
O (Kα)	0.007	0.024	0.389	1.319	0.278	0.947
Si (Kα)	0.286	0.559	0.306	0.591	0.277	0.537
Cr (Kα)	17.244	18.183	17.099	17.826	17.36	18.183
Mn (Kα)	1.138	1.136	0.707	0.698	1.201	1.191
Fe (Kα)	69.549	68.282	69.687	67.642	69.502	67.776
Ni (Kα)	9.582	8.949	9.615	8.877	9.241	8.572
Mo (Lα)	1.789	1.022	1.739	0.983	1.741	0.989

The difference between Sample 6 and Sample is the Ni layer. Temperature and time parameters are constant for both samples and are 1050°C and 180 minutes. The effect of these parameters on grain sizes is seen in detail in SEM images. In sample 6, the grain boundaries were enlarged. In some places, full penetration has been achieved, and in some places, micro-voids are still visible. There is no difference in the EDS results, and it clearly reveals the 316L elemental spectrum. It is seen that the grain boundaries in Sample 8 are not as large as in Sample 6. However, when the samples of Sample 1 and Sample 3, where the temperature is low, are examined, it is not difficult to see the obvious difference.

Table 3-9 : EDS Results (Figure 3-12-b).

Element	1		2		3	
	Weight %	**Atom %**	**Weight %**	**Atom %**	**Weight %**	**Atom %**
C (Kα)	0.347	1.576	0.559	2.551	0.51	2.392
O (Kα)	0.249	0.85	0.04	0.137	0.807	2.841
Si (Kα)	0.294	0.571	0.176	0.344	-	-
Cr (Kα)	17.521	18.392	15.202	16.016	-	-
Mn (Kα)	1.096	1.089	0.84	0.838	-	-
Fe (Kα)	69.365	67.791	65.354	64.104	1.164	1.175
Ni (Kα)	9.425	8.762	16.108	15.029	97.519	93.592
Mo (Lα)	1.703	0.969	1.72	0.982	-	

Table 3-9 : EDS Results (Figure 3-12-b) (Cont.).

Element	4		5		6	
	Weight %	**Atom %**	**Weight %**	**Atom %**	**Weight %**	**Atom %**
C (Kα)	1.754	7.347	0.449	2.046	0.447	2.027
O (Kα)	3.682	11.574	1.085	3.711	0.159	0.541
Si (Kα)	-	-	-	-	0.304	0.589
Cr (Kα)	-	-	9.707	10.218	17.457	18.303
Mn (Kα)	-	-	1.496	1.49	-	-
Fe (Kα)	1.403	1.263	29.106	28.524	70.64	68.955
Ni (Kα)	93.161	79.815	57.593	53.689	9.263	8.601
Mo (Lα)	-	-	0.565	0.322	1.731	0.984

Looking at the EDS results of Sample 8, it is seen that Ni diffuses into Fe. This situation is clearly seen when the surroundings of the interlayer are examined.

From the SEM photograph of the sample, which was diffusion bonded for 180 minutes without an intermediate layer at 1050°C, that the intermediate zone is almost completely disappeared, as in the 120 minute parameter. In sample 6, less micro-voids are still observed in region 2, where diffusion bonding between 316L materials is still observed, and the oxide layer is reduced. The formation of grain boundaries along the diffusion-binding region provides convincing evidence that diffusion-binding occurs well. However, the fact that the grains are large and rare in sample 6 supports the fact that it is less strength in the tensile test than sample 5, where the grains are smaller and denser. SEM photo of diffusion bonding made using Ni interlayer for 180 minutes is presented in Figure 3.12. In sample 8, almost complete integration of the residual Ni interface with the 316L base material is seen in the diffusion bonding region. Particularly, the disappearance of grain boundaries in the diffusion bonding region explains this situation. When the EDS results in regions 2 and 5 are examined, it is seen that the concentrations of iron and nickel are very close to each other. It is seen that the iron ratio is 65.354% by weight and the Ni ratio is 16.108% by weight in the 2nd region. In Region 5, it is seen that the iron ratio is 29.106% by weight, and the Ni ratio is 57.593%. All this shows why the Sample 8 performed the best in the tensile test.

When the SEM and EDS results are evaluated in general, it is possible to say that the obvious effect of temperature and waiting time on the microstructure and the growth of grain boundaries is seen. As the temperature and time increase, it is seen that penetration is achieved, that is, full diffusion is approached. It can also be said that the Ni interface is clearly effective in the origination of this diffusion.

3.4 Microhardness Test Results

The microhardness test was carried out 5 times for each sample, starting from the midpoint of the two main materials, towards both material directions at 30μm intervals. The locations of the measurements taken and their appearance on the materials are shared in Figure 3.13. The results of the microhardness tests performed on the samples produced for each parameter are shared in Table 3.5. As base material 316L, microhardness tests results median is 301 HV.

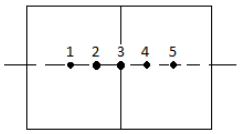

(a)

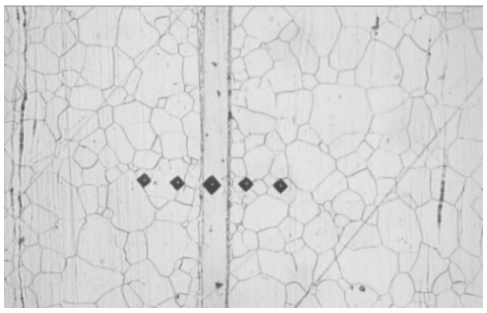

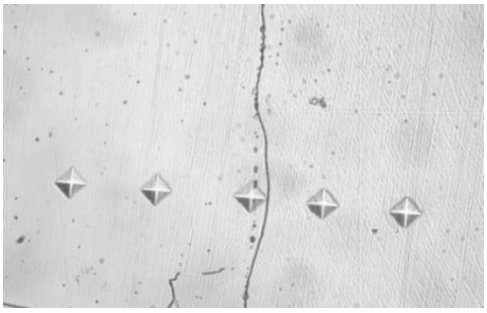

(b) (c)

Figure 3.13 : Microhardness Measurements Points. a) Schematic Draw. b) 316L – Ni – 316L Sample. c) 316L-316L Sample.

Table 3.5 : Microhardness Results.

Sample No	Microhardness Measure [HV]				
	1	2	3	4	5
1	333	311	291	299	322
2	293	298	292	258	277
3	261	262	265	288	312
4	297	312	239	295	313
5	278	284	282	276	300
6	383	351	377	370	391
7	233	235	229	238	232
8	362	398	231	370	389

The difference in the production of samples 1 and 2 was the temperature. However, it is clearly seen that the vickers microhardness value does not change with temperature. Microhardness values change in symmetrical values ranging from 255-333. It was observed that the temperature difference of 100°C did not make a significant change on the basis of these samples. Microhardness values are correlated with each other,

except for minor hardness differences in 1 and 2 locations in samples 3 and 4. This can be interpreted as the situation in samples 1 and 2. It was observed that the temperature difference of 100°C did not have a visible effect on the hardness. Samples 5 and 6 do not have a ni interlayer. For this reason, the same correlation with respect to each other continues. However, the microhardness value of the 6th sample is approximately 50% higher than the 5th sample. Even though they are produced at the same temperature, the emergence of this ratio is that the waiting time of the 6th sample is 1 hour longer than the 5th sample. Microhardness value in sample 6, which was exposed to diffusion bonding process under 8.5 MPa pressure at 1050°C for 3 hours, was higher than sample 5 due to waiting time. Considering the samples 7 and 8, we see that the hardness value is 230 HV in the region number 3, that is, in the region where the Ni interlayer is located. Looking at regions 1-2 and 4-5, it is seen that the microhardness value is higher in sample 8 exposed to 1050°C for 1 more hour. The same situation is seen in the samples 5 and 6 as well. More exposure to temperature shows that the microhardness value increases. When we look at the general situation, the effect of exposure to temperature on the hardness value is greater than the change in temperature. In other words, the exposure time as a parameter has a much greater effect on the microhardness value than the temperature. This interpretation can be made in terms of microhardness.

4. PRODUCTION AND TESTS OF PCHE

The production stages of the heat exchanger are detailed in two main headings as plate manufacturing and connecting the plates. After the plate production, the PCHE production process started. Diagram of the production process is shared in Figure 4.1.

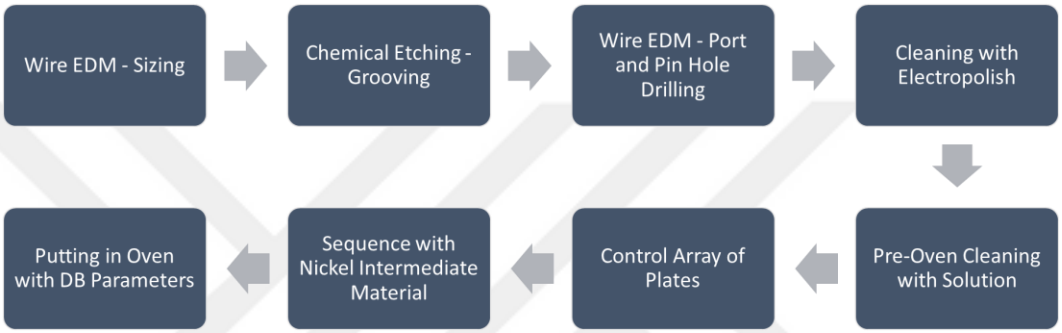

Figure 4.1 : Heat Exchanger Production Process.

After the production of PCHE, hydrostatic and leakage tests were carried out.

4.1 Manufacturing of PCHE Plates

The point to be considered during the supply of the plates is the verification of the material composition and mechanical properties with the material certificate. Differences up to ±0.05 mm tolerance were detected in the 2 mm plate thickness after the supply of verified materials. Since these geometric defects will prevent homogeneous joining on all surfaces of the plates, the parts have been tried to be corrected by double-sided grinding and lapping processes in order to eliminate these geometric defects. However, since the material of the heat exchanger is 316L from austenitic stainless steels, it shows weak magnetic properties. Therefore, grinding processes could not be performed because the 2 mm thick plates forming the heat exchanger could not be fixed. When we subjected the 2 mm thick plates to the lapping process directly instead of grinding, since the amount of sawdust removed during lapping was very small, it was necessary to do the lapping process for a long time. This

causes huge costs. In order to reduce the cost of the 2 mm thick plates in the lapping process, grinding by pulling the plates on the vacuum table instead of grinding on the magnetic table has been investigated. For this process, a company with a vacuum table could not be found. As a result, when the 2mm thick plates produced by milling could not be corrected, the milling process could not be efficient. Since the 20 mm thick lower and upper plates to be used in the outer shell of the heat exchanger can be fixed with the help of a vise, their processing was carried out with the help of grinding and lapping.

After the plates are produced with not good condition, firstly, milling defects, ie 2 mm plates that were not in good condition, were corrected with a chemical acid bath. Then, it is necessary to open a channel as a second step. The opening of channels suitable for the previously determined channel geometry was made by chemical etching. In the chemical etching process, first of all, the parts outside the channel regions are masked with dyes that do not react with acid. After the masking process was completed, the channel geometries were formed by keeping the plates in an acid bath. There are two important aspects in the chemical etching process. The first is good masking. Otherwise, abrasions that may cause transitions between the channel walls and pitting may occur on the joining surfaces. The second issue is the waiting time of the plates in the acid bath. For this process, the chemical composition of the acid bath was kept constant, and the time was optimized until the desired depth was reached. After the optimum time was determined, mass production was started.

Apart from the creation of the channel geometries, distortions occur during the sizing of the plates, the heat exchanger inlet-outlet ports and the drilling of the pin holes. For this, the wire erosion process, which applies the least thermal and mechanical load, is preferred. In addition, since the tolerance of the wire erosion process is ±0.002, more precise centering elements have been created.

After the geometrical elements of the plates were formed, the oil and dirt accumulated on the plates during processing and transportation were removed by electropolishing. The final geometry of the plates after the electropolishing process is shared in Figure 4.2 and Figure 4.3.

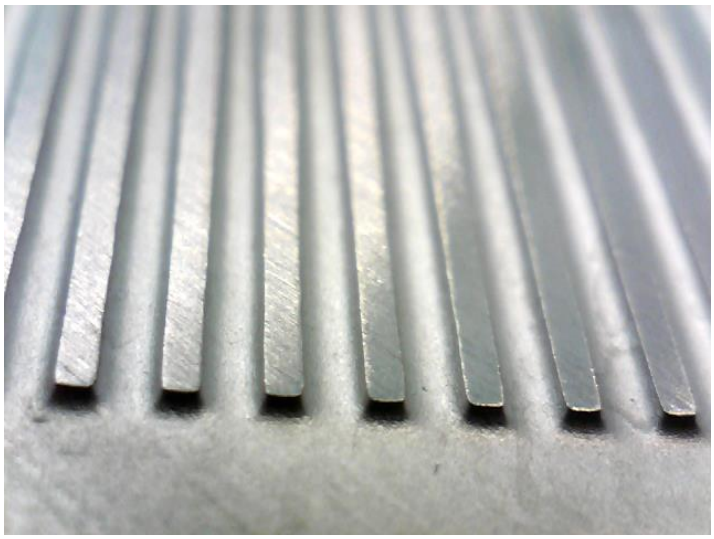

Figure 4.2 : Channel Geometries as a Result of Chemical Etching.

Figure 4.3 : Printed Circuit Heat Exchanger Plate.

4.2 Connection of PCHE Plates and Production of PCHE

In order to connect the plates, in the first step, according to the final arrangement of the heat exchanger, the plates were arranged on top of each other in a controlled manner as in Figure 5. A solution was used during arranging to clean the oil and dirt accumulated on the plates during transportation or due to the ambient atmosphere.

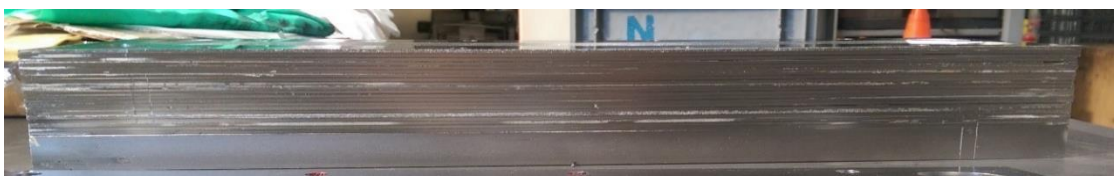

Figure 4.4 : Arrangement of PCHE Plates.

The best parameters determined during the development of the diffusion bonding methodology were obtained in samples with nickel fillers. These parameters are; It has a temperature of 1050°C, a pressure load of 8.5 MPa, an argon atmosphere and a dwell time of 180 minutes. In line with these parameters, the sequence was updated again by adding nickel filler material between the plates. An array in the form of a nickel filler material after a heat exchanger plate was formed as shared in Figure 4.5. At this stage, previously prepared Ø10 mm diameter pins were used to ensure the correct alignment of the plates and nickel filler materials. The internal stresses of the pins were removed by heat treatment so that these pins do not distort the alignment of the plates by buckling due to thermal expansion. The pins are then precision ground. A ground graphite plate is placed at the bottom of the plates to prevent the plates from tipping or slipping due to the pressure load applied during the diffusion bonding process. Also, in order to prevent the bottom plate from sticking to the graphite plate, an anti-adhesive paste was applied to the plate. Afterwards, the sequence was completed and the assembly shared in Figure 4.6, was obtained. In order to better control the temperature of the plates in the oven, a thermocouple hole has been opened on the bottom plate near the oven door. Thus, the formation of thermal balance on the parts was followed more precisely.

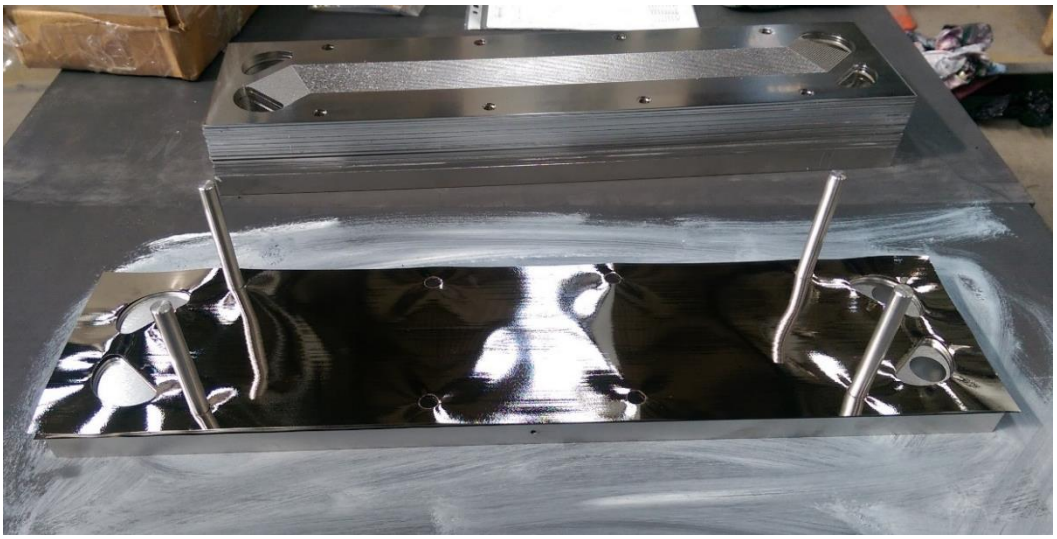

Figure 4.5 : Arrangement of PCHE Plates with Nickel Filler.

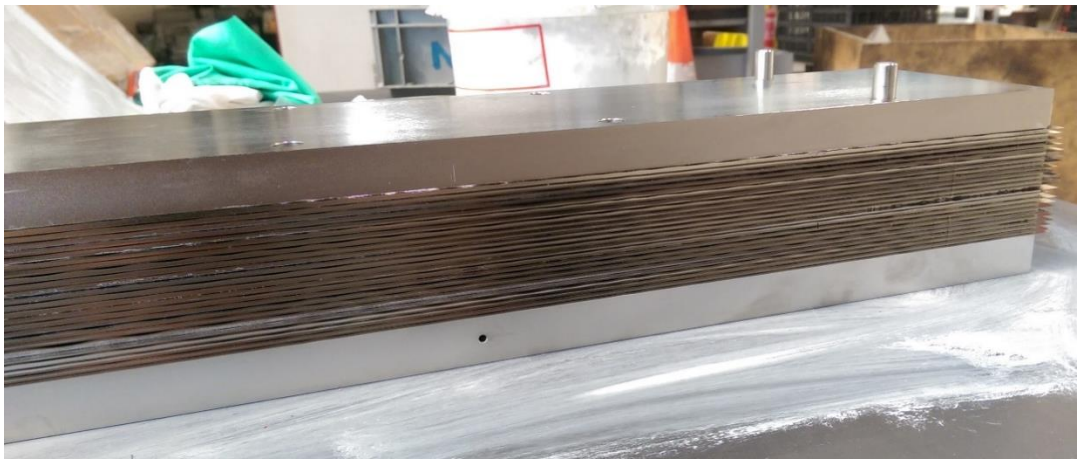

Figure 4.6 : Final Arrangement with Nickel Filler.

Connection interfaces have been created for the integration of the heat exchanger discharged from the furnace into the test setup. For this, the previously drilled port holes were threaded with a ¾" NPT guide. The reason why the connection interfaces are left after firing is to prevent leaks from occurring due to distortions in the thread areas. The final heat exchanger, manufactured by diffusion bonding process, connection ports opened, shared in Figure 4.7.

Figure 4.7 : Final PCHE Manufactured with Diffusion Bonding.

4.3 Tests and Results of PCHE

The heat exchanger, whose production was completed and connection interfaces were created, was integrated into the hydrostatic test setup. The heat exchanger is pressurized to 200 bar by means of a water pump. It has been checked from the

pressure gauges that the pressurized heat exchanger maintains a pressure of 200 bar for at least 1 hour. As a result, no pressure drop was observed and the hydrostatic test of the heat exchanger was successful.

Figure 4.8 : Hydrostatic Pressure Test of PCHE.

After the hydrostatic test, the heat exchanger was pressurized with gas to 6 bar. 15-30 minutes after pressurization. The solution was applied to the heat exchanger junction areas and junction interfaces, which showed bubbles. Afterwards, it was observed that no bubbles were formed after waiting for the specified time. Thus, the heat exchanger bubble (leakage) test has been successfully completed.

Figure 4.9 : Leakage Test of PCHE.

It has also successfully passed the PCHE performance test. PCHE sCO2 operated at 453°C and 80 bar pressure. The calculated thermal capacity value was between 24.28 - 24.92 kW. This is very close to the technical design requirement of 25 kW. The production of PCHE produced by diffusion coupling method with the measured values was successful.

Figure 4.10 : Performance Tests of PCHE.

5. CONCLUSION

In this thesis study, which was carried out within the scope of development of diffusion bonding methodology, optimum bonding parameters of AISI 316L type stainless steel pair were investigated by using diffusion welding method with and without interlayer Ni. For this purpose, diffusion bonding was carried out in an Argon gas atmosphere at 8.5 MPa pressure for 60, 120 and 180 minutes and at temperatures of 950°C to 1050°C.

As a result of the diffusion bonding tensile tests performed without using a Ni interlayer, the maximum strength was obtained as 407 MPa for the samples combined at 1050°C for 180 minutes which is coded as sample 8 in study. As a result of diffusion bonding tests using Ni interlayer, the maximum strength was obtained as 394 MPa on average for the samples joined for 120 minutes at 1050°C which is indicated in study as sample 7. At the same time, results close to each other were obtained in the parameters of 120 and 180 minutes at 1050°C.

It has been seen from the optical microstructure and SEM photographs of the joined samples that the junctions in which the intermediate region is completely eliminated were obtained in the samples produced at 1050°C with and without Ni interlayer at 120 and 180 minutes parameters. Again, from the EDS analysis, it was concluded that the diffusion rate increased with the increasing time of Fe diffusion towards the Ni interlayer and again towards the base material.

As a result of all the studies, the production of printed circuit heat exchangers by developing the diffusion bonding method was achieved for the first time in the country. The realization of this process was indirectly one of the first, by using 316L as the base material and nickel as the intermediate layer.

Printed circuit heat exchanger (PCHE) was produced by using the sample results that gave the best results. The heat exchanger has been tested at 80 bar and 453°C as performance test which meets the technical requirements. As a hydrostatic test, heat exchanger performed at room temperature, and 200 bar successfully. In addition to this PCHE also gave 25 kW power.

Thus, the diffusion bonding process developed for the designed printed circuit heat exchanger (PCHE)

REFERENCES

[1] **J. W. Seo, Y. H. Kim, D. Kim, Y. D. Choi, and K. J. Lee**, (2015), Heat transfer and pressure drop characteristics in straight microchannel of printed circuit heat exchangers, *Entropy*, vol. 17, no. 5, pp. 3438–3457, doi: 10.3390/e17053438.

[2] **L. R. and R. D. H.J.E**, (2017), *Compact Heat Exchanger: Selection, design and operation*, Second Edition. Cambridge: Oxford.

[3] **N. CONNOR**, (May 22, 2019), Overall Heat Transfer Coefficient, *Thermal Engineering*, https://www.thermal-engineering.org/what-is-heat-exchanger-heat-transfer-coefficient-u-factor-definition/ (accessed Jan. 02, 2022).

[4] **AZOM**, "Thermal Proporties of 316L and Pure Nickel."

[5] **ASME**, (2015), ASME Sec VIII Div1 2015, UG-99, New York.

[6] **S. ÇELİK**, (1996), Koruyucu Gaz Altında Saf Alüminyum ve Bakır'ın Difüzyon Kaynağı Şartlarının Belirlenmesi.

[7] **Tekin A.**, (1986), Malzemelerin Elektronik Özellikleri, İTU Yayınları, İstanbul.

[8] **TOPBAŞ M. A.**, (1993), Isıl İşlemler, Yıldız Teknik Üniversitesi, İstanbul.

[9] **W. D. CALLISTER and D. G.** (2009), RETHWISCH, *MATERIALS SCIENCE AND ENGINEERING AN INTRODUCTION*, vol. EIGHT EDITION. New Jersey: WILEY.

[10] **Fidan L.**, (2006), Saf Alüminyum ve Saf Bakırın Difüzyon Kaynağında Arafazların Oluşumu ve Etkisi, Balıkesir.

[11] **N. F. Nikolaĭ F. Kazakov**, (1985), *Diffusion bonding of materials*. Pergamon Press.

[12] **P. Sabharwall, D. E. Clark, R. E. Mizia, M. v. Glazoff, and M. G. McKellar**, (2013), Diffusion-welded microchannel heat exchanger for industrial processes, *Journal of Thermal Science and Engineering Applications*, vol. 5, no. 1, pp. 1–7, doi: 10.1115/1.4007578.

[13] **Üngören Serkan**, (2007), Ti-Al-V Alaşımlarının Difüzyon Kaynaklı Bağlantılarının Mekanik ve Mikroyapısal Özelliklerinin İncelenmesi, Kocaeli.

[14] **K.N. and G.B.**, (2013), *Modern Kaynak Teknolojisi*, vol. Epa. Ankara: Mat Basım Yayın.

[15] **Özdemir U.**, (2003), Difüzyon Kaynaklı TiAl ve Ti6Al4V alaşımlarının içyapı ve mekanik karakterizasyonu, Antakya.

[16] **Yılmaz O.**, (1999), Östenitik Paslanmaz Çelik ve Bakır Çiftinin Difüzyon Kaynağı ile Birleştirilmesinde KAynak Parametrelerinin Birleştirilmeye Etkisi, Elazığ.

[17] **Bartle P.**, (1972), *Diffusion Bonding A Look At The Future*.

[18] **Pakdil M.**, (2001), Difüzyon Kaynağı ile Birleştirilmiş Ti ve Alaşımlarının Kırılma Davranışlarının İncelenmesi, Antakya.

[19] **İpekoğlu G.**, (2003), Difüzyon Kaynaklı TiAl-TiAl Alaşımlarının İçyapı ve Mekanik Özelliklerinin İncelenmesi, Antakya.

[20] **Tuncel S.**, (1989), Yüksek Alaşımlı Bir Takım Çeliği ile Az Alaşımlı bir Islah Çeliğinin Difüzyon Kaynağı ile Birleştirilmesi Üzerine Deneysel Çalışmalar, Kocaeli.

[21] (1987), *Welding Handbook*, Eight Edition., vol. Vol.2.

[22] **Kurt A.**, (1997), Katı Hal Birleştirmeler İçin Difüzyon Kaynağının İncelenmesi, Ankara.

[23] **B. Z. Yıldırım**, (2001), Difüzyon Kaynağının Demir Dışı Hafif Malzemelere Uygulanması, Eskişehir.

[24] **D. M. R. R. G. S. ve L. I. B. A. Burroughs**, (1980), Application of Superplastic Forming/Diffusion Bonding (SPF/DB) of Titanium Structure (T-38 Landing Gear Strut Door), San Antonio.

[25] **G. İpekoğlu**, (2003), Difüzyon Kaynaklı TiAl-TiAl Alaşımlarının İçyapı ve Mekanik Özelliklerinin İncelenmesi, Antakya.

[26] **T. Nguyentat**, "VACETS," *VACETS*.

[27] **Z. X. Guo**, (1985), Diffusion Bonding of Superplastic Materials, Manchester.

[28] **FUJI**, (Jan.02,2022),FUJI denolo. http://www.fujidenolo.co.jp/english/technology/diffusion-bonding.html (accessed Jan. 02, 2022).

[29] **Intergage**, (Jan.02,2022) "Heatric,". https://www.heatric.com/diffusion_bonding.html (accessed Jan. 02, 2022).

[30] **S. Dağlılar**, (1994), AISI 304 Tipi Paslanmaz Çelik ile 6101 No'lu Aluminyum Alaşımının KAtı Hal Difüzyon KAynağı ile Birleştirilmesi, İstanbul.

[31] **Mollaoğlu H.**, (2004), SiC Partikül Takviyeli Al Metal Matrisli Kompozitlerin Difüzyon Kaynağı, İstanbul.

[32] **N. F. Kazakov**, (2013), *Diffusion Bonding of Materials*, vol. P10. Oxford: Pergamon.

[33] **A. Hill-F and E. R. Wallach**, (1989), MODELLING SOLID-STATE DIFFUSION BONDING.

[34] **K. Pongmorakot, S. Nambu, Y. Shibuta, and T. Koseki**, (Apr. 2017,), Investigation on the mechanism of steel/steel solid-state bonding at low temperatures, *Science and Technology of Welding and Joining*, vol. 22, no. 3, pp. 257–263, doi: 10.1080/13621718.2016.1222237.

[35] **C. Zhang, H. Li, and M. Li**, (Mar. 2017), Role of surface finish on interface grain boundary migration in vacuum diffusion bonding, *Vacuum*, vol. 137, pp. 49–55, doi: 10.1016/j.vacuum.2016.12.021.

[36] **Z. L. An, W. L. Luan, F. Z. Xuan, and S. T. Tu**, (Nov. 2005), High Temperature Performance of 316L-SS Joint Produced by Diffusion Bonding, *Key Engineering Materials*, vol. 297–300, pp. 2795–2799, doi: 10.4028/www.scientific.net/kem.297-300.2795.

[37] **S.T. Tu**, (2004), Environmental effect on fracture and damage, in *New Need of Structural Integrity Technology for High Temperature Applications*, S. T. T. and Z. D. W. H. Eds G.C. Sih, Ed. Zhejiang university Press, pp. 43–57.

[38] **G. V. N.S. Pradeep**, (1999), Cryogenics, vol. Vol. 39, pp. 517–527.

[39] **K. K. T. H. and K. I. T. Takeda**, (1997), Nuclear Engineering and Design, vol. 168, pp. 11–21.

[40] **T. A. and M. E. H. Nishi**, (1998), Fusion Engineering and Design, vol. 39–40, pp. 505–511.

[41] **KOÇER SERMİN**, (1998), YÜKSEK KROM NİKEL ALAŞIMLI PASLANMAZ ÇELİĞİN ALAŞIMSIZ DÜŞÜK KARBONLU ÇELİKLE DİFÜZYON KAYNAĞININ ARAŞTIRILMASI, ELAZIĞ.

[42] **B. BİLGİN**, (2007), "Ti-6Al-4V/304L MALZEME ÇİFTİNİN BAKIR ARATABAKA KULLANILARAK DİFÜZYON KAYNAĞI İLE BİRLEŞTİRİLMESİ," ELAZIĞ.

[43] **E. ATASOY**, (2007), "TİTANYUM VE DÜŞÜK KARBONLU ÇELİK ÇİFTİNİN ARABAĞLAYICI KULLANILARAK DİFÜZYON KAYNAĞI İLE BİRLEŞTİRİLEBİLİRLİĞİNİN ARAŞTIRILMASI," Zonguldak Karaelmas Üniversitesi, KARABÜK.

[44] **K. Aydin**, (2011), TİTANYUM VE BAKIR MALZEMELERİN DİFÜZYON KAYNAK YÖNTEMİ İLE BİRLEŞTİRİLEBİLİRLİĞİNİN ARAŞTIRILMASI, Karabük Üniversitesi, KARABÜK.

[45] **F. TOLUN**, (2013), BAKIR VE PORSELEN MALZEMELERİN DİFÜZYON KAYNAĞI İLE BİRLEŞTİRİLEBİLİRLİĞİNİN İNCELENMESİ VE ANALİZİ, BALIKESİR ÜNİVERSİTESİ, BALIKESİR.

[46] **A. Yildiz**, (2014), TİTANYUM VE FERRİTİK PASLANMAZ ÇELİK MALZEMELERİN NİKEL ARABAĞLAYICI KULLANILARAK DİFÜZYON KAYNAK YÖNTEMİ İLE BİRLEŞTİRİLEBİLİRLİĞİNİN ARAŞTIRILMASI, KARABÜK.

[47] **M. T. Salehi**, (1990), *Isostatic Diffuison of Some Superplastic Alloys*. Manchester: UMIST.

[48] **P. K. Samal ve J. W. Newkirk**, (2015), *Powder Metallurgy*, vol. 7. Ohio: ASM International.

[49] **W.-L. L. F.-Z. X. ve S.-T. T. Z.-L. An**, (2005), High Temperature Performance of 316L-SS Joint Produced by Diffusion Bonding, Shanghai.

[50] **Z. An and S. Tu**, (2006), Mechanical Performance and Failure Modes of Direct Diffusion Bonding Joints of 316L Stainless Steel, Shangai.

[51] **B. Sunden**, (2005), High temperature heat exchangers (HTHE), in *5th International Conference on Science, Engineering and Technology*, Vellore.

[52] **T. S. D. K. and S. J. D. X. Li**, (2009), Materials for nuclear diffusion-bonded compact heat exchangers, *ICAPP'09*.

[53] **R. M. M. V. G. ve M. M. W. P. D. Clark**, (2012), Diffusion Welding of Compact Heat Exchangers for Nuclear Applications, *Idaho Naional Laboratory, Idaho Falls*.

[54] **W. C. and W. M**, (2004), Stahlschlüssel, Marbach: Verlag Stahlschlüssel Wegst GmbH.

[55] (2004), TS 138 EN 10002-1 (Nisan 204) Metalik Malzemeler - Çekme Deneyi - Bölüm 1: Ortam Sıcaklığında Deny Metodu, Türk Standartları Enstitüsü, Ankara.

APPENDIX-1

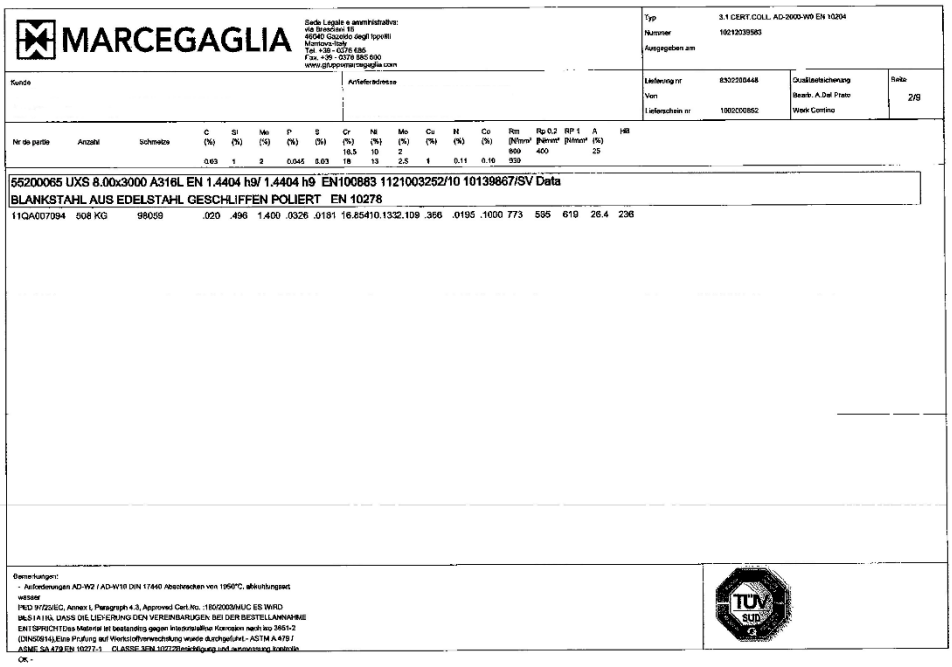

MARCEGAGLIA

Sede Legale e amministrativa:
via Bresciana 16
46040 Gazoldo degli Ippoliti
Mantova-Italy
Tel. +39 - 0376 685
Fax. +39 - 0376 685 600
www.gruppomarcegaglia.com

Typ 3.1 CERT.COLL. AD-2000-W0 EN 10204
Nummer 19212039583
Ausgegeben am

Kunde

Anlieferadresse

Lieferung nr 8302388448
Von
Lieferschein nr 1902000862

Qualitätsteicherung
Bearb. A.Del Prato
Werk Corrino

Seite 2/9

Nr de partie	Anzahl	Schmelze	C (%)	Si (%)	Mn (%)	P (%)	S (%)	Cr (%)	Ni (%)	Mo (%)	Cu (%)	N (%)	Co (%)	Rm (N/mm²)	Rp 0,2 (N/mm²)	RP 1 (N/mm²)	A (%)	HB
			0,03	1	2	0,045	0,03	16,5	10	2				500	400		25	

55200065 UXS 8.00x3000 A316L EN 1.4404 h9/ 1.4404 h9 EN100883 1121003252/10 10139867/SV Data
BLANKSTAHL AUS EDELSTAHL GESCHLIFFEN POLIERT EN 10278

11QA007094	508 KG	98059	.020	.496	1.400	.0326	.0181	16.85	410.13	32.109	.366	.0195	.1000	773	595	619	26.4	236

Bemerkungen:
- Anforderungen AD-W2 / AD-W10 DIN 17440 Abschrecken von 1050°C, abkühlungsart wasser
PED 97/23/EC, Annex I, Paragraph 4.3, Approved Cert.No. :180/2003/MUC ES IWRD
WIR BESTÄTIGEN, DASS DIE LIEFERUNG DEN VEREINBARUGEN BEI DER BESTELLANNAHME ENTSPRICHT.Das Material ist bestandig gegen interkristalline Korrosion nach iso 3651-2
(DIN50914).Eine Prüfung auf Werkstoffverwechslung wurde durchgeführt. - ASTM A 479 / ASME SA 479/EN 10272-1 CLASSE 3EN 10272Besichtigung und abmessung kontrolle
OK. -

TÜV SÜD

APPENDIX-2

16094

Certificate - Zeugnis

OUTOKUMPU

Certificate of Chemical Composition acc to EN 10204 – 2.1

Date – Datum	Load – Ladung	Certificate No – Zeugnis Nr
2010-11-12		G13594S00E

Your order – Ihre bestellung	Order-Auftrag	Invoice – Rechnung
	B11901	

Purchaser – Besteller
TURKEY

Requirements – Anforderungen
EN 10088-1 1(95)

Destination – Lieferadress
TURKEY

Product – Erzeugnisform
SHEET 2B

SECOND CHOICE MATERIAL

Grade - Werkstoff	EN	ASTM
	1.4404	

Brand mark / Herstellerzeichen	Inspectors stamp / Abname – Stempel	Melting Process / Erschmeltzungsart
OUTOKUMPU		E + CLU / AOD

Extent of delivery - Lieferumfang

Item –ID No.	No – Anzahl	Dimension – Abmess. T * W * L (mm)	Weight – Gewicht (kg)	Heat No – Schmelze Nr
		2,00 X 1000 X 2000	592	83960

Chemical Composition – Chemiche Zusammensetzung

C	Si	Mn	P	S	Cr	Ni	Mo	Ti	N		
0,021	0,46	1,76	0,03	0,0015	17,09	10,09	2		0,0423		

Test results comply with order requirements

H Buhre

Authorized Inspector & QA Manager

Outokumpu Nordic AB
Abramsons väg 2, P.O. Box 1134, SE-631 80 Eskilstuna, Sweden
Tel. +46 16 34 99 50, Fax +46 16 34 99 99, www.outokumpu.com
Reg. No. 556069-1924, Vat No. SE556069192401

CURRICULUM VITAE

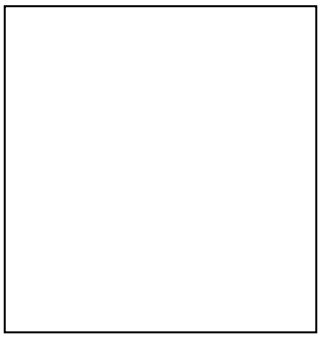

EDUCATION:

- **B.Sc.** **:** 2017, Istanbul Bilgi University, Faculty of Engineering and Natural Sciences, Department of Mechanical Engineering (Full Scholarship) (100% English), *Honor Student*
- **Second Major** **:** 2018, Istanbul Bilgi University, Faculty of Engineering and Natural Sciences, Department of Energy Systems Engineering**,** *Honor Student*
- **M.Sc.** **:** 2022, Istanbul Technical University, Department of Material Science and Engineering, Material Science and Engineering Programme